UNIVERSIDADE FEDERAL DO RIO GRANDE DO SUL
CENTRO DE BIOTECNOLOGIA
PROGRAMA DE PÓS-GRADUAÇÃO EM BIOLOGIA CELULAR E MOLECULAR

Propriedades Estruturais e Biológicas do Peptídeo Jaburetox e da Proteína de Fusão Glutationa S-Transferase-Urease Ubíqua de Soja (*Glycine max*)

MSc. Fernanda Cortez Lopes
(Farmacêutica - Bioquímica UFRGS)

Tese submetida ao Programa de Pós-Graduação em Biologia Celular e Molecular da UFRGS como requisito parcial para a obtenção do grau de Doutora em Ciências

Orientadora Profª Drª Célia Regina Ribeiro da Silva Carlini
Co-Orientador Prof. Dr. Adriano Brandelli

Porto Alegre, março 2015.

CIP - Catalogação na Publicação

Cortez Lopes, Fernanda
Propriedades Estruturais e Biológicas do Peptídeo Jaburetox e da Proteína de Fusão Glutationa S-Transferase-Urease Ubíqua de Soja (Glycine max) / Fernanda Cortez Lopes. -- 2015.
133 f.

Orientadora: Célia Regina Ribeiro da Silva Carlini.
Coorientador: Adriano Brandelli.

Tese (Doutorado) -- Universidade Federal do Rio Grande do Sul, Centro de Biotecnologia do Estado do Rio Grande do Sul, Programa de Pós-Graduação em Biologia Celular e Molecular, Porto Alegre, BR-RS, 2015.

1. Jaburetox. 2. urease. I. Ribeiro da Silva Carlini, Célia Regina, orient. II. Brandelli, Adriano, coorient. III. Título.

Elaborada pelo Sistema de Geração Automática de Ficha Catalográfica da UFRGS com os dados fornecidos pelo(a) autor(a).

MEMBROS DA BANCA EXAMINADORA

Dra. Débora Foguel
(Instituto de Bioquímica Médica Leopoldo De Meis/UFRJ)

Dr. Hugo Verli
(Programa de Pós-Graduação em Biologia Celular e Molecular/UFRGS)

Dr. Leonardo Nimrichter
(Instituto de Microbiologia/UFRJ)

Revisor e Membro suplente: Dr. Rodrigo Ligabue Braun
(Programa de Pós-Graduação em Biologia Celular e Molecular/UFRGS)

Este trabalho foi desenvolvido no Laboratório de Proteínas Tóxicas, no Departamento de Biofísica da Universidade Federal do Rio Grande do Sul. O período de doutorado-sanduíche foi realizado no Laboratorio di Chimica Bioinorganica, Dipartimento di Farmacia e Biotecnologie, Università di Bologna sob supervisão do Prof. Dr. Stefano Ciurli. Durante o doutorado, obtive bolsa de estudos financiada pela CAPES e no período do doutorado-sanduíche fui contemplada com um bolsa de estudos, também concedida pela CAPES, pelo Projeto Pesquisador Visitante PVE 054/2012, fazendo parte do Programa Ciências sem Fronteiras.

"Uma criança, um professor, uma caneta e um livro podem mudar o mundo"

Malala Yousafzai

"Feliz aquele que transfere o que sabe e aprende o que ensina"

Cora Coralina

" A dúvida é o princípio da sabedoria"

Sócrates

Dedico esta tese aos meus grandes amores:

Douglas, Mãe, Pai e Ricardo.

AGRADECIMENTOS

Primeiramente eu gostaria de agradecer à minha orientadora Célia, por ter acreditado em mim desde o início, por ter me proporcionado as melhores oportunidades, por ter sido uma orientadora dedicada; enfim, por ter sido uma verdadeira mãe para mim durante estes 4 anos. Ao meu co-orientador, Adriano, por ter fornecido as cepas bacterianas e fúngicas e por sempre deixar as portas de seu laboratório abertas para mim.

Ao meu orientador na Itália, Stefano, que me ensinou muito sobre análises de estruturas de proteínas, que sempre foi dedicado nas idas à Firenze e nas análises dos dados. À Barbara que me ensinou muito e que foi uma grande amiga durante a minha estadia em Bologna. À Olena que me ajudou muito nas análises de RMN e que foi uma excelente companhia de finais de semana e de passeios por Bologna. Ao Luca pelas discussões científicas sobre ureases e por todas as ajudas no lab. À Lucià e Cinzia pela amizade e pelas traduções simultâneas inglês-italiano que foram fundamentais para a vida em Bologna. Ao Matteo e Anna por todas as discussões científicas, elaborações de cartas em italiano para as autoridades sanitárias e ajuda com o *Permesso di soggiorno*. Agradeço a todos do lab, pelos muitos cafés e almoços que renderam ótimos momentos. Ao AllahBaksh (AB), que foi um ótimo amigo, me ensinou muito sobre clonagem e transformação em plantas, que fez a longa jornada no ônibus 35 diversas vezes e que me mostrou um pouco da cultura de seu país. Aos professores Claudio Ratti e Elena Baraldi por abrirem seus laboratórios para mim e terem me ajudado muito. Ao Massimo Lucci, do CERM, por todas as aquisições de RMN, mas principalmente por toda a simpatia. Ao professor Vladimir Uversky, por todos os ensinamentos sobre proteínas intrinscamente desordenadas.

Aos secretários mais competentes do mundo: Silvinha e Luciano! Vocês deixam nossas vidas muito mais fáceis na pós-graduação. Além de serem sempre muito simpáticos e queridos!! Muito obrigada por tudo nestes 6 anos de pós-graduação.

Ao querido Tinoko que é um anjo para o Laprotox, mas muito mais do que é isso, é um amigão. Muito obrigada por "quebrar" todos os galhos, por todos os almoços no RU e por todos papos-cabeça. À Dona Eva, que é fundamental para nosso lab, que é um amor de

pessoa e que é a pessoa mais determinada que eu conheço, que fica feliz mesmo com a pia atrolhada de vidrarias.

À Val, que foi uma amigona desde o início, minha "*roommate*", baita colega de laboratório (no Brasil e em Bologna) e companheira de Whatsapp. Quero continuar sendo tua parceria científica e que a nossa amizade não tenha fim. À Anne por ter sido uma super parceira também, dividindo comigo os "planos infalíveis" (nem tanto assim) semanais para terminar o paper da ubíqua, obrigada pela companhia nas aulas de inglês, pelas milhares de caronas, pelas caminhadas, mas principalmente pela amizade. Ao Rodrigo que foi o grande incetivador da minha entrada no Laprotox, um grande amigo, que sempre admirei como pesquisador e que me ajudou muito ao longo do doutorado (as novidades renderam muitas conversas!). À Deise, minha primeira "filha científica", que está trilhando seu caminho (quase farmacêutica) com muito sucesso e que me enche de orgulho a cada conquista. À Andressa e à Bruninha que me ajudam muito no laboratório, a Bruninha que eu vi amadurecer e que se tornou uma menina responsável e cheia de metas e à Andressa que a cada dia mostra o seu potencial e que promete ter um futuro brilhante. À Karine pela companhia no lab, na aula de inglês e pelos almoços do tipo *gourmet* que ainda virão. Ao Diogo, que me ajudou muito no mundo das proteínas (principalmente no que se refere à Espectrometria de Massas) e que sempre contou as mais divertidas histórias, ao longo dos milhares de cafés que tomamos ao longo do doutorado. À Jozi, que me deu carona durante a greve dos ônibus e que sempre foi uma amiga querida para todas as horas. À Arlete que é minha amiga desde os tempos idos de BioPlus e que sempre me ajudou e muito no Laprotox. Às queridas Angelas e à Mayara que sempre foram companhias certas para o RU (e os nossos almoços foram sempre muito divertidos!!!), sempre simpáticas e queridas. À Marina por toda a ajuda nos experimentos e por todas as ótimas reflexões sobre a vida. À Adriele por ser sempre muito prestativa (caronas, manobras inesperadas) e que juntamente com o Augusto e Deiber sempre foram muito camaradas na divisão do uso do nosso querido Äkta. A Mel que foi quem me mostrou o Laprotox e que dividiu comigo o amor pelos funguinhos. À Monica que fez milhares de cultivos comigo (que não tinham fim) e pelas muitas risadas nos cafés da tarde. Ao Leonardo, Natalia e Jimena por serem tão queridos e nos ensinarem um pouco de español. À Vanessa, Fernanda, Juliana, Monique, Rafael, Thiago, por toda a ajuda sempre. Às meninas da ULBRA, Camila, Ionara e

Roberta, pela amizade e pelas “quebradas de galho”. Obrigada a todos do Laprotox e aos que passaram por lá!!

À Karine com suas agulhinhas mágicas, que me deram muita serenidade e tranquilidade nos últimos meses de doutorado, que foram e estão sendo fundamentais para me manter equilibrada e menos estressada.

Às minhas queridas amigas do ICTA, Stela, Karla, Jamile, Eliandra, Evelise, Juliana pelas parcerias em Congressos, pelas discussões científicas “microbiológicas” e pela amizade! Vocês sempre serão as minhas microbiologistas favoritas!!!!

Às minhas amigonas da FacFar, Bruna, Tailise e Liana, pelos almocinhos e jantinhas muito divertidos, mas principalmente pela amizade de 11 anos.

Ao Douglas por ser o melhor namorado que eu poderia ter, que sempre entendeu as rotinas de trabalho longas, os finais de semana de muito trabalho, que sempre me apoiou e me motivou. Obrigada pelas longas conversas pelo Skype (diárias) quando eu estava em Bologna, elas foram muito importantes para aguentar a distância. Te amo demais!

Ao meu Pai e à minha Mãe que foram fundamentais durante estes quatro anos, que me deram muitas caronas ao vale, que sempre foram meu suporte nos momentos difíceis, que também tiveram longas conversas pelo Skype, não deixando eu me sentir sozinha, mesmo a muitos quilômetros de distância. Muito obrigada por tudo o que vocês fizeram por mim, esse título também é de vocês. Ao Ricardo, meu irmão que sempre me apoiou demais, que me ajudou muito! Obrigada por todas as nossas conversas e por ter me apresentado à ONGEP, que aflorou em mim o amor pela docência. Amo muito vocês!!

ÍNDICE

LISTA DE ABREVIATURAS

CAPITO: CD Analysis and Plotting Tool (Análise de dados de Dicroísmo Circular e Ferramenta de Plotagem)

CARA: Computer-Assisted Resonance Assignment (Assinalamento das Ressonâncias Assistido por Computador)

CD: Circular Dichroism (Dicroísmo Circular)

CFU: Colony Forming Units (Unidades Formadoras de Colônia)

EDTA: Ethylenediaminetetraacetic acid (Ácido Etilenodiamino Tetraacético)

ELISA: Enzyme-Linked Immunosorbent Assay (Enzimaimunoensaio)

eSBU: embryo-specific soybean urease (urease embrião-específica de soja)

GST: Glutathione S-Transferase (Glutationa S-Transferase)

HSQC: Heteronuclear Single-Quantum Coherence

IDP: Intrinsically Disordered Proteins (Proteínas Intrinsicamente Desordenadas)

IPTG: Isopropyl β-D-1-thiogalactopyranoside (Isopropil β-D-1-tiogalactopiranosídeo)

JBU: Jack bean Urease (urease de feijão-de-porco)

JBURE-II: Jack bean Urease II (urease de feijão-de-porco II)

LB: meio de cultura Luria Bertani

LUV: Large Unilamellar Liposomes (Lipossomas Unilamelares Grandes)

MALS: Multiple Angle Light Scattering (Espalhamento de Luz de Múltiplo Ângulo)

MoRFs: Molecular Recognition Features (Características de Reconhecimento Molecular)

MS: Mass Spectrometry (Espectrometria de massas)

NOE: Nuclear Overhauser Effect (Efeito Nuclear Overhauser)

PDB: Protein Data Bank

PONDR: Predictor of Naturally Disordered Regions (Preditor de Regiões Naturalmente Desordenadas)

QELS: Quasi Elastic Light Scattering (Espalhamento de Luz Quasi Elástico)

qPCR: quantitative PCR (PCR quantitativo)

RMN (Ressonância Magnética Nuclear) ou **NMR** (Nuclear Magnetic Resonance)

SAXS: Small Angle X-ray Scattering (Espalhamento de Raios-X a baixo ângulo)

SDS-PAGE: Sodium Dodecyl Sulfate Polyacrylamide Gel Electrophoresis (Eletroforese em Gel de Poliacrilamida-Dodecil Sufato de Sódio)

SEC: Size Exclusion Chromatography (Cromatografia de Exclusão por Tamanho)

SSP: Secondary Structure Propensity (Propensão à Estrutura Secundária)

TCEP: tris(2-carboxyethyl)phosphine [tris(2-carboxietil)fosfina]

T_m: Melting Temperature (Temperatura de Fusão)

uSBU: Soybean ubiquitous urease (urease ubíqua de soja)

RESUMO

Urease (EC 3.5.1.5) é uma metaloenzima dependente de níquel que catalisa a hidrólise da ureia à amônia e dióxido de carbono. A Soja (*Glycine max*) produz duas isoformas de urease: a urease ubíqua (uSBU) e a urease embrião-específica (eSBU). Nosso grupo demonstrou que eSBU apresenta propriedades biológicas independentes da sua atividade ureolítica, como ativação de plaquetas, atividade inseticida e inibição do crescimento de fungos fitopatogênicos, estes últimos sugestivos de envolvimento das SBUs em mecanismos de defesa da planta. Outras ureases também estudadas pelo nosso grupo, são as de Feijão-de-porco (*Canavalia ensiformis*). O Feijão-de-porco produz três isoformas de urease: Canatoxina, JBU e JBURE-II, que também apresentam atividades biológicas, não relacionadas à sua atividade enzimática. Dentre elas, a atividade inseticida tem sido a mais estudada. A toxicidade das ureases a insetos envolve a liberação de um peptídeo interno tóxico, mediante à hidrólise por enzimas digestivas do inseto. Um peptídeo equivalente foi clonado em *Escherichia coli* e denominado Jaburetox. Este peptídeo apresenta um amplo espectro de ação contra insetos e toxicidade contra fungos. Nossos objetivos nessa tese foram estudar: 1) as propriedades biológicas da urease ubíqua de soja, fusionada à Glutationa S-Transferase (GST-uSBU), e 2) as propriedades estruturais do peptídeo Jaburetox. No capítulo 1 mostramos que a GST-uSBU é tóxica contra fungos filamentosos, interferindo no metabolismo secundário fúngico e na produção de pigmentos, e também foi tóxica a leveduras, induzindo mudanças morfológicas. A proteína de fusão apresentou ainda atividade inseticida e induziu agregação de plaquetas de coelho e de hemócitos de insetos. Os dados sugerem que GST-uSBU serve de modelo para o estudos futuros de propriedades biológicas de ureases de plantas. No captítulo 2, o peptídeo Jaburetox foi estabilizado em sua forma monomérica, com a utilização do agente redutor TCEP (tris (2-carboxietil) fosfina). O Jaburetox apresentou elevado raio hidrodinâmico, característico de uma proteína intrinsicamente desordenada. Estes dados foram confirmados através de análises de Dicroísmo Circular, de preditores de desordem (PONDR) e por Ressonância Magnética Nuclear. A estrutura do peptídeo em solução foi elucidada, apresentando um motivo α-hélice na região N-terminal e duas estruturas do tipo volta, uma na região central e outra próxima da região C-terminal do peptídeo. O conhecimento da estrutura tridimensional do peptídeo será de grande importância para o entendimento do mecanismo de ação inseticida e fungitóxico do Jaburetox.

ABSTRACT

Urease (EC 3.5.1.5) is a nickel-dependent metalloenzyme that catalyzes the hydrolysis of urea to form ammonia and carbon dioxide. Soybean (*Glycine max*) produces two urease isoforms: ubiquitous urease (uSBU) and the embryo-specific urease (eSBU). Our group demonstrated that eSBU displays biological properties independent of its ureolytic activity, such as platelets activation, insecticidal activity and inhibition of phytopathogenic fungi growth. These data suggested that soybean ureases could be involved in plant defense. Other ureases also studied by our group are jack bean (*Canavalia ensiformis*) ureases. Jack bean produces three isoforms of ureases, Canatoxin, JBU and JBURE-II, which also have biological properties unrelated to enzymatic activity. Among them, the insecticidal activity has been the most studied. The toxicity of ureases against insects involves hydrolysis by insect digestive enzymes and the release of a toxic internal peptide. An equivalent peptide was cloned in *Escherichia coli* and called Jaburetox. This peptide presents a broad spectrum of activity against insects and is also fungitoxic. In this thesis, our objectives were to study: 1) the biological properties of the soybean ubiquitous urease fused to Glutathione S- Transferase (GST-uSBU), and 2) the structural properties of the peptide Jaburetox. In chapter 1, we show that GST-uSBU is toxic against filamentous fungi, interfering on the fungal secondary metabolism, in the pigments production, and also affected yeasts, inducing morphological changes. GST-uSBU also displayed insecticidal activity and induced aggregation of rabbit platelets and insect hemocytes. Thus, this fusion protein could serve as model for future studies related to biological properties on plant ureases. In chapter 2, the peptide Jaburetox was stabilized in its monomeric form by using the reducing agent TCEP (tris (2-carboxyethyl) phosphine). Jaburetox showed a large hydrodynamic radius, which is characteristic of an intrinsically disordered protein. These data were confirmed by Circular Dichroism analysis, disorder predictors (PONDR) and Nuclear Magnetic Resonance. The structure of the peptide in solution was elucidated, showing a α-helix motif in the N-terminal region and two turn-like structures, one located in the central region and another near the C-terminal of the peptide. The knowledge of Jaburetox's three-dimensional structure is an important step towards the understanding of its insectidal and fungitoxic mode of action.

1. INTRODUÇÃO

Desde os primórdios da agricultura, aproximadamente 10.000 anos atrás, o cultivo das plantas teve que competir com diversos organismos nocivos como pestes animais (insetos, ácaros, nematóides, roedores, lesmas, caracóis, pássaros), patógenos de plantas (vírus, bactérias, fungos, organismos do reino Chromista) e ervas daninhas (OERKE, 2006). Estes organismos nocivos, denominados pestes, causam elevadas perdas em culturas, no mundo todo. As perdas podem chegar a até 80 %, em culturas de beterraba e de algodão, por exemplo (OERKE & DEHNE, 2004). Para atender a demanda por alimentos para a crescente população mundial, há a necessidade de novas formas de proteção das culturas de plantas contra predadores e patógenos, bem como evitar o uso de compostos químicos no combate às pestes, pois estes compostos são prejudicais ao meio ambiente (CARLINI & GROSSI-DE-SÁ, 2002).

Em relação aos fungos, os fungicidas sintéticos tem controlado efetivamente doenças de plantas por muitos anos, mas uma crescente preocupação sobre os efeitos ambientais destes fungicidas devido à sua toxicidade residual, à falta de especificidade e ao desenvolvimento de resistência, enfatizam a necessidade do desenvolvimento de alternativas para o controle seletivo (LEE, 2007). Uma vez que as plantas estão sempre expostas a estes micro-organismos presentes no ambiente, elas dispõem de uma variedade de mecanismos potentes de defesa, incluindo a síntese de compostos de baixo peso molecular, proteínas e peptídeos que apresentam atividade antifúngica. Estas proteínas parecem estar envolvidas tanto na resistência constitutiva quanto induzida ao ataque de fungos (SELITRENNIKOFF, 2001).

Insetos não são os únicos responsáveis diretamente pelas massivas perdas nas lavouras, porém também causam perdas indiretas relevantes devido ao seu papel como vetor de vários patógenos de plantas. Estas perdas ocorrem mesmo com o uso de pesticidas e fungicidas (HILDER & BOULTER, 1999). Todas as plantas apresentam resistência endógena aos ataques dos insetos. Contudo, como resultado da co-evolução, insetos herbívoros tem se adaptado às defesas de plantas (GATEHOUSE, 2002). Plantas geneticamente modificadas, com resistência aumentada a insetos, estão revolucionando a agricultura, levando à redução do uso de pesticidas e menores gastos de produção. Atualmente, as plantas transgênicas no mercado expressam principalmente toxinas

derivadas da bactéria *Bacillus thuringiensis* (*Bt*). Contudo, existem insetos que não são susceptíveis às toxinas *Bt* e, por isso, a busca por alternativas para controle dessas pestes tem ganhado muita atenção.

Devido ao fato de que as ureases de plantas têm atividade contra insetos resistentes a toxina *Bt*, somado à toxicidade a fungos fitopatogênicos, as ureases e seus peptídeos derivados apresentam grande potencial biotecnológico. Dessa forma, o estudo das propriedades entomotóxicas e fungitóxicas das ureases de plantas é fundamental para o desenvolvimento de estratégias alternativas para proteger culturas comercialmente relevantes, contra seus inimigos naturais (CARLINI & POLACCO, 2008; VANDENBORRE, SMAGGHE, & DAMME, 2011; STANISÇUASKI & CARLINI, 2012).

2. REVISÃO BIBLIOGRÁFICA

2.1. UREASES

Ureases (EC 3.5.1.5; ureia amidohidrolase) são metaloenzimas amplamente distribuídas na natureza entre plantas, fungos e bactérias, não sendo sintetizadas por animais. Catalisam a hidrólise da ureia, formando amônia e dióxido de carbono. O substrato ureia é disponível em abundância, estando presente na urina de animais, na decomposição de compostos nitrogenados de organismos mortos e, também, devido à sua aplicação como fertilizante. Dessa forma, a produção de ureases permite aos organismos utilizarem fontes exógenas e endógenas de ureia como fonte de nitrogênio para a sua nutrição (MOBLEY & HAUSINGER, 1989; FOLLMER, 2008; KRAJEWSKA, 2009).

Ureases de plantas e de fungos são usualmente trímeros (α_3) ou hexâmeros (α_6) com subunidades de aproximadamente 90 kDa, enquanto que as ureases bacterianas são multímeros de duas ou três subunidades (usualmente $[\alpha,\beta,\gamma]_3$) (MOBLEY, ISLAND, & HAUSINGER, 1995; SIRKO & BRODZIK, 2000) (Figura 1). A subunidade única de ureases de plantas e de fungos alinha com as subunidades menores das ureases bacterianas (na ordem γ-β-α). O alinhamento das três subunidades da urease de *Klebsiella aerogenes* com a região ortóloga da urease majoritária de *Canavalia ensiformis* revelou mais de 50 % de identidade. Esta similaridade entre reinos sugere que todas as ureases são variantes do mesmo ancestral e apresentam mecanismos catalíticos similares (MOBLEY et al., 1995; SIRKO & BRODZIK, 2000; FOLLMER, 2008).

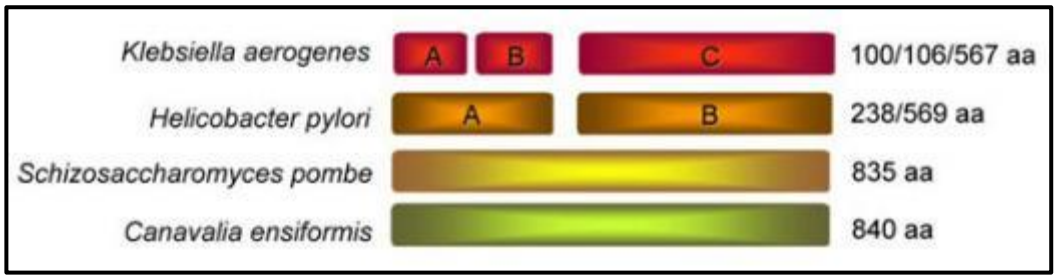

Figura 1: Organização estrutural de ureases. Em plantas (*Canavalia ensiformis*) e fungos (*Schizosaccharomyces pombe*) as ureases são formadas por um único tipo de cadeia polipeptídica. Já as ureases bacterianas apresentam três tipos de subunidades (*Klebsiella aerogenes*) ou dois tipos de cadeias polipeptídicas (*Helicobacter pylori*). Retirada de www.ufrgs.br/laprotox.

Nosso grupo demonstrou recentemente, através de estudos filogenéticos, que o ancestral das ureases possuia três cadeias, e sua transição para enzimas com uma cadeia não envolveu intermediários de duas cadeias. As variantes de urease com uma e duas cadeias podem ter derivado de um processo de fusão gênica dos três genes ancestrais (LIGABUE-BRAUN et al., 2013).

Ureases geralmente apresentam dois íons Ni^{2+} em seus sítios ativos, com poucas exceções relatadas na literatura, como a Canatoxina isolada de *C. ensiformis*, que contém zinco no sítio ativo (FOLLMER et al., 2002) e a urease bacteriana de *Helicobacter mustelae* que contém ferro (CARTER et al., 2011). Estudos genéticos e bioquímicos realizados em sistemas eucarióticos e procarióticos demonstraram que a a maioria destas enzimas requer proteínas acessórias para a correta inserção do níquel no sítio ativo (CARTER et al., 2009; ZAMBELLI et al., 2011).

Um estudo em *Arabidopsis thaliana* demonstrou que as proteínas acessórias UreD, UreF e UreG são necessárias e suficientes para ativação da urease, uma vez que plantas *knockout* para qualquer um dos genes destas proteínas acessórias não apresentavam atividade ureolítica. Neste trabalho, também foi demonstrado que a partir da co-expressão dos genes para as proteínas acessórias e do gene estrutural da urease de *A. thaliana*, foi possível a ativação da urease em células de *Escherichia coli* (WITTE, ROSSO & ROMEIS, 2005). Além disso, KIM, MULROONEY & HAUSINGER (2005) reportaram que apesar de *Bacillus subtilis* apresentar uma urease cataliticamente ativa, esta bactéria não apresenta genes para as proteínas acessórias. Os autores sugerem que *B. subtilis* pode utilizar proteínas acessórias ainda não identificadas na ativação da urease. Há na literatura, também, alguns casos de um ou mais genes de proteínas acessórias não serem encontrados no *operon* da urease de determinados organismos. Um exemplo é o *operon* da bactéria *Mycobacterium tuberculosis* linhagem Erdman, o qual não contém o gene para a UreD e mesmo assim sintetiza uma urease ativa. Os autores postulam que o gene para a UreD pode estar em outra região no cromossomo bacteriano (CLEMENS, LEE & HORWITZ, 1995).

2.1.1. UREASES DE PLANTAS

Ureia é uma importante fonte primária de nitrogênio para plantas. O catabolismo da arginina é a única rota confirmada para geração de ureia *in vivo.* A degradação das purinas e ureídos também poderia gerar ureia, porém esta segunda rota ainda é um pouco controversa. O nitrogênio somente é assimilável após a hidrólise da ureia e este é o principal papel fisiológico atribuído às ureases de plantas. A amônia resultante é assimilada pela glutamina sintetase, utilizando glutamato como substrato (REAL-GUERRA et al, 2013). A atividade ureásica está presente virtualmente em todas as espécies de plantas, sendo distribuída em todos os tecidos (POLACCO & WINKLER, 1984; TORISKY & POLACCO, 1990; WITTE, 2011).

2.1.1.1. UREASES DE SOJA (*Glycine max*)

A leguminosa Soja tem sido economicamente muito importante como fonte de várias proteínas para uso industrial. Além do fato de ser uma fonte rica de proteínas e de fácil isolamento, os subprodutos derivados de proteínas da soja são de importância para aves, para pesca e para alimentação de rebanhos leiteiros. Dentre várias proteínas presentes na soja, umas delas é urease, presente em abundância nas sementes e em menor quantidade nos outros tecidos (KUMAR, DWEVEDI, & KAYASTHA, 2009). O isolamento da urease de soja, pioneiro dentre ureases de vegetais superiores, foi realizado por Takeuchi, em 1909 (FEARON, 1923).

A urease produz duas isoformas na soja, a urease embrião-específica (eSBU) que é sintetizada somente no embrião em desenvolvimento e acumula nas sementes maduras (codificada pelo gene *Eu1*, GenBank AY230157, Phytozome Glyma05g27840) (POLACCO, & HAVIR, 1979; POLACCO & WINKLER, 1984; POLACCO & HOLLAND, 1993) e a urease ubíqua (uSBU) (codificada pelo gene *Eu4*, GenBank AY230156, Phytozome Glyma11g37250), que é encontrada em pequenas quantidades em todos os tecidos da planta (TORISKY et al., 1994). uSBU é considerada a isoforma responsável pela reciclagem de ureia. Este fato foi demonstrado pelo fato de que mutantes com silenciamento desta isoforma não acumulam ureia em nenhum tecido e não há prejuízo com o uso da ureia como única fonte de nitrogênio. No entanto, mutantes do gene

Eu4 que não expressavam uSBU, apresentaram um fenótipo característico como necroses nas extremidades das folhas e raízes, acúmulo de ureia nas folhas e sementes, além de retardamento na germinação (POLACCO & HOLLAND, 1993). O cDNA de ambas as isoformas foi sequenciado, mostrando que estas compartilham 87 % de identidade e 92 % de similaridade (GOLDRAIJ, BEAMER & POLACCO, 2003). Nosso grupo clonou a uSBU em *Escherichia coli* no plasmídeo pGEX-4T-2, expressando uSBU como uma proteína fusionada a Glutationa S-Transferase (GST) (MARTINELLI, 2007), com intuito de realizar ensaios biológicos com a mesma, uma vez que, devido às pequenas quantidades da proteína encontrada na soja, sua purificação a partir de tecidos da planta seria praticamente inviável.

Em 2010, o genoma da soja foi sequenciado (SCHMUTZ et al., 2010) e foi confirmada a presença dos dois genes de urease, *Eu1* e *Eu4*. Além disso, foi revelado um terceiro gene (Glyma08g10850), que acredita-se ser uma terceira isoforma de urease. Este parálogo é provavelmente não funcional como enzima, devido ao acúmulo de mutações (troca de aminoácidos funcionalmente essenciais, deleções parciais na sequência e um códon de parada prematuro). De acordo com as evidências de que a urease eSBU possa estar envolvida com defesa, essa também poderia ser uma função desta terceira isoforma (WITTE, 2011).

2.1.1.2. UREASES DE FEIJÃO-DE-PORCO (*Canavalia ensiformis*)

O Feijão-de-porco (*Canavalia ensiformis*) apresenta três isoformas de ureases: urease majoritária (JBU) (SUMNER, 1926), Canatoxina (CARLINI & GUIMARÃES, 1981; FOLLMER et al., 2001) e JBURE-II (PIRES-ALVES et al., 2003; MULINARI et al, 2011). Os estudos da urease majoritária de Feijão-de-porco (JBU) foram um grande marco em Bioquímica. A análise dos cristais desta urease demonstrou a natureza proteica de enzimas (SUMNER, 1926), rendendo um prêmio Nobel de Química ao pesquisador James Sumner, em 1946. Em estudos com a mesma proteína, foi descoberto um papel biológico do Ni^{2+}, que é encontrado no sítio ativo de JBU, e da grande maioria das ureases, classificando-as como metaloenzimas (DIXON et al., 1975). A Canatoxina, por sua vez, foi isolada por Carlini & Guimarães (CARLINI & GUIMARÃES, 1981) e, somente 20

anos mais tarde, essa neurotoxina foi identificada como uma isoforma de urease (FOLLMER et al., 2001). Por fim, a JBURE-II teve seu cDNA clonado em *E. coli* (PIRES-ALVES et al., 2003; MULINARI et al., 2011), apresentando alta identidade de aminoácidos com ureases de plantas (71 a 82 %), sendo, assim, caracterizada como uma terceira isoforma de urease de *C. ensiformis*. A apoJBURE-II foi obtida de forma recombinante em *E. coli* na ausência de proteínas acessórias e apresentou várias das propriedades biológicas descritas para Canatoxina e JBU (MULINARI et al., 2011),

2.1.2. UREASES MICROBIANAS

Ureases microbianas são importantes enzimas em determinados estados patológicos de humanos e de outros animais, no metabolismo de ruminantes e nas tranformações ambientais de determinados compostos nitrogenados (MOBLEY & HAUSINGER, 1989). Algumas ureases são consideradas fatores de virulência, pois apresentam importante papel na patogênese de doenças em humanos e em animais. Entre as bactérias para as quais a urease foi caracterizada como fator de virulência estão *Proteus mirabilis*, *Helicobacter pylori*, *Clostridium perfringens*, *Klebsiella pneumoniae*, *Salmonella* spp., *Staphylococcus saprophyticus*, *Ureoplasma urealyticum*, *Yersinia enterocolitica*, entre outras. A contribuição para a patogênese, na maioria desses casos, reflete os efeitos da hidrólise da ureia, que são o aumento de pH e toxicidade, pela liberação de amônia e de seus derivados. Ureia é o maior subproduto do metabolismo de nitrogênio da maioria dos animais terrestres, é produzida no fígado, carreada pela corrente circulatória até os rins e é excretada na urina. Sua concentração no soro de indivíduos saudáveis é em torno de 1-10 mM e na urina é de aproximadamente 0,5 M. Adicionalmente, é estimado que entre 20-25 % de toda ureia produzida esteja no trato gastrointestinal, sendo sua concentração no estômago de 1,7-3,4 mM. Como o K_m para ureia da maioria das ureases está na faixa de 0,1 a 5 mM, nos tecidos a atividade ureolítica ocorre em condições saturantes (MOBLEY, ISLAND & HAUSINGER, 1995; KRAJEWSKA, 2009). Por isso, em humanos, o sistema urinário e digestório são os locais mais comuns de infecções por estas bactérias (MOBLEY, ISLAND & HAUSINGER, 1995; KRAJEWSKA, 2009). A presença de atividade ureolítica foi reportada em doenças como urolitíase, pielonefrite, encefalopatia, coma hepático, infecções gastroduodenais, entre outras (MORA & ARIOLI, 2014). Uma

das ureases bacterianas mais estudada é a urease de *H. pylori*, que tem sido relacionada a úlceras pépticas e câncer de estômago (TAN & WONG, 2011).

Estudos com as leveduras *Cryptococcus neoformans* e *Coccidioides posadasii* sugerem que mudanças de pH urease-dependentes estão envolvidas na evasão dos fungos do nosso sistema imunitário e a toxicidade da amônia liberada contribui para a patogênese de modo sistêmico (RUTHERFORD, 2014). Em um trabalho publicado recentemente pelo nosso grupo, mutantes *knockout* de *Cryptococcus gattii* para o gene estrutural (URE1) ou para os genes que codificam as proteínas acessórias URE4 e URE6 foram construídos. Os dados sugerem que a ureólise mediada pela urease de *C. gattii* não é a única função desta enzima durante a infecção. Enquanto que esta atividade é aparentemente necessária para a colonização inicial dos pulmões, a ureólise não é tão importante nos estágios finais da infecção. Estes resultados sugerem que a urease de *C. gatti*i tem um importante papel na virulência, em parte possivelmente devido a mecanismo(s) independente(s) da atividade ureolítica (FEDER et al., 2015). Uma vez que humanos não produzem ureases e não possuem enzimas dependentes de níquel, as ureases tem sido propostas como potenciais alvos terapêuticos, para doenças causadas por micro-organismos produtores desta enzima (RUTHERFORD, 2014).

Ureases microbianas podem atuar de forma positiva em seres humanos e em alimentos, fatos reconhecidos apenas recentemente. Ureases produzidas pela comunidade bacteriana oral atuam na contenção de cáries, sendo que indíviduos sem cáries apresentam alta atividade ureolítica em amostras de placas bacterianas. Algumas bactérias lácticas, com documentado comportamento probiótico, são ureases-positivas. Igualmente, outras espécies de bactérias lácticas, que são amplamente utilizadas em produtos lácteos fermentados e na produção de iogurte, utilizam a atividade ureásica para conter o estresse ácido, além de fornecer dióxido de carbono e amônia para diversas rotas biossintéticas. Urease é também difundida em diversas espécies pertencentes a microbiota intestinal humana e é estimado que esta comunidade complexa tem habilidade de hidrolisar de 15-30% da ureia sintetizada em indíviduos normais (MORA & ARIOLI, 2014).

É de grande importância na agricultura a atividade ureolítica de solos. Esta atividade deriva de micro-organismos, mas principalmente de ureases do solo, proveniente de plantas e de células microbianas mortas, tornando a enzima extracelular. A urease no

solo é estabilizada ao ser imobilizada em argilas e substâncias húmicas. A presença desta forma estável de urease no solo permite o uso de ureia como um eficiente fertilizante (KRAJEWSKA, 2009). A urease de *Bacillus pasteurii* pode ser encontrada livre e enzimaticamente ativa no solo após lise celular (CONRAD, 1940). O solo ao redor das raízes das plantas, a rizosfera, contém uma vasta gama de exsudatos de raízes (WALKER et al., 2003). Atividades indutoras de secreção são comuns entre ureases microbianas e de plantas, e poderiam contribuir para a riqueza de compostos encontrados na rizosfera (OLIVERA-SEVERO et al, 2006). A urease de *Bradyrhizobium japonicum*, uma bactéria diazotrófica simbionte em soja, não está envolvida nos processos de nodulação ou fixação de nitrogênio na planta. Porém, as ureases da soja exercem um efeito quimiotático sobre *B. japonicum* e contribuem, por um mecanismo não esclarecido, para os processos de nodulação e fixação de nitrogênio pela planta (MEDEIROS-SILVA et al., 2012).

2.2. PROPRIEDADES BIOLÓGICAS DE UREASES E PEPTÍDEOS DERIVADOS

As ureases vegetais e microbianas pertencem a um grupo de proteínas multifuncionais (*moonlighting*), apresentando além da atividade ureolítica, outras propriedades independentes da hidrólise de ureia (FOLLMER et al., 2004). Estas proteínas apresentam no mínimo dois domínios proteicos distintos, responsáveis por atividades biológicas diferentes: no caso das ureases, um domínio com atividade hidrolítica sobre a ureia, tiol-dependente e suscetível de inibição por agentes oxidantes, e pelo menos mais um segundo domínio, tiol-independente, responsável por outras propriedades biológicas não relacionadas com a hidrólise de ureia (CARLINI & POLACCO, 2008).

2.2.1. PROTEÍNAS *MOONLIGHTING*

Proteínas *Moonlighting* formam uma classe especial de proteínas multifuncionais, que apresentam funções múltiplas, autônomas e muitas vezes não relacionadas. Um importante critério para proteínas *moonlighting* é a independência das diferentes funções, significando que a inativação de uma função (por exemplo, por mutação) pode não afetar outras funções e vice versa (HUBERTS & VAN DER KLEI, 2010). A definição de

proteínas *moonlighting* exclui proteínas que resultam de *splicing* alternativo, de modificações pós-traducionais e fusões de genes; proteínas capazes de utilizar múltiplos substratos e proteínas catalisando múltiplos passos na mesma rota metabólica (SRIRAM et al., 2005). Uma faceta interessante dessas proteínas é que uma proteína *moonlighting* em um organismo pode não ser uma proteína *moonlighting* em outro, sugerindo que pequenas variações na sequência da proteína são responsáveis pelas ações *moonlighting* (HENDERSON, LUND, & COATES, 2010).

2.2.2. ATIVIDADE INSETICIDA

A primeira isoforma de urease a ser testada contra insetos foi a Canatoxina, que mostrou-se letal quando ingerida por *Callosobruchus maculatus*, *Rhodnius prolixus*, *Dysdercus peruvianus*, *Nezara viridula*, porém não afetou outros insetos como *Manduca sexta*, *Schistocerca americana*, *Drosophila melanogaster* e *Aedes aegypti* (CARLINI et al., 1997; FERREIRA-DASILVA et al., 2000; CARLINI & GROSSI-DE-SÁ, 2002; STANISÇUASKI et al., 2005). A isoforma majoritária JBU foi testada contra *R. prolixus*, *D. peruvianus* e *Oncopeltus fasciatus*, mostrando o mesmo nível de atividade inseticida da Canatoxina (FOLLMER et al., 2004; STANISÇUASKI et al., 2010; DEFFERRARI et al, 2011). Por fim, a isoforma JBURE-II também apresenta efeitos entomotóxicos, causando inibição de diurese em *R. prolixus* (MULINARI et al. 2011). O efeito inseticida das ureases é dependente do ciclo de vida do inseto, afetando preferencialmente ninfas quando administrado por via oral (FERREIRA-DASILVA et al, 2000; CARLINI & GROSSI-DE-SÁ, 2002; STANISÇUASKI et al, 2005).

A urease de soja eSBU apresentou atividade entomotóxica contra *Dysdercus peruvianus* (FOLLMER et al., 2004), enquanto que a urease de feijão-guandu (*Cajan cajan*) causou mortalidade em *Callosobruchus chinensis* (BALASUBRAMANIAN et al., 2013). Por outro lado, a urease de *Bacillus pasteurii* não apresentou atividade inseticida. Como esta proteína não tem a parte da sequência que apresenta atividade inseticida das ureases, postulou-se que isso explicaria a ausência de toxicidade (FOLLMER et al., 2004). Estudos posteriores mostraram efeitos entomotóxicos diretos da JBU como inibição de diurese, interferência no transporte de água e na contração muscular (STANISÇUASKI &

CARLINI, 2012). Nosso grupo relatou a atividade inseticida de bactérias do gênero *Photorhabdus* (SALVADORI et al., 2012), indicando a existência de mais de um domínio entomotóxico nessas proteínas.

Recentemente, foi reportada a toxicidade da urease de *Yersinia pseudotuberculosis* contra a pulga (*Xenopsylla cheopis*). *Y. pseudotuberculosis* é a espécie mais próxima de *Y. pestis*, a última sendo a causadora da peste bubônica. Outros resultados deste trabalhos também evidenciaram que *Y. pestis* apresenta uma deleção na proteína acessória UreD, sendo inócua a *X. cheopis*. Mutantes de *Y. pestis* expressando esta proteína, tiveram a atividade ureolítica restabelecida e tornaram-se tóxicas a *Xenopsylla cheopis*. A inibição da atividade ureolítica em *Y. pestis* é importante, pois esta pulga é a responsável por transmitir a bactéria *Y. pestis* através de sua picada, favorecendo assim a relação simbiótica entre a bactéria e a pulga (CHOUIKHA & HINNEBUSCH, 2014).

2.2.2.1. JABURETOX

A atividade inseticida de Canatoxina é em parte dependente da liberação de um peptídeo interno de 10 kDa (Pepcanatox), liberado por hidrólise da toxina por enzimas digestivas do tipo catepsina (cisteíno e aspártico proteases) encontradas nos insetos *C. maculatus*, *R. prolixus*, *N. viridula*, *D. peruvianus* e *O. fasciatus* (FERREIRA-DASILVA et al., 2000; CARLINI & GROSSI-DE-SÁ, 2002; STANISÇUASKI et al., 2005; DEFFERRARI et al., 2011). Por outro lado, não há liberação desse peptídeo da Canatoxina quando esta é ingerida por insetos que apresentam enzimas do tipo tripsina (serino proteases), como *M. sexta*, *S. americana*, *D. melanogaster* e *A. aegypti*. A ativação proteolítica de canatoxina foi demonstrada pela digestão *in vitro* da proteína com enzimas obtidas de larvas de *C. maculatus*, os peptídeos resultantes foram fracionados por gel filtração e testados contra *R. prolixus*. Da fração mais ativa foi isolado um peptídeo tóxico de 10 kDa, denominado Pepcanatox (FERREIRA-DASILVA et al., 2000).

Baseado na sequência N-terminal do peptídeo Pepcanatox e utilizando como molde o cDNA da isoforma JBURE-II, obteve-se, por expressão heteróloga em *Escherichia coli*, um peptídeo recombinante, o Jaburetox-2Ec (apresentando um epitopo viral V5 e uma cauda com seis histidinas) (MULINARI et al., 2007). Jaburetox-2Ec apresentou um amplo

espectro de atividade inseticida, que também incluiu insetos não susceptíveis à Canatoxina como *Spodoptora frugiperda* (MULINARI et al., 2007). Jaburetox-2Ec causou a inibição da diurese em *R. prolixus* por um mecanismo que envolve GMP cíclico e distúrbio do potencial transmembrana dos túbulos de Malpighi (STANISÇUASKI et al., 2009). Além disso, Jaburetox-2Ec permeabilizou lipossomas unilamelares grandes, demonstrando a sua capacidade de desorganizar bicamadas lipídicas acídicas (PG [L-α-fosfatidil glicerol], PA [L-α-ácido fosfatídico] e PC [L-α-lisofosfatidilcolina]/PA) (BARROS et al., 2009).

Com intuito de compreender o modo de ação inseticida do Jaburetox-2Ec, estudos de modelagem molecular foram realizados sugerindo a existência de um motivo do tipo grampo β na porção C-terminal do peptídeo (MULINARI et al., 2007, BARROS et al., 2009) (Figura 2). Este motivo foi confirmado na estrutura cristalográfica de JBU (BALASUBRAMANIAN & PONNURAJ, 2010), sugerindo-se que este poderia ser a região do peptídeo com atividade sobre membranas (BALASUBRAMANIAN et al., 2013; BARROS et al., 2009). Um variante do peptídeo recombinante Jaburetox-2 Ec, sem o epitopo V5 e contendo apenas a cauda de histidina, foi clonado e expresso em *E. coli* e denominado apenas Jaburetox (POSTAL et al., 2012).

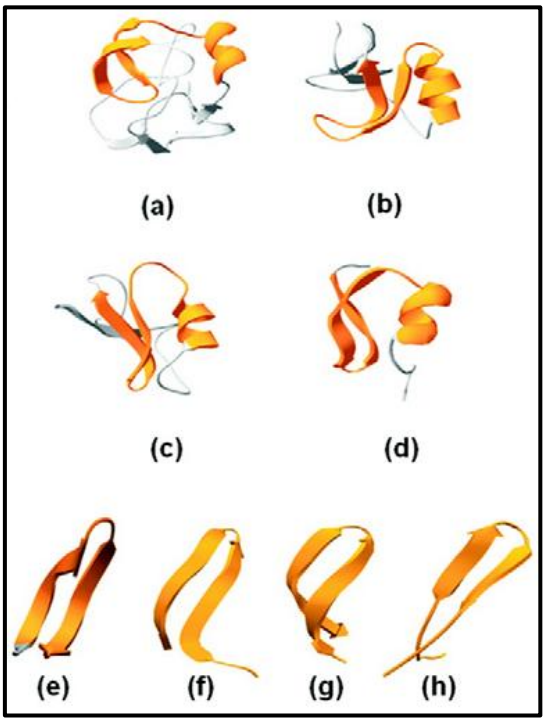

Figura 2: Similaridades Estruturais de Jaburetox-2Ec. (a) neurotoxina tipo α BMKM1 de escorpião: inibidor de canal de sódio; (b) (PDB ID: 1djt) e β-neurotoxina inibidor de canal

de Potássio; (c) (PDB ID: 1b3c) e BMKK4; (d) (PDB ID: 1s8 k). Os segmentos dos peptídeos com alta similaridade estrutural são mostradas em laranja. Para comparação, os domínios grampos β são mostrados para: Jaburetox-2Ec (e) e os peptídeos envolvidos na formação de poros/canais: protegrin-1 (f) (PDB ID: 1pg1), tachyplesin-1 (g) (PDB ID: 1wo0) and polyphemusin PV5 (h) (PDB: 1×7k). Retirada de BARROS et al., 2009).

Visando confirmar experimentalmente a importância do motivo grampo β, três mutantes do peptídeo Jaburetox foram construídos: Jbtx Δβ (mutante com deleção do grampo β), Jbtx N ter (mutante correspondente à metade N-terminal do peptídeo) e Jbtx C-ter (mutante correspondente à metade C-terminal do peptídeo, e que contem o grampo β) (MARTINELLI et al., 2014). O peptídeo com deleção do grampo β apresentou todas as propriedades biológicas da forma selvagem do peptídeo, demonstrando não ser esta a porção biologicamente ativa da molécula. Já em ensaios de injeção em *O. fasciatus* e *R. prolixus*, somente o peptídeo mutante correspondente à metade N-terminal apresentou atividade inseticida, enquanto os outros dois peptídeos foram inócuos. Contudo, Jbtx C-ter e Jbtx N-ter foram ativos quando ingeridos pelos insetos, indicando diferentes modos de ação para os peptídeos, dependendo da via de administração. Ambos os peptídeos causaram o bloqueio da junção neuromuscular da barata *Phoetalia pallida*, inibiram a secreção em túbulos de Malpighi de *R. prolixus*, além de causarem ruptura de vesículas unilamelares grandes. Estes dados sugerem que a porção N-terminal é a responsável pela atividade entomotóxica. No entanto, a região C-terminal do peptídeo contribui de forma importante na interação do Jaburetox com membranas celulares (MARTINELLI et al., 2014) (Figura 3). Comprovando a capacidade do Jaburetox de interagir com membranas, outros estudos demonstraram que o peptídeo selvagem e seus mutantes podem se inserir em bicamadas lipídicas planares e formar canais iônicos cátions seletivos. O peptídeo Jbtx N-ter é mais ativo, formando canais em membranas com potenciais negativos, enquanto que a atividade de formar canais dos outros mutantes é voltagem independente (PIOVESAN et al., 2014).

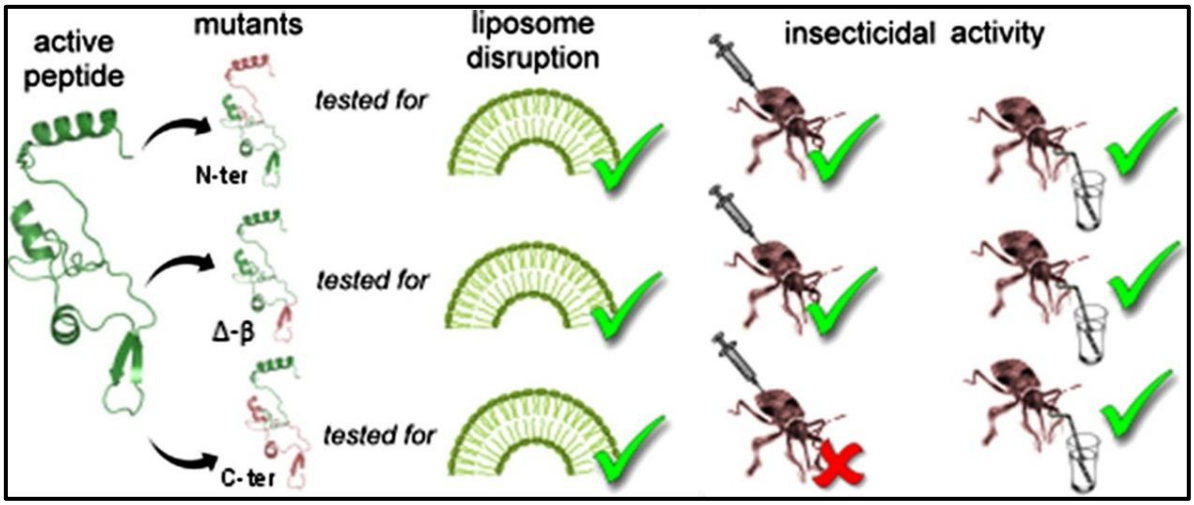

Figura 3: Efeitos dos mutantes do Jaburetox sobre LUVs e atividade inseticida pelas vias de administração injeção e ingestão. Retirada de MARTINELLI et al., 2014.

2.2.3. ATIVIDADE ANTIFÚNGICA

Canatoxina foi a primeira urease descrita por ser capaz de inibir (1 mg de proteína purificada) o crescimento radial de diversos fungos filamentosos fitopatogênicos como *Macrophamina phaseolina*, *Sclerotium rofstii* e *Colletotrichum gloesporioides* (OLIVEIRA et al., 1999). Estudos posteriores demonstraram que eSBU purificada de semente de soja inibia o crescimento e/ou germinação de esporos dos fungos filamentosos *Colletotrichum musae*, *Curvularia lunata*, *Penicillium herquei*, *Fusarium oxysporum*, *F. solani*, *Trichoderma* sp., *T. viride* e *T. pseudokoningii.* No mesmo estudo, verificou-se um espectro de ação diferenciado para a JBU (*F. solani*, *F. oxysporum*, *C. musae*, *C. lunata* e *P. herquei*) e para a urease de *H. pylori* (*P. herquei* e *C. lunata*). Estas ureases apresentavam atividade antifúngica, independente da atividade ureolítica, em concentrações de 0,27 μM (BECKER-RITT et al., 2007). Análise por microscopia eletrônica de varredura do fungo fitopatogênico *P. herquei*, após tratamento com JBU e eSBU, evidenciaram desorganização e ramificações das hifas, além de ruptura da parede celular, sugerindo assim a ocorrência de plasmólise. A urease purificada de semente de algodão (*Gossypium hirsutum*) foi fungitóxica contra os fungos *C. musae*, *C. lunata* e *P. herquei* na dose de 10 μg (MENEGASSI et al., 2008) e a apourease recombinante JBURE-IIB de *C. ensiformis* inibiu o fungo *P. herquei* (MULINARI et al., 2011).

Mais recentemente, POSTAL et al., 2012 demonstraram a atividade antifúngica de JBU sobre as leveduras *Candida parapsilosis, C. tropicalis, C. albicans, Kluyveromyces marxianus, Pichia membranifasciens* e *Saccharomyces cerevisiae* em doses de 0,18 μM. A JBU causou a inibição da proliferação das leveduras, induziu a formação de pseudo-hifas, mudanças no transporte de H^+ e no metabolismo de carboidratos, bem como permeabilização de membranas. Ainda nesse trabalho, hidrolisados de JBU foram gerados com papaína, com intuito de identificar o(s) domínio(s) antifúngicos de JBU. Os peptídeos fungitóxicos obtidos foram analisados por espectrometria de massas, identificando-se um um fragmento contendo a região N-terminal do Jaburetox. Testado para efeitos fungitóxicos, o Jaburetox foi ativo contra os fungos filamentosos *Mucor* sp. e *P. herquei* e contra as mesmas leveduras sensíveis à JBU, porém em doses mais elevadas como 9 e 18 μM, sugerindo a existência de pelo mais outra região fungitóxica na JBU, além daquela correspondente ao Jaburetox.

O grupo indiano do Dr. Karthe Ponnuraj relatou que a urease de feijão-guandu (*Cajanus cajan*) inibiu o crescimento dos fungos *Colletotrichum* sp., *C. lunata*, *Fusarium moniliforme* e *Macrophomina phaseolina* e inibiu a germinação dos esporos de *Colletotrichum* sp., *C. lunata*, *Fusarium moniliforme*, *Botrytis* sp e *F. oxysporum*. Esta urease também afetou a germinação de escleródios de *M. phaseolina* (BALASUBRAMANIAN et al., 2013).

Recentemente, evidências *in planta* da participação de uSBU na resistência da soja a fungos foram obtidas. Plantas de soja transgênicas construídas para super-expressar a uSBU apresentaram silenciamento do transgene e ainda co-supressão dos genes endógenos de urease, resultando em plantas "nulas" para urease. Ensaios com folhas dessas plantas mostraram maior susceptibilidade aos fungos *P. herquei* (patógeno de milho), *Phomopsis* sp. e *Rhizoctonia solani* (patógenos de soja). Inoculadas com o fungo biotrófico *Phakospora pachyrhizi*, responsável pela doença denominada ferrugem asiática na soja, as plantas silenciadas mostraram maior número de lesões causadas pelo patógeno. Alem disso, cultivares de soja resistentes à ferrugem asiática (PI561356) apresentaram altos níveis de expressão de uSBU após a infecção com *P. pachyrhizi*, em comparação com um cultivar susceptível (Embrapa-48). Estes dados corroboram com um possível papel de defesa de uSBU contra a infecção por fungos em soja (WIEBKE-STROHM et al., 2012).

2.2.3.1. SOYURETOX

O peptídeo Soyuretox é o equivalente ao peptídeo Jaburetox obtido a partir da urease de soja. Para a clonagem em *E. coli* foi utilizado como molde o gene da uSBU, previamente clonado em pGEX-4T-2 (MARTINELLI, 2007). Para a determinação da região equivalente ao Soyuretox, foi realizado um alinhamento das sequências de nucleotídeos do gene da urease ubíqua de soja e de JBURE-II, a partir da qual foi realizada a clonagem do Jaburetox-2Ec (MULINARI et al., 2007). Dos 101 aminoácidos do Soyuretox, 74 (71,8 %) são idênticos em ambos os peptídeos e dos 27 diferentes, 20 de 21 estão localizados na região N-terminal. Igualmente ao peptídeo Jaburetox, o Soyuretox também apresentou tendência a oligomerização (KAPPAUN, 2014).

Estudos de caracterização biológica do peptídeo foram realizados, sendo que o peptídeo recombinante apresentou atividade antifúngica contra os fungos filamentosos *P. herquei* e *C. lunata* e contras as leveduras *C. albicans, C. tropicalis* e *S.cerevisae* nas doses de 9 e 18 µM. Além disso, o Soyuretox foi superexpresso em raízes de soja do cultivar Williams 82, o qual é susceptível a nematóides. Raízes superexpressando Soyuretox exibiram uma redução significativa de 50% na presença do nematóide *Meloidogyne javanica* e de seus ovos, comparando com raízes de plantas tranformadas com o plasmídeo vazio e de plantas não transformadas. Os resultados indicam que, utilizado como um transgene, o Soyuretox confere um efeito protetor contra nematóides e fungos em plantas de soja (RECHENMACHER et al., em preparação).

2.2.4. OUTRAS PROPRIEDADES BIOLÓGICAS DE UREASES

A Canatoxina administrada intraperitonealmente a ratos e camundongos (LD_{50} 0,4-0,6 e 2-3 mg/kg, respectivamente) induziu dificuldade respiratória, convulsão e morte (CARLINI & GUIMARÃES, 1981; CARLINI et al., 1984) em até 24 horas. Em doses subconvulsivantes, a Canatoxina promoveu em ratos um aumento dos níveis plasmáticos de gonadotrofinas (RIBEIRO-DASILVA, PIRES-BARBOSA & CARLINI, 1988) e de insulina (RIBEIRO-DASILVA & PRADO, 1993), além de causar efeitos pró-inflamatórios

nos animais (BENJAMIN, CARLINI, & BARJA-FIDALGO, 1992). *In vitro*, a Canatoxina apresentou potente atividade secretagoga, em doses nanomolares, em diversos sistemas celulares isolados, incluindo agregação e secreção de plaquetas (BARJA-FIDALGO, GUIMARÃES, & CARLINI, 1991; CARLINI, GUIMARÃES & RIBEIRO, 1985), secreção de dopamina e serotonina por sinaptossomas (BARJA-FIDALGO, GUIMARAES & CARLINI, 1991), liberação de histamina por mastócitos (GRASSI-KASSISSE & RIBEIRO-DASILVA, 1992) e secreção de insulina por ilhotas pancreáticas isoladas (BARJA-FIDALGO, GUIMARAES & CARLINI, 1991a; BARJA-FIDALGO, GUIMARAES, & CARLINI, 1991). A Canatoxina inibiu o transporte de cálcio pela Ca^{2+}, Mg^{2+}-ATPase de membranas de vesículas do retículo sarcoplasmático, sem contudo inibir a hidrólise de ATP (ALVES et al., 1992) e alterou o fluxo de Ca^{2+} da membrana plasmática de plaquetas com canais de Ca^{2+} inibidos por verapamil (GHAZALEH et al., 1997). A urease de *Helicobacter pylori* (HPU) também induziu inflamação *in vivo* no modelo de edema de pata em camundongo. Adicionalmente, a HPU inibiu a apoptose e ativou neutrófilos humanos a produzir espécies reativas de oxigênio (ROS), efeitos que poderiam contribuir para a patogênese causada por *H. pylori* (UBERTI et al., 2013).

Como inicialmente descrito para a Canatoxina, outras ureases, vegetais (JBU e eSBU) ou microbianas (*B. pasteurii* e *H. pylori*) também induziram a agregação de plaquetas de coelho e de humanos (FOLLMER et al., 2004; OLIVERA-SEVERO et al., 2006; WASSERMANN et al., 2010). Ao contrário de Canatoxina, JBU não apresentou toxicidade quando injetada intraperitonealmente em camundongos (FOLLMER et al., 2001), mas ambas são ativas se administrada por via endovenosa. Além disso, Canatoxina e JBU interagem com polisialogangliosídeos (GD1b e GT1b) e sialoproteínas (mucina, tireoglobulina, fetuína) na superfície de eritrócitos e também de forma isolada (CARLINI & GUIMARÃES, 1991; FOLLMER et al., 2001).

2.3. ESTUDOS DAS PROPRIEDADES ESTRUTURAIS DE PROTEÍNAS E PEPTÍDEOS

A Biologia Estrutural encontra-se na interface entre a biologia molecular, a bioquímica e a biofísica, e tem como foco a investigação da estrutura de macromoléculas.

A partir desta, busca-se elucidar a relação entre a estrutura e a função de uma determinada molécula. Os últimos vinte anos testemunharam um grande crescimento do número de estruturas de proteínas, elucidadas com alta resolução, depositadas no Banco de Dados Protein Data Bank. Este progresso em Biologia Estrutural foi dirigido pelo desenvolvimento da Tecnologia de Expressão Recombinante de Proteínas, bem como nos avanços em metodologias, análises de dados e bioinformática. A bactéria *Escherichia coli* é o hospedeiro mais utilizado para expressar proteínas recombinantes para estudos estruturais, os quais requerem quantidades elevadas de amostra com adequado grau de pureza (WIEDEMANN, BELLSTEDT, & GO, 2013, MALUF et al., 2014). Quantidades significativas de proteína, usualmente entre 5 e 50 mg, dependendo do tamanho da proteína e da técnica experimental utilizada, são requeridas para cada projeto de biologia estrutural, independente da técnica de elucidação da estrutura utilizada, incluindo cristalografia de Raios X, RMN e criomicroscopia eletrônica (PETI & PAGE, 2007).

2.3.1. ESTRUTURAS TRIDIMENSIONAIS DE UREASES JÁ ELUCIDADAS

As estruturas tridimensionais de poucas ureases foram elucidadas até o momento. As estruturas das ureases microbianas já conhecidas são as de *Klebsiella aerogenes* (1FWJ) (JABRI et al., 1995), de *Bacillus pasteurii* (4UBP) (BENINI et al., 1999), de *Helicobacter pylori* (1E9Z) (HA et al., 2001) e de *Helicobacter mustelae* (3QGA).

Dentre as estruturas de ureases de plantas resolvidas, a primeira foi a da urease majoritária de *C. ensiformis*, JBU (3LA4) (BALASUBRAMANIAN & PONNURAJ, 2010), obtida somente 83 anos após o relato da cristalização de JBU por Sumner (SUMNER, 1926). O mesmo grupo também resolveu a estrutura da urease de feijão guandu (*Cajanus cajan*) (4G7E) (BALASUBRAMANIAN et al., 2013).

Todas as ureases tiveram suas estruturas tridimensionais elucidadas por Cristalografia de Raios X, devido à elevada massa molecular das ureases, incompatível atualmente para serem resolvidas por Ressonância Magnética Nuclear.

2.3.2. PROTEÍNAS INTRINSICAMENTE DESORDENADAS

A maioria das proteínas necessita adotar uma estrutura tridimensional definida, a fim de exercer suas funções. Isto é exemplificado pelas estruturas de diversas enzimas que precisam apresentar um determinado enovelamento, para, assim, exercer sua função, que é a catálise. Contudo, na última década foi demonstrado que grande parte dos genomas, dos mais diversos organismos, codificam proteínas que não adotam uma estrutura tridimensional definida em condições nativas e funcionais. Este grupo de proteínas é denominado proteínas intrinsicamente ou nativamente desordenadas, ou regiões de proteínas intrinsicamente desordenadas (IDPs, do inglês, intrinsically disordered proteins ou IDPRs, intrinsically disordered protein regions) (DYSON & WRIGHT, 2005; TOMPA & FERSHT, 2009; TOMPA, 2011; UVERSKY & DUNKER, 2010). A falta de uma estrutura globular rígida em condições fisiológicas, pode representar uma considerável vantagem funcional para as proteínas desenoveladas, pois sua grande plasticidade permite que elas interajam eficientemente, com alta especificidade, com diversos alvos. Além disso, uma transição de desordem/ordem induzida em IDPs, durante a ligação a alvos especificos *in vivo*, pode representar um mecanismo simples de regulação de numerosos processos celulares, incluindo regulação da transcrição e tradução, e o controle do ciclo celular (UVERSKY, 2002).

As IDPs apresentam na sua sequência de aminoácidos algumas particularidades, detectadas por algoritmos que as caracterizam como desordenadas, dentre elas, baixo número de resíduos hidrofóbicos e grande quantidade de resíduos carregados, o que pode resultar em uma elevada carga líquida (UVERSKY, GILLESPIE, & FINK, 2000). A maioria das IDPs contem poucos aminoácidos promototes de ordem como Isoleucina, Leucina, Valina, Triptofano, Fenilalanina, Tirosina, Cisteína e Asparagina, e são ricas em resíduos promotores de desordem: Ácido Glutâmico, Lisina, Arginina, Glicina, Glutamina, Serina, Prolina e Alanina (UVERSKY, 2002). IDPs possuem elevados volumes hidrodinâmicos, baixo conteúdo de estrutura secundária e são caracterizadas pela alta heterogeidade estrutural e elevada flexibilidade conformacional (UVERSKY, 2010).

As proteínas podem assumir quatro estados termodinâmicos possíveis: ordenada (ou nativa), tipo *Molten globule*, *Pre-molten globule* e tipo *Random coil*. O estado termodinâmico de uma proteína pode ser diferenciado em função do grau de enovelamento

da cadeia polipeptídica (Figura 4). A aquisição de função de uma proteína pode estar associado à uma transição entre estes estados (UVERSKY, 2002.)

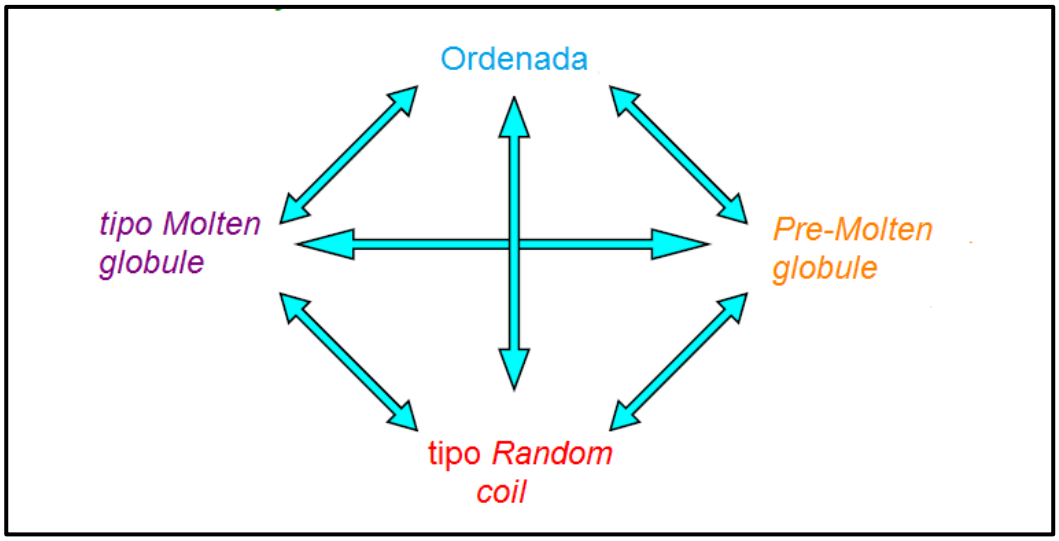

Figura 4: Proteínas podem apresentar quatro conformações das suas cadeias polipeptídicas (forma ordenada, tipo *Molten globule*, *Pre-Molten globule* e do tipo *Random coil*) definidos conforme o grau de enovelamente das moléculas. Adaptada de UVERSKY, 2002 e de ZAMBELLI, B. Aula do Curso Metodi Chimico-Molecolari per lo studio delle proteine.

Uma estratégia importante no estudo de IDPs e IDPRs tem sido o uso de algoritmos preditores de desordem, como por exemplo, os algoritmos do tipo PONDR (Predictors of Natural Disoreded Regions). Este método é vantajoso em termos de tempo e custo para estudar as proteínas desordenadas, comparados aos métodos experimentais tradicionais. Desordens estruturais também podem ser estudadas em grande detalhe por diversas técnicas experimentais e o avanço mais pronunciado foi atingido através da aplicação da técnica de Ressonância Magnética Nuclear multidimensional. Esta técnica normalmente é complementada por outras técnicas estruturais, como Espalhamento de Raios-X a baixo ângulo (SAXS) (TOMPA, 2012).

3. OBJETIVOS

3. 1. OBJETIVO GERAL

Nesta tese tivemos como objetivos gerais: 1) estudar as propriedades biológicas da proteína de fusão GST-uSBU; e 2) estudar as propriedades estruturais do peptídeo Jaburetox em solução.

3.2. OBJETIVOS ESPECÍFICOS

Capítulo I: OTIMIZAÇÃO DA PRODUÇÃO E PROPRIEDADES BIOLÓGICAS DA PROTEÍNA DE FUSÃO GST-uSBU

- Otimizar a produção da proteína de fusão GST-uSBU para a realização de estudos de suas propriedades biológicas;
- Avaliar as propriedades biológicas da proteína de fusão GST-uSBU: atividade antifúngica (fungos filamentosos e leveduras), antibacteriana, inseticida e indutora de agregação de plaquetas de coelho e de hemócitos de inseto.

Capítulo II: PROPRIEDADES ESTRUTURAIS DO PEPTÍDEO JABURETOX

- Otimizar a produção e obter o peptídeo Jaburetox estável em solução;
- Determinar a estrutura secundária por Dicroísmo Circular;
- Determinar o raio hidrodinâmico e a massa molecular por Espalhamento de Luz;
- Determinar a T_m do peptídeo em diferentes condições;
- Determinar estrutura tridimensional por Ressonância Magnética Nuclear.

4. RESULTADOS

4.1. CAPÍTULO I: OTIMIZAÇÃO DA PRODUÇÃO E PROPRIEDADES BIOLÓGICAS DA PROTEÍNA DE FUSÃO GST-uSBU

Manuscrito a ser submetido à publicação ao **Archives of Biochemistry and Biophysics**.

As regras usuais de formatação do periódico foram adaptadas para a melhor leitura do manuscrito.

Production Optimization and Biological Properties of the Fusion Protein Glutathione S-Transferase - Soybean Ubiquitous Urease

Fernanda Cortez Lopes, Anne Helene Souza Martinelli, Valquiria Broll, Marina Schumacher Defferrari, Karine Kappaun, Deise Michele Tichota, Diogo Ribeiro Demartini, Melissa Postal, Monica de Medeiros Silva, Arlete Beatriz Becker-Ritt, Giancarlo Pasquali, Célia Regina Carlini

Resumo: Ureases são enzimas níquel dependentes que catalisam a hidrólise da ureia a amônia e dióxido de carbono. A soja (*Glycine max*) produz duas isoenzimas, a urease embrião-específica (eSBU) e a urease ubíqua (uSBU). Nosso grupo demonstrou que eSBU, purificada de sementes de soja, apresenta atividade antifúngica contra fungos filamentosos fitopatogênicos, entomotoxicidade contra *Dysdercus peruvianus* e induz agregação de plaquetas de coelho. Estas propriedades de eSBU não requerem hidrólise da ureia. Neste trabalho, nosso objetivo foi investigar as propriedades biológicas da apo-uSBU fusionada a Glutationa S-Transferase (GST), que é enzimaticamente inativa. A produção da proteína de fusão foi otimizada a 5 mg por litro de cultivo, utilizando a Metodologia de Superficie de Resposta. As condições ótimas de indução foram 24 °C, 0,55 mM de IPTG e 14 h. A remoção da GST afetou a estabilidade da apo-uSBU, por isso os bioensaios foram

realizados com GST-uSBU. A proteína de fusão apresentou toxicidade contra fungos filamentosos e afetou o metabolismo secundário fúngico, aumentando ou diminuindo a produção de pigmentos por *Fusarium oxysporum* e *Penicillium herquei*, respectivamente. *Candida albicans* e *C. tropicalis* foram susceptíveis à GST-uSBU com a formação de pseudo-hifas. A proteína de fusão apresentou atividade inseticida contra *Rhodnius prolixus*, acompanhada pela agregação de hemócitos *in vivo*. A agregação de plaquetas de coelho também foi observada na presença da proteína fusionada. A atividade antibacteriana não foi observada. Portanto, uSBU apresenta as mesmas propriedades biológicas descritas para eSBU, reforçando o papel proposto para ureases de plantas em mecanismos de defesa.

Production Optimization and Biological Properties of the Fusion Protein Glutathione S-Transferase - Soybean Ubiquitous Urease

Fernanda C. Lopes[a#], Anne H. S. Martinelli[b#], Valquiria Broll[a], Marina S. Defferrari[e], Karine Kappaun[a], Deise M. Tichota[a], Diogo R. Demartini[a], Melissa Postal[a], Monica M. Silva[a], Arlete Beatriz Becker-Ritt[c], Giancarlo Pasquali[a,d], Célia Regina Carlini[a,b,e,*]

[a] Graduate Program in Cellular and Molecular Biology – Center of Biotechnology, Universidade Federal do Rio Grande do Sul, Porto Alegre, RS, CEP 91501-970, Brazil

[b] Department of Biophysics, UFRGS, Porto Alegre, RS, CEP 91501-970, Brazil

[c] Graduate Program in Cellular and Molecular Biology Applied to Health, Genetics Applied Toxicology, Universidade Luterana do Brasil – ULBRA, Canoas, RS, Brazil

[d] Department of Molecular Biology and Biotechnology, UFRGS, Porto Alegre, RS, CEP 91501-970, Brazil

[e] Instituto do Cérebro - InsCer, Pontifícia Universidade Católica do Rio Grande do Sul (PUCRS), Av. Ipiranga 6690, CEP 90610-000 Porto Alegre, RS, Brazil.

# these authors contributed equally to this work

* Corresponding author: Célia R. Carlini. Department of Biophysics & Center of Biotechnology, Universidade Federal do Rio Grande do Sul, Av. Bento Gonçalves, 9500. Prédio 43.431, Porto Alegre, RS, 91501-970, Brazil. Tel.: +55 51 3308 7606; fax: +55 51 3308 7003. E-mail address: ccarlini@ufrgs.br

ABSTRACT

Ureases are nickel-dependent enzymes that catalyze the hydrolysis of urea to ammonia and carbon dioxide. Soybean (*Glycine max*) produces two isoenzymes, the embryo-specific urease (eSBU) and the ubiquitous urease (uSBU). Our group demonstrated that eSBU, purified from soybean seeds, has antifungal properties against phytopathogenic filamentous fungi, entomotoxicity against *Dysdercus peruvianus* and induces rabbit platelet aggregation. These properties of eSBU do not require hydrolysis of urea. Here we aimed to investigate the biological properties of the enzymatically inactive apo-uSBU fused to Glutathione S-Transferase (GST). The production of the fusion protein was optimized to 5 mg per liter of culture using Response Surface Methodology. The optimal induction conditions were 24 °C, 0.55 mM IPTG and 14 h. Removal of the GST affected apo-uSBU stability, so bioassays were carried out with GST-uSBU. The fused uSBU was toxic against filamentous fungi and affected the fungal secondary metabolism, increasing or decreasing pigment production by *Fusarium oxysporum* and *Penicillium herquei*, respectively. *Candida albicans* and *C. tropicalis* were susceptible to GST-uSBU with formation of pseudo-hyphae by the treated yeasts. The fusion protein showed insecticidal activity against *Rhodnius prolixus* accompanied by *in vivo* hemocyte aggregation. Rabbit platelet also aggregated in the presence of the fused protein. No antibacterial activity was observed. Thus, uSBU displays the same biological properties described for eSBU, even fused to GST, reinforcing the proposed role of plant ureases in defense mechanisms.

Keywords: soybean ubiquitous urease, fusion protein, antifungal activity, fungal pigments, pseudo-hyphae.

Introduction

Ureases (EC 3.5.1.5, urea amidohydrolase), metalloenzymes that catalyze the hydrolysis of urea to produce ammonia and carbon dioxide, are produced by plants, fungi and bacteria, but not by animals (Follmer, 2008; Krajewska, 2009). Ureases contain two catalytically important atoms of nickel in their structures (Dixon et al., 1975), which require a set of accessory proteins to be placed in active site of the apoenzymes (Carter et al., 2009; Zambelli et al., 2011). In plants, ureases are abundant in some plant tissues, mainly seeds of some members of the families Fabaceae and Curcubitacea (Follmer, 2008). It has been postulated that these enzymes are not only involved in nitrogen bioavailability, but also in defense processes in plants (Polacco and Holland, 1993). Over the last two decades our group has demonstrated that ureases from different organisms are multifunctional proteins that display a number of biological properties unrelated to their enzyme nature, including platelet aggregating, insecticidal and antifungal activities (Carlini and Polacco, 2008).

Soybean (*Glycine max*) produces two urease isoenzymes: the embryo-specific urease (eSBU), encoded by the *Eu1* gene (GenBank accession AY230157, Phytozome accession Glyma05g27840.1), synthesized only in the developing embryo, and the ubiquitous urease (uSBU), encoded by *Eu4* gene (GenBank accession AY230156, Phytozome accession Glyma11g37250.1), present in small amounts in all plant tissues (Real-Guerra et al., 2013; Torisky et al., 1994). While the uSBU is responsible for recycling metabolically-derived urea, the role of eSBU remains elusive. Mutants lacking eSBU do not accumulate urea in any tissue and do not have any impairment on the use of urea as sole nitrogen source (Polacco and Sparks, 1982; Polacco et al., 1985; Stebbins and

Polacco, 1995; Witte et al., 2002). The SBU isoforms share 87% of identity and 92% of similarity at the cDNA level (Goldraij et al., 2003).

Soybeans are susceptible to many predators and pathogens, including insects, nematodes, fungi and viruses. These pathogens and pests, usually tissue-specific, cause damage to seeds, roots, leaves, stems and pods, and despite control measures, can reduce soybean production by almost 28 % worldwide (Oerke and Dehne, 2004). Development of new technologies to control these pests is quite urgent, and exploring plant natural compounds represents a major strategy to this end (Carlini and Grossi-De-Sá, 2002). In agreement with data obtained for other ureases, we have demonstrated that eSBU, purified from soybean seeds, display several biological properties that are independent of its ureolytic activity (Real-Guerra et al., 2013) such as the activation of rabbit blood platelets, insecticidal activity against *Dysdercus peruvianus* (Follmer et al., 2004) and also *in vitro* growth inhibition of the phytopathogenic fungi *Colletotrichum musae*, *Curvularia lunata*, *Fusarium oxysporum*, *F. solani*, *Penicillium herquei*, *Trichoderma* sp., *T. viride* and *T. pseudokoningii* (Becker-Ritt et al., 2007).

In contrast, uSBU, which occurs in such low concentrations in plant tissues that conventional purification is very difficult (Polacco & Havir, 1979), was less explored in the literature. In a recent study, soybean mutants were obtained in which silencing of the uSBU gene resulted in co-suppression of all ureases genes (Wiebke-Strohm et al., 2012). These urease-null plants were more susceptible to *P. herquei* (maize pathogen), *Phomopsis* sp. and *Rhizoctonia solani* (soybean pathogens) and to the biotrophic fungus *Phakospora pachyrhizi*, agent of the Asian rust disease (Wiebke-Strohm et al., 2012); corroborating the hypothesis that uSBU could also be involved in plant defense.

Aiming a better understanding of the roles of ureases in plants, here we describe the expression optimization of the fusion protein Glutathione-S-Transferase~ (apo)uSBU using a Response Surface Methodology and the characterization of some biological properties of this recombinant protein.

Materials and Methods

GST-uSBU expression and purification

Escherichia coli BL21-CodonPlus (DE3)-RIL (Stratagene) cells were transformed by heat shock with the construct pGEX-4T-2-*GST-uSBU* that expresses the fusion protein GST-uSBU (Martinelli, 2007). This construct contains only the structural gene of uSBU, the product is an apo-uSBU, with no nickel atoms placed in its active site, rendering it enzymatically inactive. Cells were cultured in 50 mL falcons containing 15 mL of 2-XYT medium (16 $g.L^{-1}$ tryptone, 10 $g.L^{-1}$ yeast extract, 5 $g.L^{-1}$ sodium chloride, pH 7.0), ampicillin (100 $\mu g.mL^{-1}$) and chloramphenicol (40 $\mu g.mL^{-1}$), overnight, at 37 °C and 200 rpm. Aliquots of 2 mL of the pre-inoculum were inoculated in 1 L Erlenmeyer containing 200 mL of 2-XYT medium and were incubated at 37 °C, 200 rpm until A_{600nm} reached 0.7. Then, 1 mM of IPTG (isopropyl-β-D-thiogalactoside) was added to the culture, the temperature was cooled down to 28 °C and incubated for additional 16 h at 200 rpm. Cells were centrifuged for 10 min at 10,000 x g. Cell pellets were suspended in 20 mL PBS (140 mM NaCl, 2.7 mM KCl, 10 mM Na_2HPO_4, 1.8 mM KH_2PO_4, pH 7.3) and the suspension was sonicated (20 cycles of 1 min, 20 kHz of frequency). The cells lysate was centrifuged for 40 min at 14,000 x g and supernatant was used in the affinity chromatography (Martinelli, 2007).

A column with 2 mL of Glutathione Sepharose 4B resin (GE Healthcare) was equilibrated with 40 mL PBS, according to the manufacturer´s instruction. The cell lysate supernatant was incubated with the resin by running the sample through the column 3 times. Unbound proteins were washed out with 10 mL PBS. The GST-uSBU fusion protein was eluted in 10 mL of 50 mM Tris-HCl, 10 mM reduced glutathione, pH 8.0. Samples were dialyzed against 50 mM sodium phosphate buffer, pH 7.5, 1 mM EDTA, 5 mM β-mercaptoethanol to remove the reduced glutathione and stored at 4 °C. For the bioassays the samples were concentrated by ultracentrifugation using a 30 kDa Amicon for 15 min at 4,000 x g. In order to investigate the activity of GST- uSBU truncated proteins the samples were ultra-centrifuged using a 50 kDa Amicon for 30 min at 2,500 x g, to obtain two fractions (>50 kDa and <50 kDa).

Protein concentration was measured by Bradford assay (Bradford, 1976) and the purity was checked in a 10 % SDS-PAGE.

Recombinant Glutathione-S-Transferase (rGST) Production and Purification

rGST, used as control in the biological tests, was produced by culturing *E. coli* cells carrying the empty vector pGEX-4T-2-*GST*. The conditions of induction were: 37 °C, 1 mM of IPTG for 3 h. The purification of rGST was performed using the same protocol above (Martinelli, 2007).

Western blot analyses

Western blot analyses were performed according to (Towbin et al., 1979). Briefly, proteins were electrophoresed, transferred by gravity from 10 % SDS-PAGE to PVDF membranes (Hybond-P, GE). The membranes were blocked with 5% casein in Tris

buffered saline (TBS), washed, incubated with rabbit anti-Jaburetox-2Ec (Jaburetox 2Ec is a recombinant peptide derived from *Canavalia ensiformis* urease; Mulinari et al., 2007) polyclonal antibody (1:7,500) or mouse anti-GST monoclonal antibody (1:2000) (donated by Dr. Henrique Bunselmeyer Ferreira, Centre of Biotechnology, UFRGS) for 2 h at room temperature. After washing with TBS, the membranes were then exposed to anti-rabbit IgG (1:20,000) alkaline phosphatase conjugate (Sigma Chem. Co.) or anti-mouse IgG (1:20,000) alkaline phosphatase conjugate (Sigma Chem. Co.), respectively. The colorimetric detection was carried out by using 5-bromo-4-chloro-3-indolyl-phosphate p-toluidine salt and nitro-blue tetrazolium chloride. Jack bean urease (*Canavalia ensiformis*) was used as positive control (Urease type C-III Sigma Aldrich) and Bovine Serum Albumin (BSA, Sigma Aldrich) as a negative control.

Mass Spectrometry

GST-uSBU band (120 kDa) was excised and minced in small pieces. Digestion was performed according to Martinelli et al. (2014). Peptides generated were subjected to reversed phase chromatography (NanoAcquity UltraPerformance LC®-UPLC®, Waters, Milford, United States) in a Nanoease C18, 75 mm ID at 35 ^{O}C. The column was equilibrated with 0.1% trifluoroacetic acid (TFA) and the peptides were eluted in 20 min gradient, ramping from 0 to 60% ACN in 0.1% TFA at 0.6 nL/min constant flow. Eluted peptides were subjected to electro spray ionization and analyzed by mass spectrometry using a Q-TOF Micro™ spectrometer (Micromass, Waters, Milford, United States). The voltage applied to the cone for the ionization was 35 V. The three most intense ions in the range of m/z 200–2000 and +2 or +3 charges were selected for fragmentation. The acquired MS/MS spectra were processed using Proteinlynx v.2.0 software (Waters,

Milford, US) and the generated .mgf files were used to perform database searches using the MASCOT software (version 2.4.00) (Matrix Science, London, UK) against the NCBI database, restricting the organism to "*Glycine max* (taxid:3847)", november 2012. Tripsin/P was selected as enzyme. Search parameters allowed a maximum of one missed cleavage, the carbamidomethylation of cysteine, the possible oxidation of methionine, peptide tolerance of 1.2 Da, and MS/MS tolerance of 1.2 Da. A minimum of two unique non overlapping peptides was defined as a criterium for protein match.

Urease activity

E. coli BL21 RIL expressing GST-uSBU were grown 24 h at 37 ºC in LB agar plates containing 100 $\mu g.mL^{-1}$ ampicillin, 40 $\mu g.mL^{-1}$ chloramphenicol, 1 mM IPTG, 100 μM $NiCl_2$, 0.35 $mg.mL^{-1}$ cresol red and 60 $mg.mL^{-1}$ urea. Alkalization due to urease activity results in a reddish color around the colonies (Gee et al., 1999).

Expression Optimization of the recombinant GST-uSBU

In order to determine the best conditions of GST-uSBU expression, the effects of the temperature, IPTG concentration and time of induction on the protein yield were evaluated using a 2^3 experimental model with 5 replicates of the central point, resulting in 19 experiments (Table 1). In the statistical model, the coded variables corresponded to temperature (X_1), IPTG concentration (X_2) and time (X_3), which were the independent variables, while the protein concentration (Y) was the dependent variable (Haaland, 1989). The software Statistica version 6.0 (Statsoft Inc., Tulsa, Okla, USA) was used in the regression analysis of experimental results. The quality of fit of the first-order model

equation was expressed by R^2, the coefficient of determination, and its statistical significance was determined by F-test (Fischer's F Test).

The optimization of protein production was performed in 2-XYT medium (25 mL of the medium in 125 mL Erlenmeyer flask), ampicillin (100 $\mu g.mL^{-1}$) and chloramphenicol (40 $\mu g.mL^{-1}$). *E. coli* was cultured at 37° C, 200 rpm up to an OD_{600nm} 0.7 and then induced with IPTG. Cells were harvested by centrifugation, suspended in PBS, and disrupted by sonication (five shorts bursts, 30 s each on ice). The lysed cells were centrifuged at 12,000 x g for 25 min, and the supernatant was further analyzed.

GST-uSBU quantification by Enzyme-Linked Immunosorbent Assay (ELISA)

The concentration of GST-uSBU in supernatants was quantified by ELISA. Aliquots of cell lysate supernatants (50 µL) were adsorbed onto ELISA plates, overnight at 4 °C. After blocking the wells with 50 µL 5% casein in TBS solution for 2 h, 3 washes were performed with TBS, then 50 µL of the primary antibody anti Jaburetox 2Ec (1:500) in 2% casein-TBS were added to each well. After 2 h, the wells were washed again and further incubated for 2 h with 50 µL of the secondary anti-rabbit IgG antibody conjugated with alkaline phosphatase (1: 10,000) (Sigma Chem. Co.) in 2% casein-TBS. The color reaction was developed with 50 µL of 1 mM p-nitrophenylphosphate, 10 mM sodium borate, 0.25 mM $MgCl_2$, pH 9.8. Absorbances were determined on a SpectraMax M3 (Molecular Devices) plate reader at 405 nm. The concentration of the fusion protein was calculated using a standard curve prepared with the purified fusion protein (0.01-1 µg). The results were expressed in $mg.L^{-1}$.

Table 1: Experimental design and results of the 2^3 factorial design.

Run	X_1 Temperature (°C)	X_2 IPTG (mM)	X_3 Time of induction (h)	Y_1 GST-uSBU concentration ($mg.L^{-1}$)
1	(-1) 20	(-1) 0.28	(-1) 5.20	0.921
2	(1) 28	(-1) 0.28	(-1) 5.20	0.000
3	(-1) 20	(1) 0.82	(-1) 5.20	0.021
4	(1) 28	(1) 0.82	(-1) 5.20	0.000
5	(-1) 20	(-1) 0.28	(1) 14.76	0.000
6	(1) 28	(-1) 0.28	(1) 14.76	1.066
7	(-1) 20	(1) 0.82	(1) 14.76	0.000
8	(1) 28	(1) 0.82	(1) 14.76	2.653
9	(-1.68) 18	(0) 0.55	(0) 9.98	3.564
10	(1.68) 30	(0) 0.55	(0) 9.98	0.099
11	(0) 24	(-1.68) 0.10	(0) 9.98	4.254
12	(0) 24	(1.68)1.00	(0) 9.98	3.061
13	(0) 24	(0) 0.55	(-1.68) 2.00	2.927
14	(0) 24	(0) 0.55	(1.68) 18.00	3.477
15	(0) 24	(0) 0.55	(0) 9.98	5.362
16	(0) 24	(0) 0.55	(0) 9.98	5.522
17	(0) 24	(0) 0.55	(0) 9.98	5.056
18	(0) 24	(0) 0.55	(0) 9.98	5.367
19	(0) 24	(0) 0.55	(0) 9.98	5.267

Antifungal Assays

The filamentous fungi *Colletotrichum musae*, *Curvularia lunata*, *Fusarium oxysporum*, *Rhizoctonia solani* and *Trichoderma viride* were donated by Dr. José Tadeu Abreu de Oliveira from the Department of Biochemistry and Molecular Biology, Universidade Federal do Ceará, CE, Brazil and Dr. Lidia Fiuza, Universidade do Vale dos Sinos, São Leopoldo, RS, Brazil. *Penicillium expansum* M-02 was donated by Dr. Isa Beatriz Noll from the Laboratory of Toxicology, Food and Science Technology Institute, Universidade Federal do Rio Grande do Sul, RS, Brazil. *Cercospora chevalier*, *Fusarium lateritium*, *Mucor* sp., *Penicillium herquei*, *Phomopsis* sp., *Pythium oligandrum* and the yeasts *Candida parapsilosis* (CE002), *Candida tropicalis* (CE017), *Candida albicans* (CE022), *Kluyveromyces marxiannus* (CE025), *Pichia membranifaciens* (CE015) and *Saccharomyces cerevisiae* (1038) were kindly provided by Dr. Valdirene Gomes from the Laboratory of Physiology and Biochemistry of Microorganisms, Center of Bioscience and Biotechnology, Universidade Estadual do Norte Fluminense, Campos dos Goytacazes, RJ, Brazil.

Antifungal activity against filamentous fungi and yeasts was assayed according to (Postal et al., 2012) with minor modifications. Briefly, filamentous fungi were cultured on Potato Dextrose Agar at 28 °C until sporulation. Spores were washed with sterile distilled water, quantified in a Neubauer chamber, and 10^6 spores.mL^{-1} were inoculated in 96 wells flat bottom plates, containing GST-uSBU or rGST at 2 µM (considering the monomeric form of the proteins) final concentration in Potato Dextrose Broth. GST-uSBU and rGST were dialyzed previously against Tris-HCl buffer 10 mM, pH 7.0. The dialysis buffer was used as negative control and 0.1% hydrogen peroxide (H_2O_2), as a positive control. The

plates were incubated at 28 °C and monitored turbidimetrically at 620 nm at 24 h intervals for 48 h.

Yeasts were cultured in Sabouraud Agar for 24 h at 28 °C. Cells were washed with saline solution (NaCl 0.85 %) and quantified in a Neubauer chamber. Samples at 2 μM were incubated with 10^4 cells.mL^{-1} of each yeast in U-bottom microplates, in Sabouraud Broth at 28 °C for 24 h. Controls were the same as above. After 24 h of incubation, 20 μL of each well content were 10-fold serially diluted in saline and plated in Sabouraud agar (drop plate method) to determine the number of Colony Forming Units (CFU) after 24 h at 28 °C. Three independent bioassays with triplicated groups were carried out. Results shown are means ± standard deviations.

Evaluation of yeast cell permeability

The permeabilization of the plasma membrane was assessed with the fluorescent dye SYTOX Green (Invitrogen, Grand Island, NY, USA) as described by Postal et al. (2012). This dye forms a fluorescent complex with nucleic acids, entering cells when the integrity of their plasma membrane is compromised. Fungal cells were incubated with the test samples for 24 h and then exposed to 0.2 M SYTOX Green for 30 min at room temperature. The cells were observed under a microscope (Axioskop 40 – Zeiss) equipped with a filter for fluorescence detection (excitation wavelength 450–490 nm and emission 500 nm).

Antibacterial activity

Bacillus cereus ATCC 14579 was donated by Dr. Adriano Brandelli, Laboratory of Biochemistry and Applied Microbiology, Food and Science Technology Institute,

Universidade Federal do Rio Grande do Sul, RS, Brazil. *Escherichia coli* ATCC 25922, *Staphylococcus aureus* ATCC 25923, *Pseudomonas aeruginosa* ATCC 27853 were kindly provided by Pharmacist Elaine Staatlander, Hospital Presidente Vargas, Porto Alegre RS, Brazil. Bacteria were inoculated in 5 mL Luria Bertani (LB) broth, at 37 °C, overnight. The cultures were diluted with LB broth until 0.5 McFarland scale (corresponding to 10^8 CFU.mL^{-1}) then added to 96 wells flat plates and incubated at 37 °C for 24 h. The dialysis buffer was used as negative control and 0.1% hydrogen peroxide (H_2O_2), as a positive control. After 24 h of incubation, 20 µL of each well were 10-fold serially diluted in saline and plated in LB agar (drop plate method) to determine the number of Colony Forming Units (CFU) after 24 h at 37 °C (Pompilio et al., 2011, with modifications). Three independent bioassays with triplicated groups were carried out. Results shown are means ± standard deviations.

Insecticidal Activity and in vivo hemocyte aggregation in Rhodnius prolixus

Fifth instars *Rhodnius prolixus* (insect's mean weight 50 mg) were kindly provided by Dr. Hatisaburo Masuda and Dr. Pedro Oliveira (Institute of Medical Biochemistry, Universidade Federal do Rio de Janeiro, RJ, Brazil) and by Dr. Denise Feder (Universidade Federal Fluminense, RJ, Brazil). Samples were injected into the hemocoel of *R. prolixus* using a Hamilton Microliter 900 series syringe (Hamilton). Groups of 5 insects were injected with GST-uSBU or rGST (0.05 µg. mg^{-1} of insect body weight), prepared in *R. prolixus* saline (NaCl 150 mM, KCl 8.6 mM, $CaCl_2$ 2.0 mM, $MgCl_2$ 8.5 mM, $NaHCO_3$ 4.0 mM, glucose 34.0 mM, HEPES 5.0 mM, pH 7.0 (Lane et al., 1975). In the control group 5 insects were injected with *R. prolixus* saline previously used as the dialysis buffer while preparing the proteins (Martinelli et al., 2014). The insects were

observed for 96 h, lethality being recorded at 24 h interval. Two independent bioassays were carried out. Results shown are means ± standard errors.

Hemocyte aggregation was performed according to (Defferrari et al., 2014). Unfed insects were injected into the hemocoel with GST-uSBU or rGST diluted in *R. prolixus* saline to a final dose of 6 μg protein per insect. Control insects were injected solely with saline. Six hours after injection, the insects had their surface sterilized by immersion in 70% ethanol and hemolymph was collected from a cut in one of the legs. Hemolymph samples were immediately diluted in cold anticoagulant solution (EDTA 10 mM, glucose 100 mM, NaCl 62 mM, sodium citrate 30 mM, citric acid 26 mM, pH 4.6) at a ratio of 1:5 (anticoagulant: hemolymph). The number of cells and aggregates (defined as a cluster of nine or more cells) in the samples was then determined by counting in a Neubauer chamber. Three independent bioassays were carried out. Results shown are means ± standard errors.

Rabbit Platelet Aggregation

The methods described in (Follmer et al., 2004) and (Wassermann et al., 2010) were followed. Briefly, platelet-rich plasm (PRP) was prepared from rabbit blood collected from the ear central artery in the presence of sodium citrate (0.313 % v/v, final concentration). Blood was centrifuged at 200 x g for 20 min, at room temperature, to give a PRP suspension. Platelet aggregation was monitored turbidimetrically using a Lummi-Aggregometer (Chrono-Log Corporation, Havertown, PA, USA). PRP (300 μL) was pre-incubated for 2 min at 37 °C, with constant agitation and then the test sample (30 μL) was added: GST-uSBU at 275 nM and 800 nM final concentrations, rGST, 800 nM. Positive controls were ADP (20 μM) and Collagen 20 $mg.mL^{-1}$ (Sigma Chem. Co.).

For fluorescence microscopy, Fluorescein isothiocyanate (FITC)-labeled GST-uSBU was prepared according to manufacturer's instructions. Rabbit PRP was incubated with 800 nM FITC-GST-uSBU, under vortex stirring for 5 min at room temperature. Platelets aggregates were recovered by centrifugation, the pellets were smeared on glass slides and observed under a Zeiss Axioskop 40 – Zeiss) fluorescence microscopy (Wassermann et al., 2010).

Statistical analysis

The results were submitted to analysis of variance (ANOVA) and the significance of differences among means was determined by the Tukey test, with $p \leq 0.05$ considered statistically significant. The analyses were performed with the software GraphPad Prism 5.0.1. for Windows.

Results

GST-uSBU production and purification

Initially we obtained 2 mg of the fusion protein per one liter of culture. Fractions of the purification steps are shown in Fig. 1. Together with the intense band of the fusion protein of ~ 120 kDa (uSBU: 90 kDa and rGST: 26 kDa), other bands of smaller masses could be seen in the gel. Since these bands were also eluted from the affinity column, they probably represented GST fused to truncated (incompletely translated) uSBU (the construct has GST fused on the N-terminal region of urease). Part of the trucated GST-uSBU was successfully removed by ultrafiltration in 30 kDa membranes (fig.1, lane 4).

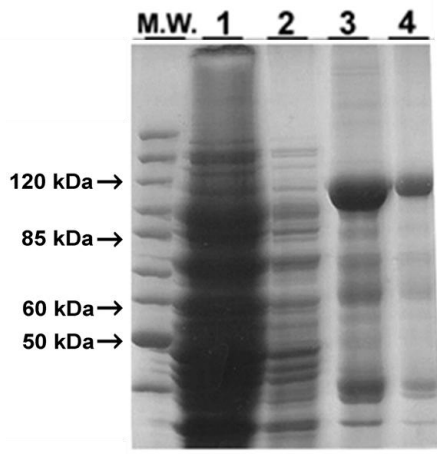

Fig. 1. 10 % SDS-PAGE of purification steps using Glutathione Sepharose resin. M.W. Molecular ladder marker; Lane 1: crude extract; Lane 2: Unbound fraction; Lane 3: Eluted fraction; Lane 4: Sample after concentration in a 30 kDa cut off membrane.

Western Blot and Mass Spectrometry Analyses

In order to exclude the presence of contaminants after the purification, we performed Western Blot analyses (Fig. 2). The smaller mass proteins reacted with both the anti-Jaburetox 2Ec (confirming they are uSBU fragments) and the anti-GST antibodies.

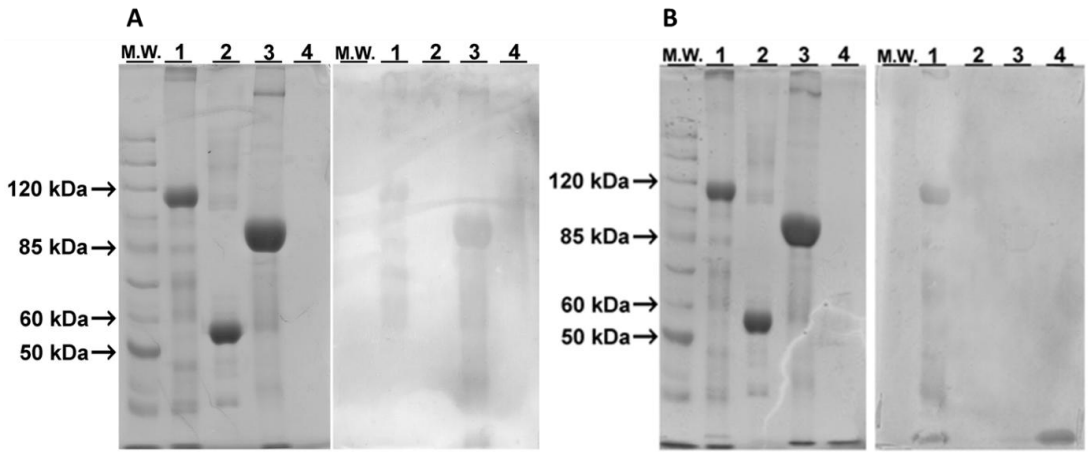

Fig. 2. 10 % SDS – PAGE (left) and Western blot (right). Panel (A) anti-Jaburetox (1: 7,500): M.W. Molecular ladder marker, Lane 1: uSBU–GST; Lane 2: BSA; Lane 3: JBU, Lane 4: rGST. Panel (B) anti-GST (1: 8,000): M.W. Molecular ladder marker, Lane 1:

uSBU–GST; Lane 2: BSA; Lane 3: JBU, Lane 4: rGST. Samples of 12 μg of each protein were applied to the gels.

Additional confirmation of the identity of fused protein was obtained by mass spectrometry of the major band (~120 kDa band) seen in the gel. The data showed 20 % of coverage of soybean ubiquitous urease sequence (Fig. S1), confirming the identity of uSBU.

Expression Optimization - Experimental Design

The analysis of the effects of three independent variables (temperature, IPTG concentration and time after induction) on the expression yield was performed. The conditions used and the concentration of GST-uSBU in the 19 experiments are shown in Table 1. The central point conditions were the most favorable: 24 °C, 0.55 mM of IPTG and approximately 10 h, increasing the yield of GST-uSBU to more than 5 mg per liter of culture (Fig. 3 and Table 1). For convenience, we chose induction for 14 h (overnight) which also fitted in region of optimal production of the surface response curve (Fig. 3B and 3C).

The equation 1 (Eq. 1) describes the yield (protein concentration) of GST-uSBU according to the independent variables.

(Eq. 1): Y (protein concentration) = $5.40 – 0.22X_1 -1{,}70X_1^2 – 1.05\ X_2^2 + 0.27\ X_3 – 1.21\ X_3^2 + 0.31\ X_1X_2 + 0.58\ X_1X_3 + 0.32\ X_2X_3$

Table 2 shows the effect of the independent variables on GST-uSBU production. The linear effect of the time of induction, within the time frame of 5.20 h to 14.76 h, was the most expressive variable, increasing in 0.54 $mg.L^{-1}$ the concentration of GST-uSBU. The increase of temperature from 18 °C to 30 ° C (quadratic) or from 20 °C to 28 °C (linear) decreased the protein expression in 3.41 $mg.L^{-1}$ and 0.45 $mg.L^{-1}$, respectively. The increase in the concentration of IPTG from 0.10 mM to 1.0 mM (quadratic) also decreased the protein expression in 2.11 mg. L^{-1}.

Table 2: Main effects and interaction analysis for GST-uSBU production

Factors	Effect (GST-uSBU concentration)	Standard error	*t* value	*p* value
Mean	5.42238	0.076022	71.3266	0.000000*
Temperature (L)	-0.44621	0.092155	-4.8419	0.008388*
Temperature (Q)	-3.40822	0.092279	-36.9338	0.000003*
IPTG (L)	-0.19308	0.092155	-2.0951	0.104226
IPTG (Q)	-2.11428	0.092279	-22.9118	0.000021*
Time (L)	0.54248	0.092155	5.8866	0.004163*
Time (Q)	-2.43706	0.092279	-26.4097	0.000012*
Temperature X IPTG	0.62175	0.120353	5.1661	0.006670*
Temperature X Time	1.16525	0.120353	9.6819	0.000637*
IPTG X Temperature	0.62175	0.120353	5.1661	0.006670*

Software Statistica, L: Linear, Q: Quadratic, confident level of 95 % and R^2 of 0.75.

* Significant factors, $p < 0.05$

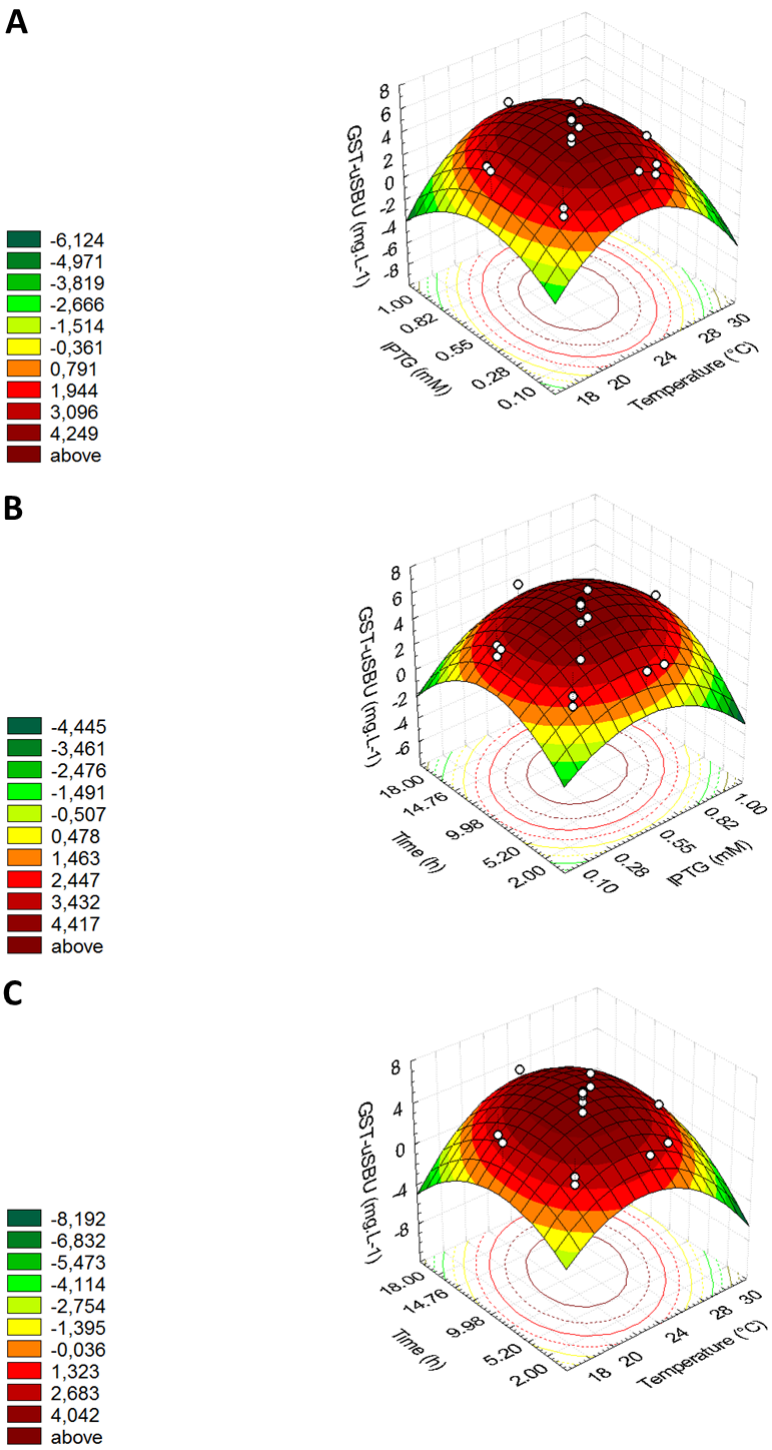

Fig. 3. Response surfaces for GST-uSBU production as a function of (A) IPTG concentration and temperature, (B) time and IPTG concentration, (C) time and temperature.

The ANOVA of the regression model showed its significance with a calculated F value of 4.13, higher than the tabulated F value 3.23, for a significance level of 95 %. Therefore, the model is considered significant.

Biological characterization of GST-uSBU

Urease activity

The fusion protein GST-uSBU is not competent for urea hydrolysis. No enzymatic activity of the purified GST-uSBU was detected by (Martinelli, 2007) using the Phenol-Hypochlorite method. Accordingly no change in coloration of the urea segregation agar was seen after a 24 h culture of GST-uSBU expressing *E. coli*. The lack of enzymatic activity reflects the fact that only the structural gene was cloned in the construct pGEX-4T-2-*GST-uSBU*. The genes for the accessory proteins were not included in the construct (Martinelli, 2007).

Antifungal activity

The effect of GST-uSBU on the fungal growth was evaluated. *C. lunata*, *F. lateritium*, *F. oxysporum*, *P. expansum*, *P. herquei* and *T. viride* were susceptible to the fusion protein at 2 μM concentration (Fig. 4). rGST alone also showed some antifungal effect after short incubation times but much less pronounced than that observed for the fusion protein. In order to investigate whether GST truncated proteins observed in SDS-PAGE (Fig. 1) could also be active against fungi, the samples were ultrafiltrated in a 50 kDa cutoff device. Only the fraction with molecules of >50 kDa retains antifungal effect against *C. tropicalis*, demonstrating that peptides and/or proteins smaller than 50 KDa are not active (Fig S2).

Besides the inhibition, changes in the pigment production by the fungi *P. herquei* and *F. oxysporum* was also observed (Fig. 5). Usually *P. herquei* produces high amounts of red pigments that diffuse to the potato dextrose agar; *F. oxysporum*, on the other hand, produces small amounts of purple pigments in the same culture medium. The inhibition of the red pigmentation in the diffusion agar experiments was also observed for *P. herquei* treated with eSBU purified from seeds (Martinelli, 2004). No changes in the pigmentation were seen for the negative control or rGST-treated fungi.

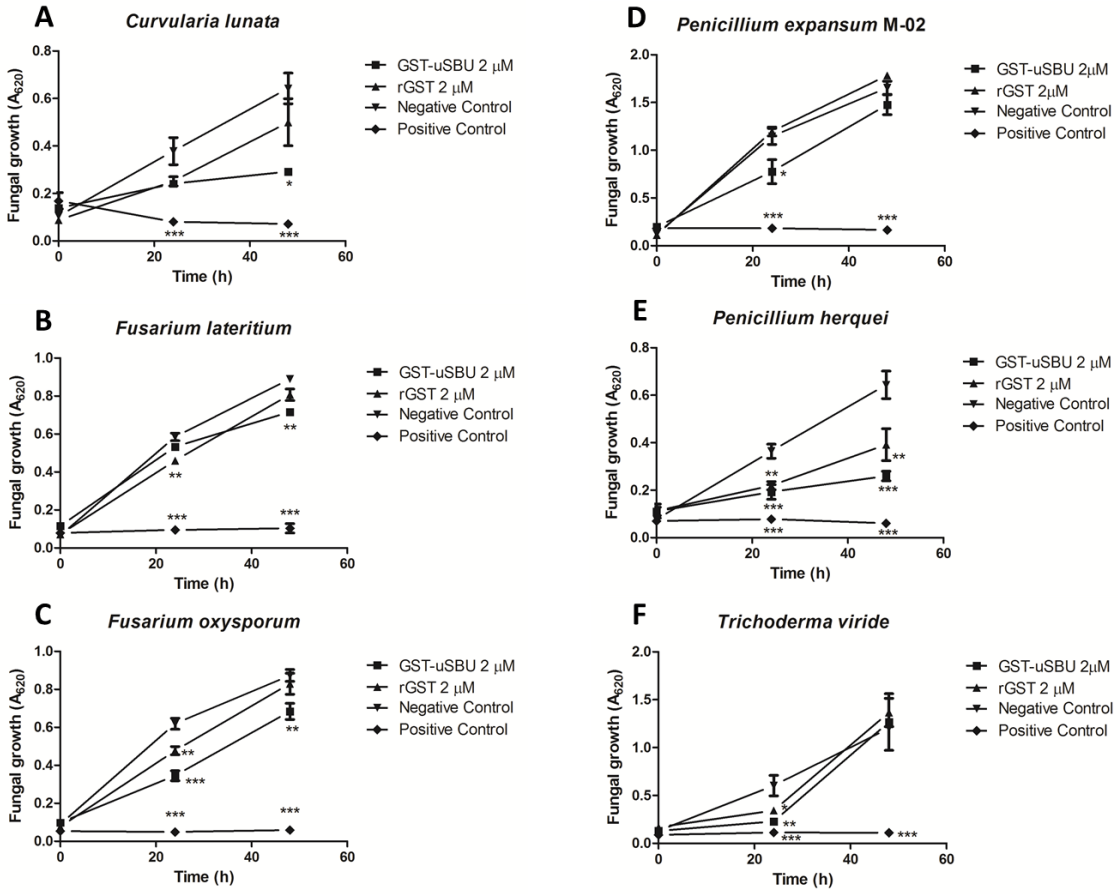

Fig. 4. Effect of GST-uSBU on fungal growth. Spores (10^6 spores.mL^{-1}) were incubated on 96-wells plates containing Potato Dextrose Broth, with 2 μM GST-uSBU; 2 μM rGST (negative control) or 0.1 % hydrogen peroxide (positive control). The incubation was

performed for 48 h, at 28 °C and fungal growth was estimated at 24 h intervals (absorbance at 620 nm ($A_{620\ nm}$). N= 3, * p≤ 0.050, ** p≤ 0.020, *** p ≤ 0.0001.

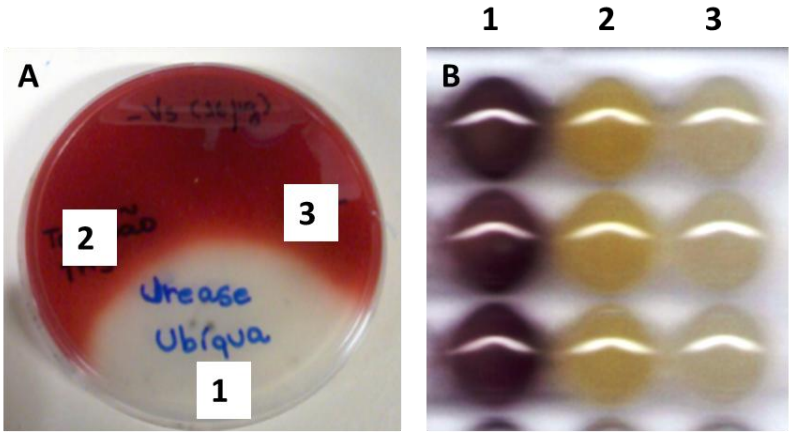

Fig. 5. Effect of GST-uSBU on the pigmentation of (A) *Penicillium herquei* and (B) *Fusarium oxysporum*. (1) GST-uSBU; (2) Negative Control (Tris-HCl buffer 10 mM, pH 7.0); (3) rGST.

The effect of GST-uSBU on yeast growth was also evaluated. The susceptible yeasts were *Candida albicans* and *C. tropicalis* (Fig. 6). rGST was not fungitoxic against the tested yeast at the same dose.

The yeast cell permeability after incubation with GST-uSBU was evaluated using the fluorescent dye SYTOX Green. A weak fluorescence was observed under dark field for *C. tropicalis* and also for *P. membranifasciens*, despite the fact that no growth inhibition was seen for the last yeast with the 2 μM dose of the fusion protein (Fig. 7). Pseudo-hyphae formation in GST-uSBU-treated *C. tropicalis* (Fig 7A) and *P. membranifasciens* was observed (Fig 7C). JBU also induced pseudo-hyphae formation in yeasts (Postal et al., 2012). Figure 8 illustrates macroscopic changes in the phenotype of *C. albicans* after exposition to the fusion protein. According to (Radford et al., 1994), the regular extreme-

jagged shaped colonies observed for GST-uSBU-treated *C. albicans* are indicative of a nearly pure culture of pseudo-hyphae yeasts, supporting the microscopic observations for the other yeast species seen in Fig.7.

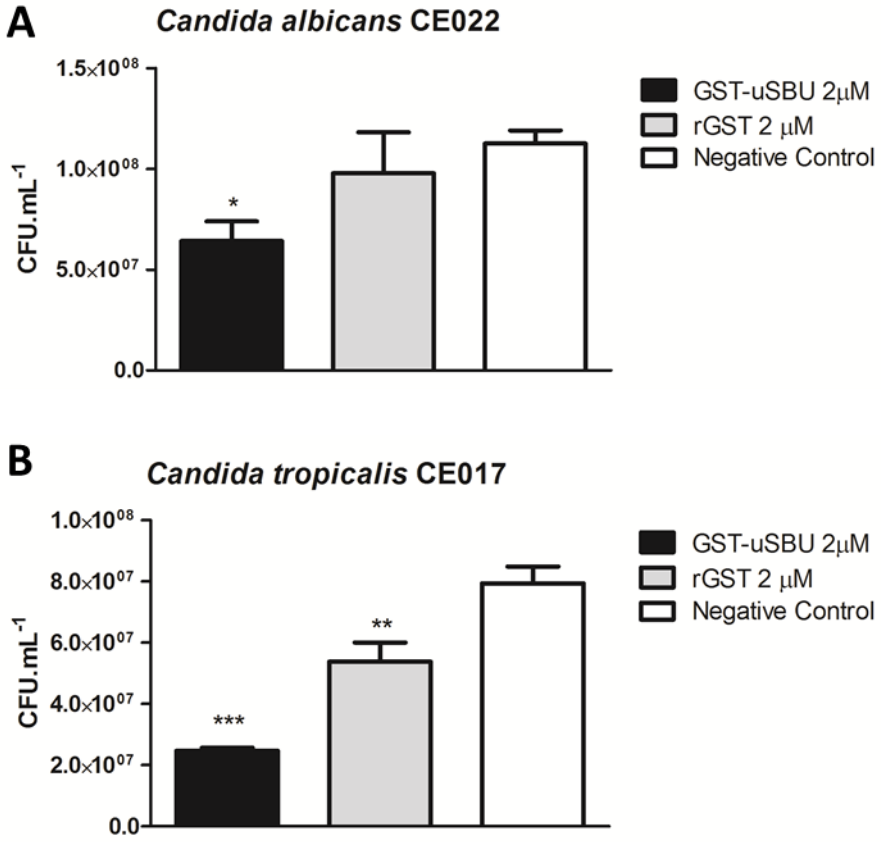

Fig 6. Colony Forming Unit (CFU) assay of yeasts. 10^4 cells.mL^{-1} were incubated on U-shaped 96-wells plates containing Sabouraud Broth, with 2 μM GST-uSBU, 2 μM rGST, Tris-HCl buffer 10 mM, pH 7.0 (negative control) or 0.1 % hydrogen peroxide (positive control). The incubation was performed for 24 h, at 28 °C and after that, the CFU was determined for each yeast. N=3, * $p \leq 0.0475$, ** $p \leq 0.0121$, *** $p \leq 0.0001$.

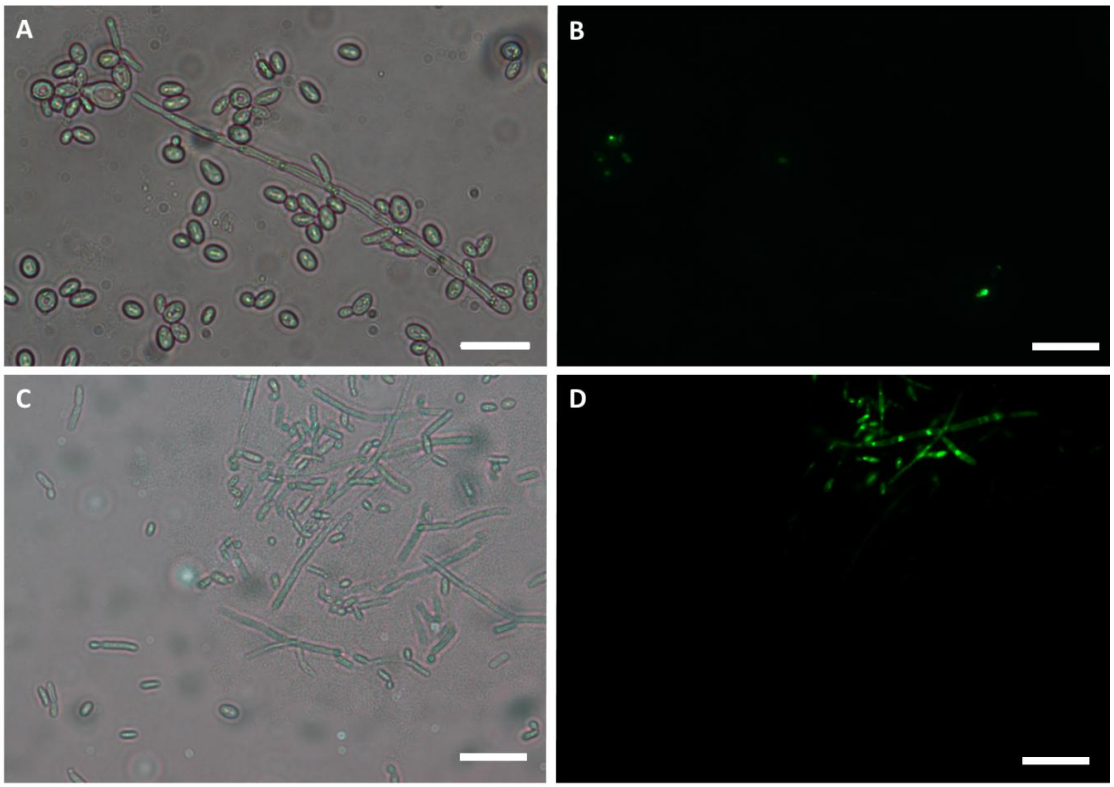

Fig 7. Fluorescence microscopy of *C. tropicalis* (A and B) and *P. membranifasciens* (C and D) treated cells with GST-uSBU 2 µM and SYTOX Green. A and C correspond to the Bright Field and B and D correspond to the Dark Field. Bars correspond to 20 µm. Typical results are shown.

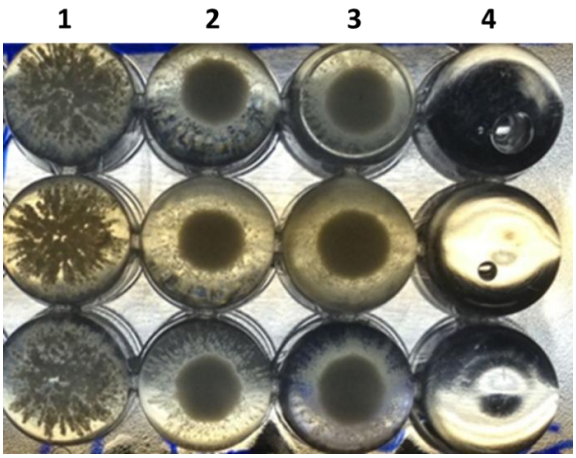

Fig 8. Changes in phenotype of GST-uSBU treated *C. albicans* (1) after 24 h incubation with 2 μM GST-uSBU (1). This change was not observed in: Negative Control (2), Tris-HCl buffer 10 mM, pH 7.0, 2 μM rGST (3) and Positive Control (4, H_2O_2). The photo shows microplate wells seen from their bottom. Typical results are shown.

Antibacterial activity

No antibacterial activity of GST-uSBU against *P. aeruginosa*, *E. coli* and *S. aureus* was observed at 2 μM. On the other hand, *B. cereus* was susceptible to GST-uSBU and also to rGST. This fact suggests that the antibacterial molecule, in this case, is rGST and not uSBU (Fig S3).

Insecticidal activity

A survival rate of 26 % was obtained for *R. prolixus* 96 h after injection of a dose of 0.05 $\mu g.mg^{-1}$ GST-uSBU (Fig. 9). rGST showed no deterrent effect when injected into the insects. This result indicates that GST-uSBU shares the entomotoxic properties observed for eSBU and jack bean ureases (Stanisçuaski and Carlini, 2012).

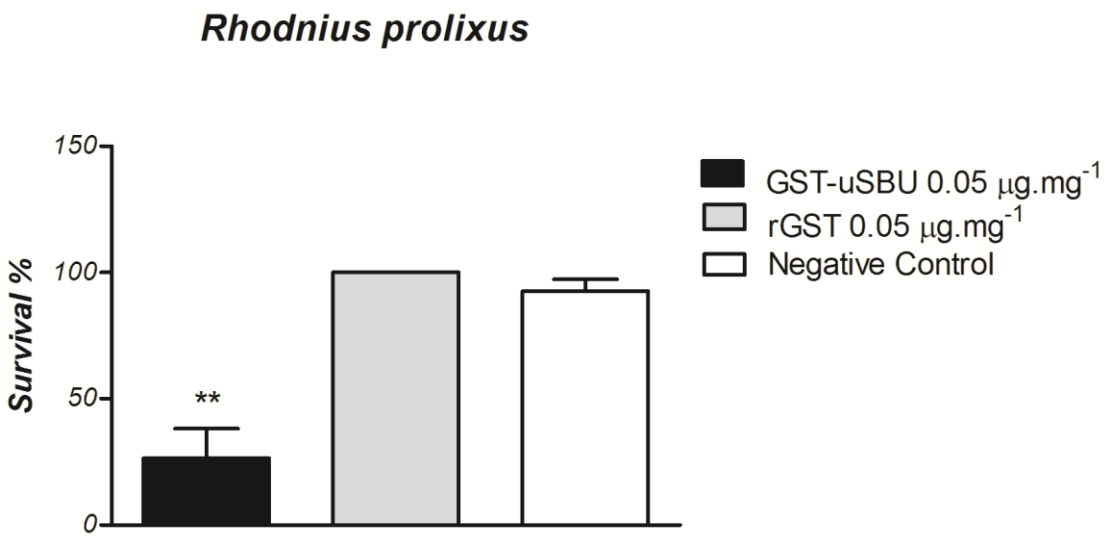

Fig. 9. Insecticidal effect of GST-uSBU on fifth instar *R. prolixus* 96 h after of hemocoel injection. No lethality was seen in the insects injected with rGST. A group of insects was injected with *R. prolixus* saline as negative control. N=5 per group, ** $p \leq 0.0014$.

Hemocytes and rabbit platelet aggregation

The presence of aggregated hemocytes in the *R. prolixus* hemolymph was evaluated 6 h after hemocoel injection of 6µg of GST-uSBU, rGST or saline. Aggregates were observed only in the hemolymph of GST-uSBU treated-insects (more than 200 aggregates per µL of hemolymph) (Fig. 10), indicating that the fusion protein displays this same entomotoxic effect described for JBU (Defferrari et al., 2014). Again, rGST was inactive.

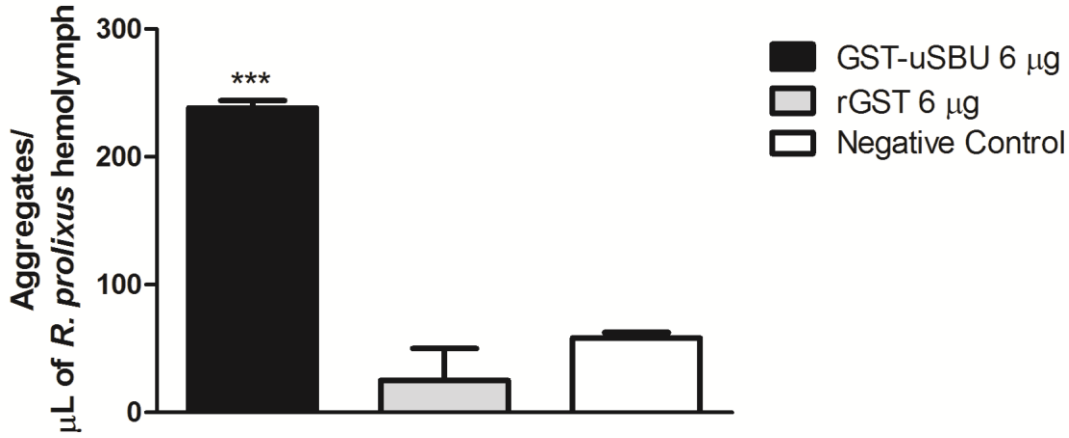

Fig.10. *In vivo* hemocyte aggregation induced by GST-uSBU. *R. prolixus* were injected with GST-uSBU or rGST (both, 6 µg per insect) or saline, as negative control. After 6 h, the hemolymph was collected and the aggregates were quantified using a Neubauer chamber. N=3, *** $p \leq 0.0001$.

Rabbit platelets were also activated by GST-uSBU in the concentrations of 275 nM and 800 nM (Fig. 11A). rGST at 800 nM did not cause platelet aggregation. FITC-labeled GST-uSBU was used to visualize platelets aggregates induced by the fusion protein (Fig 11B). As demonstrated by (Wassermann et al., 2010), the residual erythrocytes (indicated by an arrow in the bright field) Fig. 11B1 present in PRP were fluorescent in the dark field (Fig 11B2), indicating that GST-uSBU interacted only with the platelets.

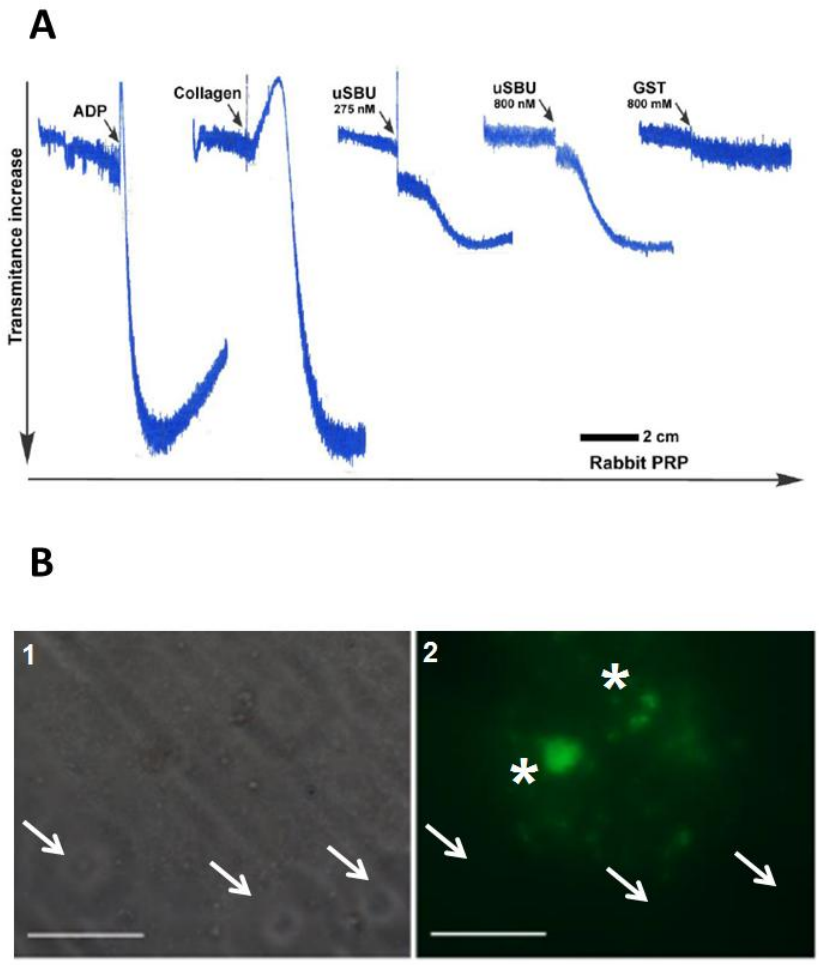

Fig. 11. GST-uSBU aggregates rabbit platelets. (A) Rabbit platelet aggregation promoted by 275 nM and 800 nM GST-uSBU. Positive controls with ADP (20 µM) and Collagen (20 mg. mL^{-1}) are also shown. The negative control was rGST 800 nM. (B) Panels demonstrating the formation of platelets aggregates induced by FITC-labeled GST-uSBU. B1 is the dark field and B2, the bright field. Arrows indicated erythrocytes and stars indicate platelet aggregates. Bars correspond to 20 µm.

Discussion

We performed the optimization and the biological characterization of the fusion protein GST-uSBU. GST-uSBU is not enzymatically active, in the present case this was an advantage, avoiding the use of generally toxic urease inhibitors during the assays of its non-enzymatic biological properties. rGST was employed as a control in all assays, to ensure that the biological effects seen were indeed related to uSBU.

It has been previously reported that the fusion of a protein to a large affinity tag, such as GST, can be advantageous in terms of increased expression, enhanced solubility (the hydrophilic surface of GST makes the fusion protein soluble), protection from proteolysis, improved folding, stability of the recombinant protein in the soluble fraction besides enabling protein purification via affinity chromatography (Zhan et al., 2001; Smyth et al., 2003; Young et al., 2012). Martinelli (2007) performed the cleavage of GST from GST-uSBU using thrombin, observing short term precipitation of the cleaved protein. The GST tag helps to maintain the fusion protein GST-uSBU soluble and stable for at least 14 days at 4°C. Even so, GST-uSBU had a tendency to aggregate upon more prolonged storage (data not shown), as also noted for JBU (Follmer et al., 2004a). Addition of EDTA and β-mercaptoethanol to the storage buffer decreased the rate of precipitation. Hence, the buffer exchange to Tris-HCl, needed for the biological assays, was performed one day before the assays.

The optimization of recombinant proteins expression is generally performed using a trial-and-error approach, with the different expression variables being tested independently from each other. Therefore, variables interactions are lost, which makes the trial-and-error approach time-consuming. Moreover, a significant amount of protein is required for every biological study, then the traditional trial-and-error method has been progressively

replaced by factorial approaches (Papaneophytou and Kontopidis, 2014). We performed the optimization using the variables temperature, IPTG concentration and time. The best conditions of GST-uSBU production were defined as 24 °C, 0.55 mM IPTG and 14 h, yielding more than 5 mg of the fusion protein per liter of culture. The production of the recombinant protein PsaA from *Streptococcus pneumoniae* serotype 14 was optimized using the same variables chosen in this present study. Low temperature (25 °C) and low IPTG concentration (0.1 mM) also favored the expression of PsaA, as well as long periods of cultivation (16 h) (Leites et al., 2011). According to Papaneophytou and Kontopidis (2014), high temperature promotes cell growth, but is detrimental to heterologous protein expression, because a higher growth rate could lead to a higher probability of plasmid loss. Therefore some proteins greatly benefit from a slower, longer induction period which generally requires a low temperature (Papaneophytou and Kontopidis, 2014). Besides, the use of low temperatures and low IPTG concentration optimizes costs of the bioprocess, making it more eco-friendly.

GST-uSBU showed all the biological properties previously reported by our group for plant ureases, such as antifungal and insecticidal effects, and aggregation-inducing activity upon insect hemocytes and rabbit platelets. As observed for GST-uSBU, the filamentous fungi *C. lunata, F. oxysporum, P. herquei and T. viride* were also susceptible to 0.57 µM eSBU purified from soybean seeds (Becker-Ritt et al., 2007). The similar spectrum of inhibition agrees with the high amino acid identity between the two isoforms (Goldraij et al., 2003). In addition, the oomycete *Pythium oligandrum* was not susceptible to GST-uSBU, as it was observed also for JBU (Postal et al., 2012). The cell walls of oomycetes are mainly composed of -1,3-glucan polymers and cellulose, and unlike fungal cell walls, they contain little chitin (Kamoun, 2003). These results suggest that chitin could

be important in the antifungal mode of action of ureases. Recently, it was reported the cellulolytic activity of a purified urease of pigeon pea (*Cajanus cajan*), but no chitinase activity was detected (Balasubramanian et al., 2013). Then, whether there is any interaction between chitin and plant ureases, this interaction apparently does not cause the hydrolysis of chitin.

The fusion protein affected the secondary metabolism of filamentous fungi, causing an increase or decrease of pigments production in *F. oxysporum* and *P. herquei*, respectively. The pigments produced by *F. oxysporum* were isolated and characterized as naphthoquinones and anthraquinones (Baker and Tatum, 1998; Tatum et al., 1987). The fungal pigments, naphthoquinones, are active against bacteria, yeast, fungi, protozoa (*Leishmania brasiliensis*) and insect (*Calliphora erythrocephala*). The pigments also have cytotoxic activity against mouse leukemia and *HeLa* cells, as well as, mutagenic and carcinogenic properties. Fungal naphthoquinones are typical representatives of the secondary metabolites and are synthesized under conditions of inhibition or total cessation of fungal growth (Medentsev and Akimenko, 1998). Therefore, the increase of the pigmentation of *F. oxysporum* could be a defense mechanism of the fungus against the toxic protein, GST-uSBU. On the other hand, the pigments produced by *P. herquei* belong to the class of phenalenones, such as atrovenetin, herqueinones, sclerodin, hequeichrysin. Phenalenones showed diverse and significant biological activities, including antimicrobial, anticancer and cytotoxic activities (Elsebai et al., 2014). We could not find a direct explanation of why *P. herquei* pigments were inhibited after treatment with GST-uSBU. We hypothesize that GST-uSBU may interfere on its pigment production pathway and as a consequence the fungus becomes more susceptible to the fusion protein. *P. herquei* is the most susceptible fungus to the effects of eSBU and JBU identified so far. Because of this

high susceptibility, it was the fungal model used in the scanning electronic microscopy studies (Becker-Ritt et al., 2007).

The antifungal activity of eSBU against yeasts was not previously determined. On the other hand JBU and Jaburetox were active, in the same concentration range as GST-uSBU, against the same *Candida* species tested here, and also against *K. marxiannus*, *P. membranifasciens* and *S. cerevisiae* (Postal et al., 2012). We observed the formation of pseudo-hyphae after treatment of *C. albicans* (Fig. 9, lane 1), *C. tropicalis* and *P. membranifasciens* with the fusion protein (Fig 8A and 8C). Pseudohyphal growth allows yeasts to escape from unfavorable growth conditions and to penetrate natural barriers. The elongated morphology provides more surface area, in comparison with oval shape, and allows pseudo-hyphae a more efficient absorption of nutrients (Abu-Elteen and Hamad, 2005). Inhibition of β-(1,3)-glucan syntethase, the mechanism of antifungal action of echinocandins, results in cytological and ultrastructural changes in fungi, characterized by growth as pseudo hyphae, thickened cell wall and buds failing to separate from mother cells (Abu-Elteen and Hamad, 2005). The pseudo hyphae shape observed for GST-uSBU treated yeasts could indicate an effect of uSBU on the yeast cell wall and/or cell membrane, or a defense mechanism of the fungi against its fungitoxic action, by assuming a more infective shape. More studies are necessary at this point to clarify the fungitoxic mode of action of ureases.

Jaburetox, a 93 amino acids recombinant peptide derived from JBU, shows antifungal activity, but its activity is lower comparing with the entire protein (Postal et al., 2012). Here no antifungal activity was detected for the GST-uSBU truncated fragments with $\leq$ 50 kDa. We are presently carrying out some experiments with Soyuretox, the

Jaburetox equivalent peptide in uSBU (Kappaun, 2014) and these studies will help us to determine the antifungal region of uSBU.

Antibacterial properties of ureases were so far investigated only for eSBU. Martinelli (2004) reported that eSBU purified from soybean seeds did not affect the growth of the phytopathogenic bacteria *Ralstonia solanacearum, Xanthomonas campestris* and *Xanthomonas axonopodis* (Martinelli, 2004). Similarly, GST-uSBU did not affect *P. aeruginosa*, *E. coli* and *S. aureus* suggesting that ureases are devoid of bactericidal properties.

Regarding to the insecticidal activity of soybean ureases, there are reports of feeding trials with eSBU in *Dysdercus peruvianus*. The insects were fed with diets containing 0.02-0.1 % (w/w) of eSBU and an LD_{50} of 0.052 % was determined (Follmer et at., 2004). Here we used hemocoel injection as the administration route to test lethality induced by GST-uSBU in *R. prolixus*. (Stanisçuaski et al., 2010), reported previously that JBU caused 96% mortality in 5^{th} instar *R. prolixus* after hemocoel injection at 0.25 $\mu g.mg^{-1}$ body weight. Using almost the same dose of GST-uSBU we used here, 0.06 $\mu g.mg^{-1}$, 25 % of survival was observed for *R. prolixus* injected with JBU (Defferrari, M.S., personal communication). In addition, GST-uSBU was able to induce the aggregation of *R. prolixus* hemocytes, suggesting deterrent effect on the insect's immune system. Defferrari and co-workers reported for JBU, at the same dose, findings of more than 400 aggregates per µL of *R. prolixus* hemolymph (Defferrari et al., 2014).

Aggregation of rabbit platelet has been described as a property of the jack bean and soybean (eSBU) ureases (one chain), *Helicobacter pylori* (two chains) and *Bacillus pasteurii* (three chains) ureases, which differ in their quaternary structures (Follmer et al., 2004; Wassermann et al., 2010). Additionally, as previously reported for *H. pylori* urease

(Wassermann et al., 2010), GST-uSBU bound only to platelets, not erythrocytes. Aggregation of rabbit platelets induced by eSBU was reported by Follmer and co-workers, with an EC_{50} of 40.74 nM (Follmer et al., 2004). Since the level of identity between eSBU and uSBU is greater than that shared by plant and bacterial ureases, the less potent aggregating effect observed here for GST-uSBU could be due to some steric hindrance imposed by the GST moiety or to an "incomplete" folding of uSBU that affected its "platelet-aggregating" domain.

Hence, all the biological properties of plant ureases screened for GST-uSBU are displayed by uSBU, even fused to GST. The fusion of GST to the N-terminal amino acid of uSBU did not destroy or "hide" the biologically active domains responsible for these properties.

To our knowledge, JBURE-IIb, an urease isoform of *C. ensiformis*, was the only plant urease expressed heterologously in *E. coli* before this work (Mulinari et al., 2011). rJBURE-IIb was expressed in the absence of accessory protein and when bacterial cells were induced in liquid medium, an enzymatically inactive protein was produced. Nevertheless, this recombinant urease displayed biological properties demonstrated for JBU and Canatoxin, the other two ureases isoforms produced by *C. ensiformis* such as inhibition of *P. herquei* growth and, also the inhibition of diuresis of *R. prolixus* isolated Malpighian tubules (Mulinari et al., 2011).

Conclusions

Our results show the potentialities of GST-uSBU as a model to study plant ureases. The fusion protein showed the same properties displayed by the native ureases, eSBU and JBU, isolated from seeds, with the advantages of high yield production and one-step

purification protocol. Moreover, it was possible to explore more deeply the effect caused by ureases on fungi. GST-uSBU was capable to interfere in the secondary metabolism of filamentous fungi and caused morphology changes in yeasts. Altogether, these results further support the hypothesis of the defense role of plant ureases.

Acknowledgments

This work was supported by Coordenadoria de Aperfeiçoamento de Pessoal de Ensino Superior (CAPES), Conselho Nacional de Desenvolvimento Científico e Tecnológico (CNPq), and Fundação de Amparo à Pesquisa do Estado do Rio Grande do Sul (FAPERGS).

References

[1] K. H. Abu-Elteen, M. Hamad, Fungi Biology and Applications (2005).

[2] R.A. Baker, J.H. Tatum, J. Ferment. Bioeng. 85 (1998) 359–361.

[3] A. Balasubramanian, V. Durairajpandian, S. Elumalai, N. Mathivanan, A.K., Munirajan, K. Ponnuraj, K., Int. J. Biol. Macromol. (2013.58) 301–309.

[4] A.B. Becker-Ritt, A.H.S. Martinelli, S. Mitidieri, V. Feder, G.E. Wassermann, L. Santi, M.H.,Vainstein, J.T. Oliveira, L.M., Fiuza, G. Pasquali, C.R. Carlini. Toxicon 50, (2007) 971–983.

[5] M.M. Bradford. Anal. Biochem. 72 (1976) 248–254.

[6] C.R. Carlini., M.F. Grossi-De-Sá. Toxicon 40 (2002) 1515–1539.

[7] C.R. Carlini, J.C. Polacco, Crop Sci. 48 (2008) 1665–1672.

[8] E.L. Carter, N; Flugga, J.L Boer, S.B. Mulrooney, R.P. Hausinger, Metallomics 1 (2009) 207–221.

[9] M.S. Defferrari, R. Silva, I. Orchard, C.R. Carlini, Toxicon 82 (2014) 18–25.

[10] N.E. Dixon, C. Gazzola, R.L. Blakeley, B. Zerner, J. Am. Chem. Soc. 97 (1975) 4131–4133.

[11] M.F. Elsebai, M. Saleem, M. V Tejesvi, M. Kajula, S. Mattila, M. Mehiri, A. Turpeinen, A.M. Pirttilä, Nat. Prod. Rep. 31 (2014) 628–45.

[12] C. Follmer. Phytochemistry 69 (2008) 18–28.

[13] C. Follmer, F.V. Pereira, N.P. Da Silveira, C.R. Carlini. Biophys. Chem. 111(2004a) 79–87.

[14] C.Follmer, R. Real-Guerra, G.E. Wasserman, D. Olivera-Severo, C.R. Carlini, C.R.,. Eur. J. Biochem. 271 (2004) 1357–1363.

[15] D.J.M.C. Gee, C. A. May, R.M., Garner; J.M., Himpsl, H.L.T.Mobley, J. Bacteriol. 181 (1999) 2477–2484.

[16] A. Goldraij, L.J. Beamer, J.C. Polacco. Plant Physiol. 132 (2003) 1801-1810.

[17] H. J.Tatum, A. R. Baker, E.R. Berry, Phytochemistry 26(1987) 2499–2500.

[18] P.D. Haaland, 1989 CRC press.

[19] S. Kamoun, Eukariotic Cell 2 (2003) 191–199.

[20] K. Kappaun, Dissertation, Universidade Federal do Rio Grande do Sul, 2014.

[21] B. Krajewska, J. Mol. Catal. B Enzym. 59 (2009) 9–21.

[22] N.J. Lane, R.A. Leslie, L.S. Swales, J. Cell Sci. 18(1975)179–197.

[23] A. Leites, A. Paula, A., C. Argondizzo, S. Esteves, E., Jessouron, R. Galler, M. Alberto, Protein Expr. Purif. 78(2011) 38–47.

[24] A.H.S. Martinelli, Trabalho de Conclusão de Curso, Universidade do Vale do Sinos, 2004.

[25] A.H.S. Martinelli, Dissertation, Universidade Federal do Rio Grande do Sul, 2007.

[26] A.H.S. Martinelli, K. Kappaun, R. Ligabue-Braun, M.S. Defferrari, A.R. Piovesan, F. Stanisçuaski, D.R. Demartini, C.A. Dal Belo, C.G.M. Almeida, C. Follmer, H. Verli, C.R. Carlini, G. Pasquali, Biochim. Biophys. Acta - Gen. Subj. 1840 (2014) 935–944.

[27] A.G. Medentsev, V.K. Akimenko, Phytochemistry 47(1998)935–959.

[28] F.Mulinari, A.B. Becker-Ritt, D.R., Demartini, R. Ligabue-Braun, F. Stanisçuaski, H. Verli, R.R. Fragoso, E.K. Schroeder, C.R. Carlini, M.F. Grossi-de-Sá,. Biochim. Biophys. Acta 1814 (2011) 1758–68.

[29] F. Mulinari, F. Stanisçuaski, L.R. Bertholdo-Vargas, M. Postal, O.B. Oliveira-Neto, D.J. Rigden, M.F. Grossi-de-Sá, C.R. Carlini, Peptides 28 (2007) 2042–50.

[30] E.C. Oerke, H.W. Dehne, Crop Prot. (2004)23 275–285.

[31] C.P. Papaneophytou, G. Kontopidis, Protein Expr. Purif. 94 (2014) 22–32.

[32] J.C. Polacco, M.A. Holland, Int. Rev. Cytol. 145 (1993) 65–103.

[33] J.C. Polacco, R.W. Krueger, R.G. Winkler, Plant Physiol. 79 (1985) 794–800.

[34] J.C. Polacco, R.B. Sparks,. Plant Physiol. 70 (1982) 189–194.

[35] J.C. Polacco, E.A. Havir. J. Biol. Chem. (1979) 1707–1715.

[36] A. Pompilio, M. Scocchi, S. Pomponio, F. Guida, A. Di Primio, E. Fiscarelli, R, Gennaro, G. Di Bonaventura, Peptides 32(2011) 1807–1814.

[37] M. Postal, A.H.S. Martinelli, A.B. Becker-Ritt, R., Ligabue-Braun, D.R. Demartini, S.F.F. Ribeiro, G. Pasquali, V.M. Gomes, C.R. Carlini, Peptides 38 (2012) 22–32.

[38] D.R. Radford, S.J. Challacombe, J.D. Walter, J. Med. Microbiol.40 (1994) 416–423.

[39] R. Real-Guerra, F. Stanisçuaski, C.R. Carlini, Intech (2013) 317-340.

[40] D.R. Smyth, M.K. Mrozkiewicz, W.J. Mcgrath, P. Listwan, B. Kobe, Protein Sci. (2003) 1313–1322.

[41] F. Stanisçuaski, C.R. Carlini, Toxins 4 (2012) 55–67.

[42] F. Stanisçuaski, V. Te Brugge, C.R. Carlini, I. Orchard, J. Insect Physiol. 56 (2010) 1078–1086.

[43] N.E. Stebbins, J.C. Polacco, Plant Physiol. 109 (1995)169–175.

[44] R.S. Torisky, J.D. Griffin, R.L. Yenofsky, J.C. Polacco, Mol. Gen. Genet. 242 (1994) 404–414.

[45] H.Towbin, T. Staehelin, J. Gordon, Proc. Natl. Acad. Sci. U. S. A. 76 (1979) 4350–4354.

[46] G.E. Wassermann, D. Olivera-Severo, A.F. Uberti, C.R. Carlini, J. Cell. Mol. Med. 14 (2010) 2025–2034.

[47] B. Wiebke-Strohm, G. Pasquali, M. Margis-Pinheiro, M. Bencke, L. Bücker-Neto, A.B. Becker-Ritt, A.H.S. Martinelli, C. Rechenmacher, J.C. Polacco, R. Stolf, F.C. Marcelino, R.V. Abdelnoor, M S. Homrich, E.M. Del Ponte, C.R. Carlini, C.R., M.C.C.G. de Carvalho, M.H Bodanese-Zanettini, Plant Mol. Biol. 79 (2012) 75–87.

[48] C.P. Witte, S.A. Tiller, M.A. Taylor, H.V. Davies, Plant Physiol. 128(2002) 1129–1136.

[49] C.L. Young, C.L., Z.T. Britton, A.S. Robinson, Biotechnol. J. 7 (2002) 620–634.

[50] B. Zambelli, F. Musiani, S. Benini, S. Ciurli, Acc. Chem. Res. 44 (2011) 520–530.

[51] Y. Zhan, X. Song, G.W. Zhou, Gene 281 (2001) 1–9.

Supplementary Material

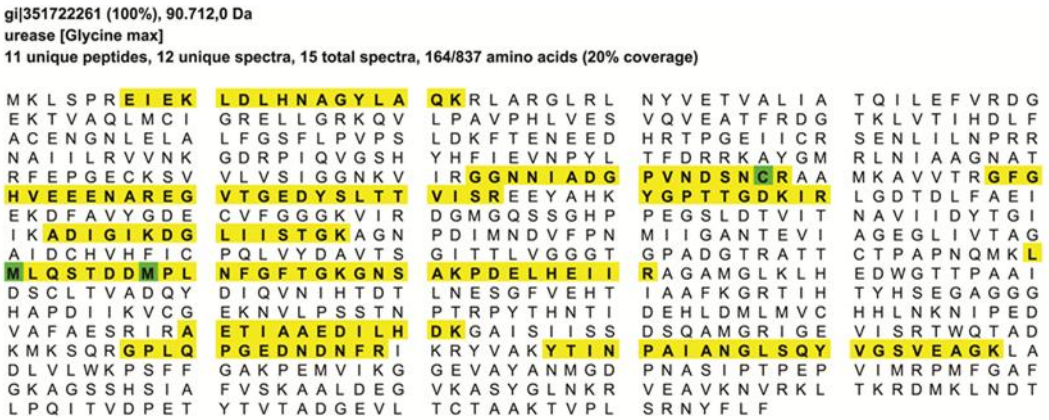

Fig. S1: Peptides found in the excised 120 kDa band. Peptides are highlighted in yellow. The amino acids highlighted in green are modified amino acids after the digestion process, due to the use of Iodoacetamide and Dithiothreitol.

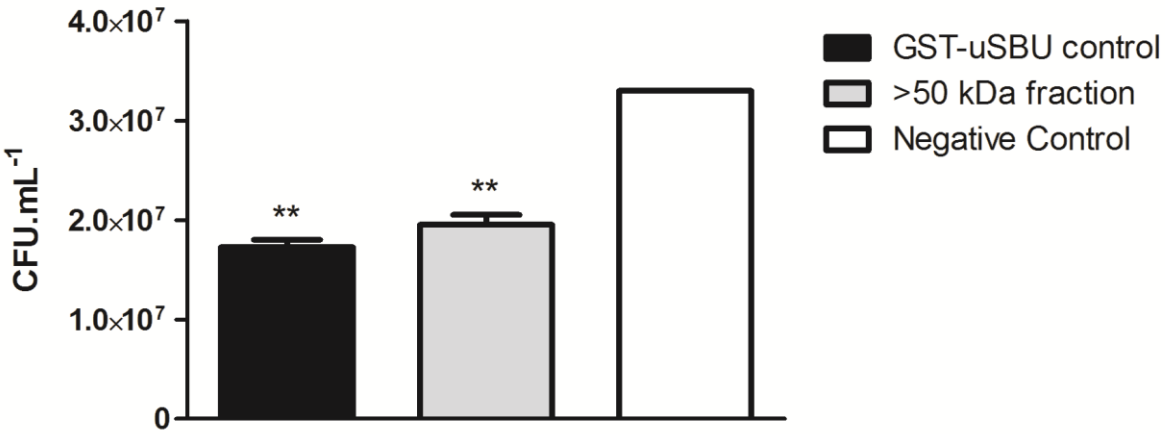

Fig S2. Antifungal effect on *Candida tropicalis* evaluating after concentration in a 50 kDa amicon. The antifungal activity is found in the >50 kDa fraction. N=3, ** $p \leq 0.0011$.

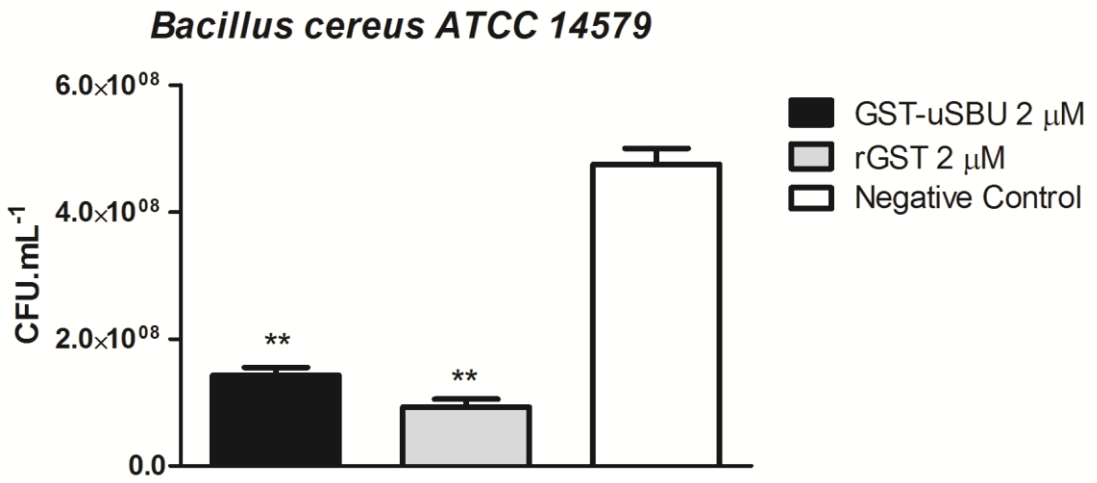

Fig S3. Antibacterial effect of GST-uSBU and GST on *Bacillus cereus*. 10^8 CFU.mL^{-1} were incubated on 96-wells plates containing LB, with 2 μM GST-uSBU, 2 μM GST, Tris-HCl buffer 10 mM, pH 7.0 (negative control) or 0.1 % hydrogen peroxide (positive control). The incubation was performed for 24 h, at 37 °C and after that, the CFU was determined. N=3 ** $p \leq 0.0011$.

4.2. CAPÍTULO II: PROPRIEDADES ESTRUTURAIS DO PEPTÍDEO JABURETOX

Artigo publicado no periódico **The FEBS Journal**.

Pliable natural biocide: Jaburetox is an intrinsically disordered insecticidal and fungicidal polypeptide derived from jack bean urease

Fernanda C. Lopes, Olena Dobrovolska, Rafael Real-Guerra, Valquiria Broll, Barbara Zambelli, Francesco Musiani, Vladimir N. Uversky, Célia R. Carlini, Stefano Ciurli

Resumo: Jaburetox é um polipeptídeo derivado da urease de feijão-de-porco (*Canavalia ensiformis*) e tóxico para um amplo espectro de insetos, fungos filamentosos fitopatogênicos e leveduras de importância médica. A elucidação das bases estruturais do peptídeo, para a compreensão do modo de ação do Jaburetox é o foco deste estudo multifacetado. Jaburetox em solução é um monômero de 11 kDa apresentando um elevado raio hidrodinâmico, sugestivo de um polipeptídeo desordenado. A natureza intrinsicamente desordenada do Jaburetox foi predita teoricamente por uma abrangente análise de bioinformática e confirmada experimentalmente por espalhamento de luz, bem como dicroísmo circular e espectroscopia de RMN. Os sinais de RMN foram assinalados e forneceram os deslocamentos químicos do *backbone* que indicaram que o Jaburetox apresenta baixa propensão de assumir uma estrutura secundária estável. Os estudos de relaxação do ^{15}N revelaram significativa mobilidade do *backbone*, especialmente na porção N-terminal do peptídeo. A estrutura em solução do Jaburetox apresentou um motivo α-hélice próximo ao N-terminal e duas estruturas tipo volta situadas na porção central da proteína e próxima ao C-terminal. Regiões similares foram preditas como potenciais locais de interação proteína-proteína utilizando ferramentos computacionais. O conhecimento das propriedades estruturais do Jaburetox em solução é um passo fundamental para correlacionar sua estrutura com suas atividades biológicas.

the FEBS Journal

Pliable natural biocide: Jaburetox is an intrinsically disordered insecticidal and fungicidal polypeptide derived from jack bean urease

Fernanda C. Lopes[1], Olena Dobrovolska[2], Rafael Real-Guerra[3], Valquiria Broll[1], Barbara Zambelli[2], Francesco Musiani[2], Vladimir N. Uversky[4,5,6], Célia R. Carlini[1,3,7] and Stefano Ciurli[2]

1 Graduate Program in Cellular and Molecular Biology – Center of Biotechnology, Federal University of Rio Grande do Sul, Porto Alegre, Brazil
2 Laboratory of Bioinorganic Chemistry, Department of Pharmacy and Biotechnology, University of Bologna, Italy
3 Department of Biophysics and Center of Biotechnology, Federal University of Rio Grande do Sul, Porto Alegre, Brazil
4 Department of Molecular Medicine and USF Health Byrd Alzheimer's Research Institute, Morsani College of Medicine, University of South Florida, Tampa, USA
5 Institute for Biological Instrumentation, Russian Academy of Sciences, Pushchino, Moscow Region, Russia
6 Department of Biological Science, Faculty of Science, King Abdulaziz University, Jeddah, Saudi Arabia
7 Instituto do Cérebro, Pontifícia Universidade Católica do Rio Grande do Sul, Porto Alegre, Brazil

Keywords
Canavalia ensiformis; circular dichroism; Jaburetox; light scattering; NMR spectroscopy; urease

Correspondence
S. Ciurli, Laboratory of Bioinorganic Chemistry, Department of Pharmacy and Biotechnology, University of Bologna, Via Giuseppe Fanin 40, 40127 Bologna, Italy
Fax: +39 051 209 6203
Tel: +39 051 2096204
E-mail: stefano.ciurli@unibo.it
V. N. Uversky, Department of Molecular Medicine and USF Health Byrd Alzheimer's Research Institute, Morsani College of Medicine, University of South Florida, Tampa, FL 33612, USA
Fax: +1 813-974-7357
Tel: +1 813-974-5816
E-mail: vuversky@health.usf.edu
C. R. Carlini, Graduate Program in Cellular and Molecular Biology – Center of Biotechnology, Federal University of Rio Grande do Sul, Av. Bento Gonçalves 9500, Porto Alegre, RS, CEP 91501-970, Brazil
Fax: + 55 51 3308 7003
Tel: + 55 51 3308 7606
E-mail: ccarlini@ufrgs.br

(Received 9 October 2014, revised 13 January 2015, accepted 14 January 2015)

doi:10.1111/febs.13201

Jaburetox is a polypeptide derived from jack bean (*Canavalia ensiformis*) urease and toxic to a broad spectrum of insects, phytopathogenic filamentous fungi and yeasts of medical importance. The elucidation of the structural basis for the mode of action of Jaburetox is the focus of this multifaceted study. Jaburetox in solution is a monomer of 11.0 kDa featuring a large hydrodynamic radius, suggestive of a disordered polypeptide. The intrinsically disordered nature of Jaburetox was theoretically predicted by a comprehensive bioinformatics analysis and experimentally confirmed by light scattering as well as by circular dichroism and NMR spectroscopy. NMR signal assignment provided backbone secondary chemical shifts that indicated that Jaburetox has a low propensity to assume a stable secondary structure. ^{15}N relaxation studies revealed significant backbone mobility, especially in the N-terminal portion of the polypeptide. The solution structure of Jaburetox shows the presence of an α-helical motif close to the N terminus, together with two turn-like structures situated in the central portion of the protein and close to the C terminus. Similar regions were predicted as potential protein–protein interaction sites using computational tools. The knowledge of the structural properties of Jaburetox in solution is a key step to correlate its structural and biological activities.

Abbreviations
HSQC, heteronuclear single quantum coherence; IDP, intrinsically disordered protein; JBU, jack bean urease; LUV, large unilamellar vesicle; MALS, multiple-angle light scattering; MoRF, molecular recognition feature; QELS, quasi-elastic light scattering; SEC, size exclusion chromatography; SSP, secondary structure propensity; TCEP, tris(2-carboxyethyl)phosphine.

Introduction

Ureases (EC 3.5.1.5) are non-redox nickel dependent enzymes [1] that catalyze urea hydrolysis into ammonia and carbon dioxide [2–5]. Jack bean (*Canavalia ensiformis*) urease (JBU) (Fig. 1A) represents an important milestone in the history of biochemistry. It was the first enzyme ever crystallized [6], and also the first enzyme found to have nickel ions in its active site [7]. In addition to JBU, *C. ensiformis* displays two additional isoforms of urease, named JBURE-II [8,9] and canatoxin [10].

Canatoxin, a toxic protein isolated from *C. ensiformis* seeds [11] and identified 20 years later as an isoform of urease [10], displays insecticidal properties [12]. This toxicity involves an internal polypeptide of 10 kDa (pepcanatox), released from the protein upon hydrolysis by cathepsin-like digestive enzymes of insects such as *Callosobruchus maculatus*, *Rhodnius prolixus*, *Nezara viridula*, *Dysdercus peruvianus* and *Oncopeltus fasciatus* [13–16] (Fig. 1A,B). Based on the N-terminal sequence of pepcanatox and using as a template the cDNA of the urease isoform JBURE-II,

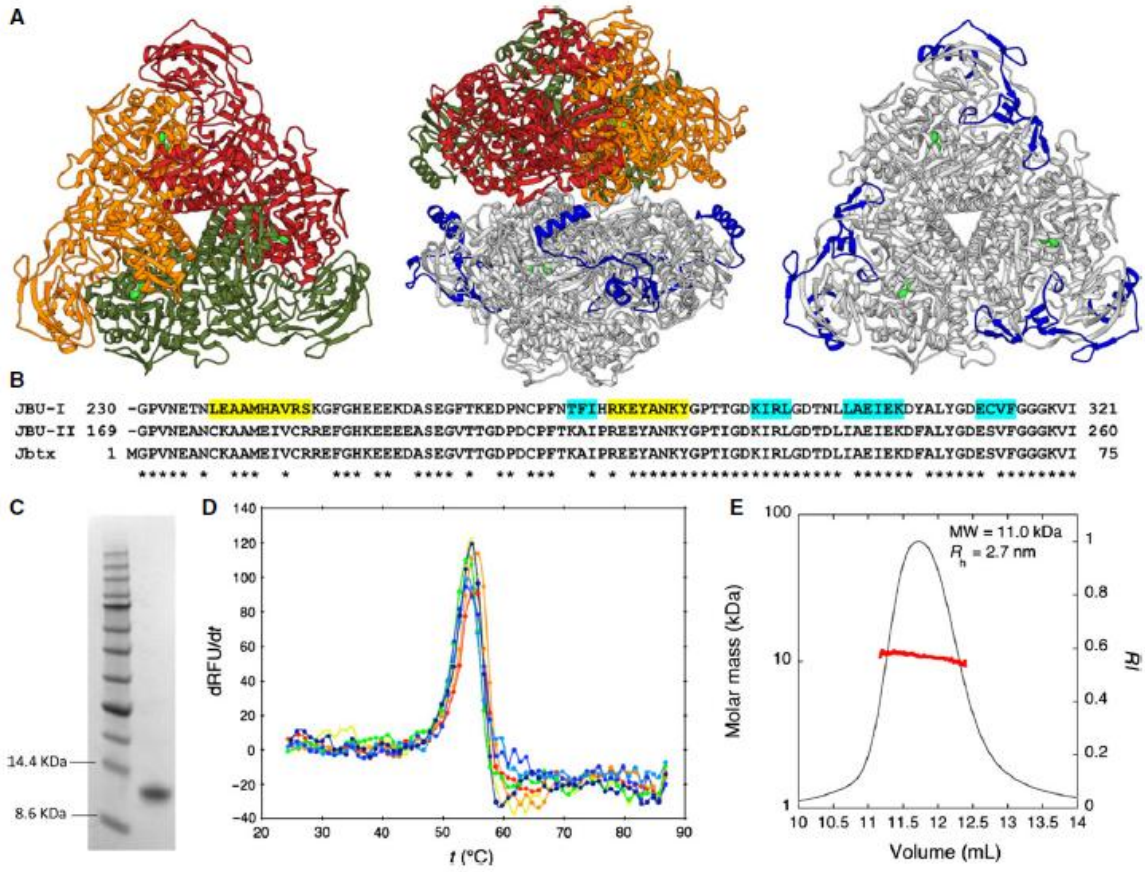

Fig. 1. Purification, stability and hydrodynamics of Jaburetox. (A) Ribbon scheme of the structure of jack bean urease: the α_6 hexamer is shown in the central panel, while the left and right panels display the two trimers that compose the overall protein tilted by 90° along the horizontal axis; the trimer on top is colored red, orange and green for the three α subunits, while the trimer on the bottom highlights in blue the protein portion that corresponds to the Jaburetox polypeptide; the nickel atoms in the active site are shown as green spheres. (B) Sequence alignment of Jaburetox (abbreviated as Jbtx) with the corresponding sequence of the two isoforms of urease in jack bean; α-helices and β-strands in the crystal structure of JBU-I are highlighted in yellow and cyan, respectively. (C) SDS/PAGE profile of the final purified Jaburetox (right lane) and the molecular mass reference markers (left lane). (D) Thermal denaturation assay of Jaburetox using Thermofluor. The plot represents the first derivative of the melting curve of the raw data obtained at pH 3.5 (red), pH 4.5 (orange), pH 5.5 (yellow), pH 6.5 (green), pH 7.5 (cyan), pH 8.5 (blue) and pH 9.5 (indigo). The T_m values correspond to the apex. (E) Molar mass distribution of Jaburetox eluted from a SEC column and evaluated using MALS-QELS. The solid line indicates the trace from the refractive index detector, whereas the dots are the weight-averaged molecular masses measured every second.

the recombinant polypeptide Jaburetox-2Ec (carrying a V5 epitope and a His-tag) was produced heterologously in *Escherichia coli* [17]. Jaburetox-2Ec shows a broader spectrum of insecticidal activity, which also includes insects not susceptible to the full-length canatoxin such as *Spodoptera frugiperda* [17] because the hydrolysis of the protein to release the polypeptide is no longer required. Jaburetox-2Ec causes inhibition of diuresis in *R. prolixus* by a mechanism that involves cGMP and disturbance of the transmembrane potential of Malpighian tubules [18]. Moreover, Jaburetox-2Ec permeabilizes large unilamellar vesicles (LUVs), displaying membrane-disruptive activity on acidic lipid bilayers [19]. A variant form of the recombinant polypeptide, corresponding to the His-tagged urease-derived sequence with no V5 epitope and simply named Jaburetox, also displays antifungal properties against filamentous fungi (*Mucor* sp. and *Penicillium herguei*) and yeasts (*Candida* (*Ca.*) *albicans*, *Ca. parapsilosis*, *Ca. tropicalis*, *Kluyveromyces marxianus*, *Pichia membranisfaciens* and *Saccharomyces cerevisiae*), in addition to its entomotoxic activity [20].

In order to understand the mode of action of Jaburetox-2Ec, molecular modeling studies were carried out that suggested the existence of a β-hairpin motif at the C-terminal portion [17,19]. This motif was indeed subsequently observed in the crystallographic structure of JBU [21], suggesting that it could be a factor for the membrane-disturbing activity of Jaburetox [19,22]. In order to confirm the importance of this β-hairpin for the biological activity of Jaburetox, three mutated versions of this polypeptide were analyzed: one lacking the β-hairpin motif, and two additional peptides corresponding to the N-terminal and the C-terminal portions of the recombinant Jaburetox, respectively [23]. The peptide lacking the β-hairpin motif showed all the properties of the wild-type Jaburetox, thus excluding this region as the biologically active portion of the molecule. On the other hand, injection assays into *O. fasciatus* and *R. prolixus* showed that only the N-terminal portion of Jaburetox carries its insecticidal activity. However, both parts caused almost the same mortality rate seen for the N-terminal peptide upon feeding to *R. prolixus*, indicating different modes of action for the two peptides depending on the different tissues of the insect. Although with different potencies, both the N- and C-terminal portions of Jaburetox caused the neuromuscular blockage of the cockroach *Phoetalia pallida* nerve-coxal muscle preparation, while both peptides were equipotent in inhibiting the fluid secretion in the Malpighian tubules of *R. prolixus* and in disrupting LUV membranes. These data suggested that the N-terminal portion carries the entomotoxic activity of Jaburetox, and that its C terminus probably contributes to the polypeptide activity by interacting with cell membranes [23]. Other studies have demonstrated that Jaburetox and its mutants can form well-resolved, highly cation-selective channels. The peptide corresponding to the N-terminal part of Jaburetox is more active in negative potentials, while the ion-channel activity of Jaburetox and the other mutants do not display voltage dependence [24].

The objective of the present study was the experimental characterization of the structural, dynamic and folding properties of Jaburetox. The hydrodynamic properties of the polypeptide were determined using size exclusion chromatography (SEC) coupled with light scattering experiments. The protein folding was examined using circular dichroism (CD), differential scanning fluorimetry and high resolution NMR spectroscopy. Based on NMR data, backbone mobility studies were carried out and the 3D structure of Jaburetox was determined. The properties that were established indicate the presence of a large ensemble of highly disordered conformers in solution with three more ordered segments.

Results

Jaburetox expression and purification

Jaburetox was expressed and purified as a His-tagged polypeptide in order to avoid additional steps in the purification protocol that might have led to decreased yields. Indeed, the presence of this tag does not interfere with the biological insecticidal [17] and fungicidal [20] activities of this urease-derived peptide. The expression protocol of Jaburetox was optimized in this work to typically yield 30 mg of Jaburetox per liter of culture. The previously described protocol had a protein yield of 10 $mg \cdot L^{-1}$ [20,23]. Screening of different culture conditions allowed a maximal yield of protein expression at 19 °C, 0.87 mM IPTG and 16 h of expression time to be obtained. Moreover, before protein induction, LB medium was exchanged with fresh M9 minimal medium and the biomass was four-fold concentrated, according to a previously reported method [25]. In addition to the advantage of increasing the cellular performance by removing secondary metabolites that might inhibit cellular growth, this method reduces isotope consumption for producing NMR samples: indeed, the majority of cell biomass is generated using unlabeled media, while labeled protein is produced in a reduced volume of isotopically labeled minimal medium. The purification protocol was improved by adding a SEC separation after the first

affinity chromatography purification step. The SDS/PAGE profile of the final purified protein is shown in Fig. 1C. Notably, although the predicted molecular mass determined from the amino acid sequence of Jaburetox with the six-histidine extension is 11 kDa, the protein exhibited a 2 kDa shift in the SDS/PAGE and migrated as a 13 kDa polypeptide. This aberrant migration during SDS/PAGE experiments is a typical feature of intrinsically disordered proteins (IDPs) [26,27], determined by their unusual amino acid compositions typically characterized by a high ratio of charged to hydrophobic residues. As a result, these disordered proteins interact less efficiently with SDS and are characterized by a decreased migration velocity, giving an apparent molecular mass that is higher than the real one [28].

Jaburetox stability by thermal differential scanning fluorimetry

Jaburetox tends to aggregate after long-term storage [19,23], a process that negatively affects the biological activity of this protein [29]. In order to find conditions to stabilize the protein solutions, the effect of pH was explored by performing thermal denaturation assays using differential scanning fluorimetry (Thermofluor [30]). In this assay, a fluorescent probe (SYPRO Orange) added to the protein solution binds to exposed hydrophobic residues, thereby increasing its fluorescence. Maximal fluorescence intensity is expected when the protein unfolds, which corresponds to a peak in the first derivative plot occurring at the melting temperature (T_m). Similar curves and melting temperatures were consistently observed in the pH range between 3.5 and 9.5 (Fig. 1D). These curves revealed the presence of an unfolding process occurring at an average melting temperature of 54.6 ± 0.9 °C. If Jaburetox were totally unfolded at room temperature, no melting transition would be observed [30], thus indicating the presence of some degree of folding that is largely independent of pH. Substitution of the reducing agent β-mercaptoethanol, previously used in the storage buffer [20,23], with tris (2-carboxyethyl)phosphine (TCEP) significantly decreased the tendency of Jaburetox to aggregate both at 25 °C and at low temperatures (−80 °C), and the same oligomeric state was obtained after freezing and thawing. No difference was observed in the melting temperatures in the absence and in the presence of TCEP, suggesting that the improved effect of TCEP versus β-mercaptoethanol is related to the more efficient reduction of disulfide bonds that could form over time by oxidation of cysteine thiol groups, and not to an overall stabilization of the protein fold.

Hydrodynamic properties and aggregation state

Light scattering measurements were carried out in order to study the aggregation state of Jaburetox in solution by combining in-line SEC, static multiple-angle light scattering (MALS) and dynamic quasi-elastic light scattering (QELS) (Fig. 1E). SEC experiments showed a single peak eluting from the column, indicating that, in solution, Jaburetox exists in a single and homogeneous oligomeric form. The latter, according to MALS measurement, presents a molar mass of 11.03 ± 0.01 kDa, fully consistent with the theoretical molar mass of the monomeric protein (10 951 Da) based on its amino acid sequence that includes the six histidines (http://web.expasy.org/protparam/). The hydrodynamic radius measured by QELS is 2.7 ± 0.1 nm. This value is larger than the expected value of 1.74 nm for a well-folded protein of the same molecular mass [31], and is very close to that predicted for intrinsically disordered pre-molten globular proteins (2.46 nm) or random coil proteins (2.77 nm) of the same molecular mass [31]. This observation supports the idea that Jaburetox exists in an extended conformation in solution, probably due to the lack of secondary or tertiary contacts. To experimentally evaluate the amount of secondary structure of the protein in solution, CD spectroscopy was applied.

Secondary structure of Jaburetox by circular dichroism

The CD spectrum of the protein under native conditions (Fig. 2A) presents features typical of a random coil conformation, with a minimum centered at 200 nm. No strong negative signals above 205 nm, characteristic of α-helix or β-sheet structures, were observed. Accordingly, the software CAPITO (http://capito.nmr.fli-leibniz.de/), a tool that distinguishes different folding states of polypeptides on the basis of their far-UV CD spectra [32], indicated that the CD spectrum of Jaburetox is compatible with a native ensemble of disordered conformations in a pre-molten globular state, featuring a small amount of secondary structure (Fig. 2B). The CD spectrum of the protein undergoes minor changes upon temperature increase (Fig. 2A), suggesting a modest influence of temperature on the structural distribution among the ensemble of protein conformers. In particular, at 90 °C the minimum at 200 nm shifts to 202 nm, and the ellipticity at 222 nm, typical of α-helical composition, slightly

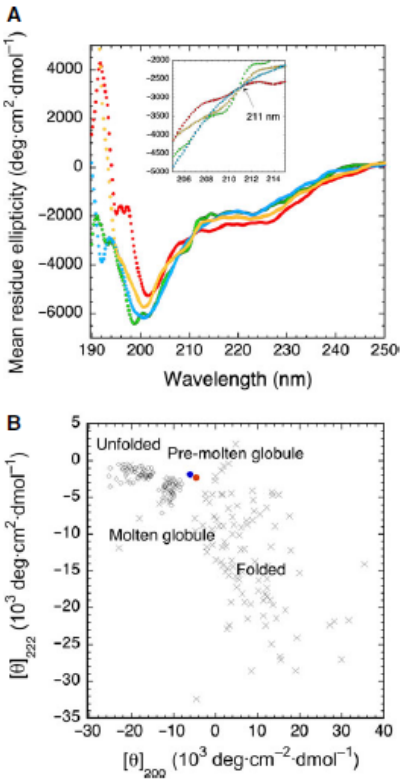

Fig. 2. Circular dichroic properties of Jaburetox. (A) CD spectrum of Jaburetox at 298 K (green), 323 K (yellow), 363 K (red) and 298 K after cooling temperature (cyan); the inset shows the region closer to the dichroic point at 211 nm. (B) Conformational classification of Jaburetox according to its CD spectrum performed using the web server CAPITO (http://capito.nmr.fli-leibniz.de/).

increases. In addition, a positive band appears at 192 nm indicative of the presence of some α-helices or β-strand elements. The spectrum of the protein at 50 °C is intermediate between the spectrum at 25 °C and at 90 °C. Overall, this reveals a small expansion of the secondary structure content at high temperature. This behavior was previously reported for IDPs [33,34] and can be explained by the known increased strength of hydrophobic interactions at higher temperatures. The effect is particularly significant in the case of strong electrostatic repulsions by a large number of electric charges that destabilize the hydrophobic attractions at lower temperatures [33]. The spectrum of the native Jaburetox at 25 °C was fully recovered after cooling the temperature, indicating that the changes induced by temperature onto the secondary structure composition are fully reversible (Fig. 2A). The superimposition of the spectra obtained at different temperatures reveals an isodichroic point at 211 nm, with a mean residue ellipticity of −2700 deg·cm^2·dmol^{-1} (Fig. 2A, inset). The presence of a wavelength in which the molar absorptivity is the same for two (or more) protein spectra is indicative of the presence of two prevalent conformational states in equilibrium. For proteins with prevalence of α-helices, isodichroic points are observed around 203 nm and are related to the helix–coil transition upon protein unfolding [35]. On the other hand, isodichroic points at higher wavelengths have been observed upon conformational transitions of IDPs, such as α-synuclein [36], and have been interpreted as indicative of conformational transitions within the random coil ensemble [37]. The presence of a conformational change between two different population states observed here is consistent with the thermal differential scanning fluorimetry experiments, which showed the presence of a transition induced by temperature.

Computational analysis of disorder propensity

In a previous study [23], the tertiary structure of Jaburetox was calculated by homology modeling, suggesting that Jaburetox contains very few secondary structure elements, with ~ 70% of the protein in the random coil conformation. A 13-residue α-helix was modeled in the N-terminal portion of the protein, while the C-terminal fragment was proposed to contain a β-hairpin. Molecular dynamics simulations suggested that the protein undergoes a further increase of the random coil conformation that, at the end of the simulation, comprised 84% of the protein structure, with the N-terminal portion losing the α-helical content and a short β-sheet appearing at the C terminus [23]. Previous molecular dynamics studies [17,19,22] also suggested that Jaburetox adopts a β-hairpin in its C-terminal region, as observed in the X-ray crystallographic structure of JBU [21].

Consistently with the intrinsically disordered nature of Jaburetox revealed by CD and hydrodynamic analyses, various computational tools indicated that this polypeptide is characterized by high intrinsic disorder propensity. First, we used the known fact that the amino acid compositions of ordered proteins and IDPs are very different, with disordered proteins being systematically enriched in disorder-promoting residues (A, R, G, Q, S, E, K and P) and depleted in order-promoting residues (W, Y, F, I, L, V, C and N) [38,39]. The results of this analysis are shown in Fig. 3A, which illustrates that Jaburetox is depleted in major order-promoting amino acids and enriched in

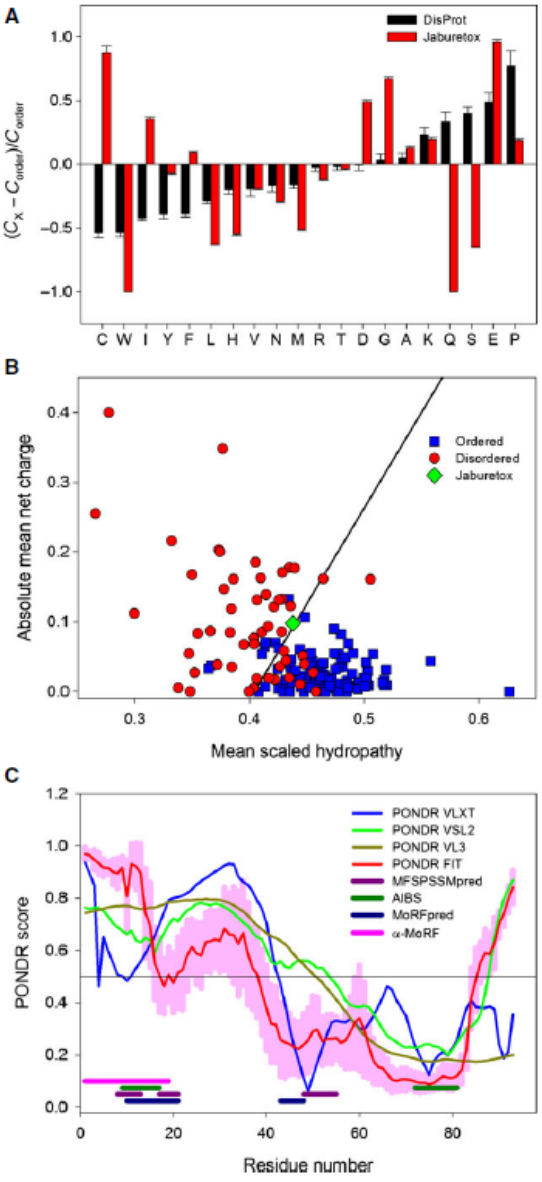

Fig. 3. Evaluation disorder propensity of Jaburetox. (A) Compositional analysis of Jaburetox in comparison with the composition of typical ordered proteins. The compositional profile of typical IDPs from the DisProt database is shown for comparison (black bars). Positive bars correspond to residues found more abundantly in Jaburetox than in ordered proteins, whereas negative bars show residues in which Jaburetox is depleted. (B) Charge–hydropathy plot for Jaburetox; data for ordered and disordered proteins are shown as blue squares and red circles, respectively, whereas the position of Jaburetox is shown as a green diamond. The black line represents a boundary separating compact and extended proteins. (C) Evaluating the per-residue intrinsic disorder propensity of Jaburetox using four members of the PONDR family: PONDR VL-XT (blue line), PONDR VSL2 (green line), PONDR VL3 (dark yellow line), PONDR-FIT (red line); sections with scores higher than 0.5 correspond to disordered regions. Light pink shadow around the PONDR-FIT line corresponds to standard errors of disorder prediction by PONDR-FIT. Location of potential binding sites predicted by MFSPSSMPRED, ANCHOR, general MORFPRED and α-MORF-PRED are shown as bold dark pink, dark green, dark blue and pink bars respectively.

some disorder-promoting residues, particularly D, G, A, K, E and P, relatively to typical ordered proteins. Also, the Uversky plot of mean net absolute charge versus mean hydrophobicity [40] (access to which is available at the PONDR® website http://www.pondr.com [41]) indicated that this protein is predicted as disordered even though it lies close to the boundary between proteins predicted to be extended and compact (Fig. 3B). Analysis of the per-residue disorder propensity of Jaburetox by a family of PONDR predictors revealed the presence of long disordered regions in this protein (PONDR scores above 0.5), especially in its N-terminal part (Fig. 3C).

It is known that protein–protein interactions are commonly mediated by disordered regions that undergo disorder to order transitions as a result of binding. Amino acid sequences of such disordered binding regions contain specific signals that can be identified by several specialized computational tools, such as A-MORF-PRED [42,43], general MORFPRED [44], MFSPSSMPRED [45] and ANCHOR [46]. Figure 3C shows that Jaburetox contains several potential disorder-based binding sites, such as α-MoRFs, general MoRFs, sites identified by MFSPSSMPRED and ANCHOR-indicated binding sites (AiBSs), which completely or partially overlap with each other. A larger agreement is observed among the various tools in the case of a potential binding site located in the N-terminal region (residues 1–21) compared to that found in the central portion (residues 43–55) or in the C-terminal region (residues 72–81). This is probably due to the fact that the potential binding site at the N terminus has a stronger α-helical signal, which is recognized by the computational tools used in this study.

The presence of these potential disorder-based binding sites is an indication that one of the functions of the disordered Jaburetox might be related to providing an interaction platform with various binding partners. Notably, earlier studies revealed that the majority of the biological activity of this protein resides preva-

lently in the N-terminal portion of Jaburetox [23], as opposed to the β-hairpin presumably located within the C-terminal portion [17,19,22]. In order to derive experimental structural information for Jaburetox, NMR spectroscopy was applied.

Assignment of the NMR spectra of Jaburetox

Figure 4 shows the ^{1}H-^{15}N heteronuclear single quantum coherence (HSQC) spectrum of Jaburetox. The spectrum is characterized by low signal dispersion in the proton dimension, indicative of a disordered state of the protein. Heteronuclear 2D and 3D triple resonance NMR spectra of Jaburetox were recorded and analyzed, and the assignment of the chemical shifts of backbone ^{1}H, ^{15}N and ^{13}C nuclei was obtained using the scalar connectivities derived by a computer-assisted resonance assignment software (CARA) [47], following a standard sequential assignment procedure. The identification of backbone ^{1}HN and ^{15}N amide peaks was obtained for 84 of the expected 86 residues of the protein, corresponding to 97.7% (not counting P3, P38, P41, P47 and P57, in addition to M1, usually featuring an $-NH_3^+$ group and not readily observable because of exchange with solvent, and G2, which is placed between the two unassigned residues M1 and P3). Residues E14, D61 and D77 were tentatively assigned based on their chemical shifts. The only unassigned residues were E49 and K62. Nearly complete assignments were achieved for the other backbone nuclei (100% for $^{13}C\alpha$, 100% for $^{13}C\beta$ and 85.2% for ^{13}CO) while side chain assignments are complete to 80.2% considering only aliphatic ^{1}H and ^{13}C nuclei. The resonance assignments were deposited in the BioMagResBank (http://www.bmrb.wisc.edu) under accession number 19830.

Secondary structure propensity of Jaburetox from NMR chemical shifts

Disordered proteins tend to feature only few long-range tertiary contacts, and therefore local structural constraints on the backbone are important in order to describe the ensemble of possible conformers of the protein. In this perspective, the structural information encoded in the chemical shifts of backbone nuclei has emerged as a key indicator of IDP ensemble properties [48]. Therefore, the experimental chemical shifts of backbone Cα, Cβ and Hα nuclei of Jaburetox were used to predict the residue-specific secondary structure propensity (SSP) for this polypeptide in solution using the program SSP [49]. A positive SSP score indicates a propensity for α-structure, while a negative score indicates a propensity for β-structure or extended loops. Residues in fully formed α-helices and β-strands are given scores of +1 and −1, respectively. Figure 5A

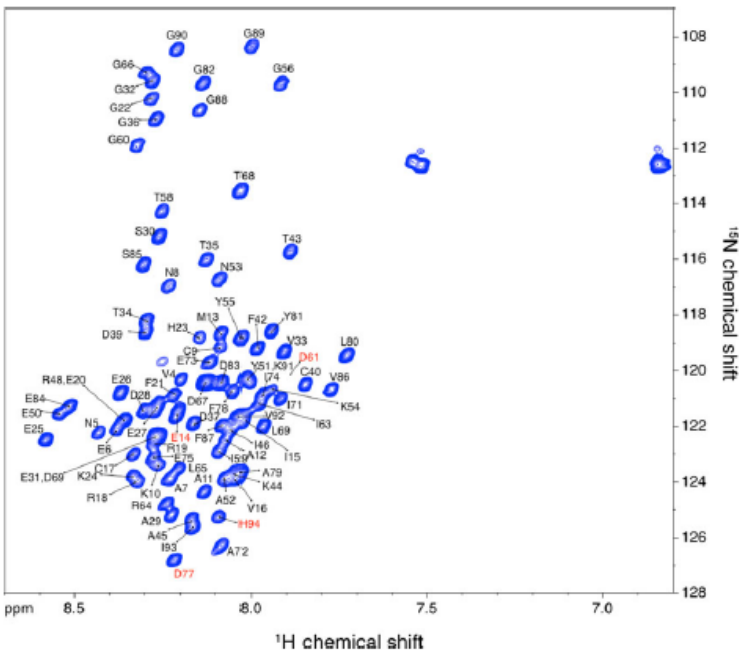

Fig. 4. *In vitro* NMR spectrum of Jaburetox. 800 MHz ^{1}H-^{15}N HSQC spectrum of Jaburetox in 90% H_2O, 10% D_2O, pH 6.5, T = 298 K. Assigned cross-peaks are labeled with one-letter amino acid type and sequence number. Tentatively assigned residues, as well as the initial histidine of the His tag, are indicated by red labels.

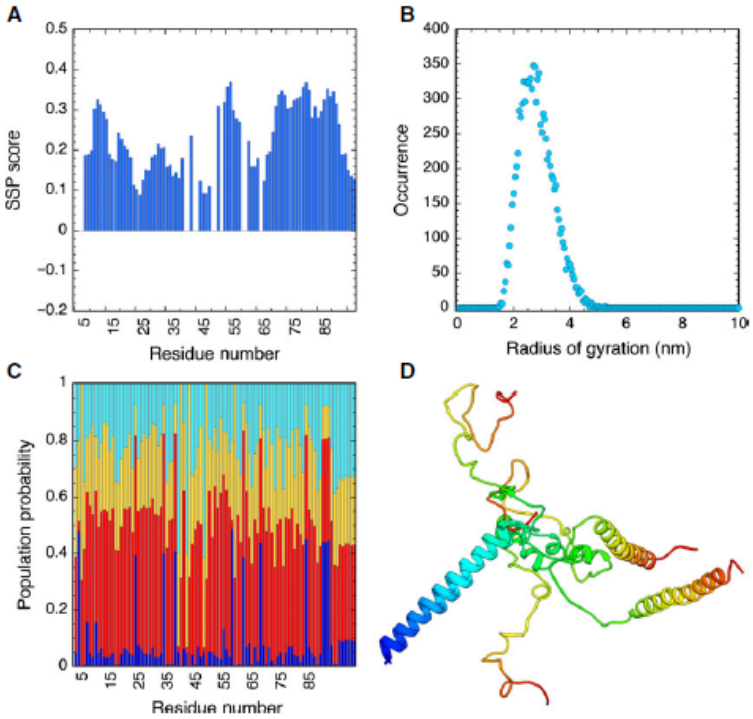

Fig. 5. Secondary structure of Jaburetox. (A) SSP scores calculated using Cα and Cβ chemical shifts for Jaburetox. Residues in fully formed α-helices and β-strands are expected to give scores of +1 and −1, respectively. (B) Radius of gyration distribution profile calculated for 10 000 conformers of Jaburetox using FLEXIBLE-MECCANO. (C) Population probability of secondary structure (cyan, β-sheet; yellow, polyproline II; red, α-helix; blue, random coil) calculated for 10 000 conformers of Jaburetox using FLEXIBLE-MECCANO. (D) Representative conformers of the structural clusters that are most populated by Jaburetox according to the FLEXIBLE-MECCANO/SSP analysis. Ribbons are colored from deep blue in the proximity of the N terminus to red at the C terminus. The structures are superimposed on residues 1–36 for clarity.

shows that Jaburetox is largely disordered, featuring only a small helical propensity, with slightly smaller SSP values in the N-terminal (larger predicted disorder) compared to the C-terminal portion (smaller predicted disorder). The average SSP score is 0.23 ± 0.08. Some correlation is observed between the SSP score based on chemical shifts and the score calculated using PONDR (Fig. 3). An analogous approach carried out using TALOS+ [50] did not yield any secondary structure with acceptable level of confidence, consistent with the picture obtained using SSP, suggesting a very small propensity to assume any organized secondary structure.

The results of the SSP analysis were used as input to calculate a structural ensemble representing Jaburetox in solution using FLEXIBLE-MECCANO [51]. This approach entails the use of amino acid specific statistical coil sampling to describe the unfolded state of the protein on the basis of the primary sequence; we further implemented the residue-by-residue conformational propensities, calculated by SSP as described above, into the calculation. The large range of gyration radii calculated using FLEXIBLE-MECCANO (Fig. 5B) suggests a largely diversified ensemble of conformers. The resulting average value of R_g (2.7 ± 0.7 nm), together with the hydrodynamic (Stokes, R_S) radius of 2.7 ± 0.1 nm determined experimentally using QELS (Fig. 1E), provides support for the nature of Jaburetox as an intrinsically disordered polypeptide that retains considerable residual structure in solution: indeed the R_g/R_S ratio is predicted to be ~ 0.775, ~ 0.9 or ~ 1.5 for proteins in a globular, pre-molten globular or fully unfolded state [52,53]. The probability of each residue existing in α-helix, β-sheet, polyproline II or random coil conformations was also calculated using FLEXIBLE-MECCANO (Fig. 5C), further supporting the preponderant presence of helices along the sequence, with slightly larger probability for helical propensity in the N-terminal portion of the polypeptide compared to the C-terminal region. Clustering analysis of the 10 000 structures of Jaburetox explicitly calculated using FLEXIBLE-MECCANO was performed using the g_cluster module of GROMACS 4.6 [54–57] and the GROMOS algorithm [58]. A 1.5 nm cutoff for the rmsd was used to include structures in the same cluster. A total of 71 clusters were identified, with the first five clusters accounting for 64% of the overall conformational ensemble. Figure 5D shows the superimposition of the representative structures of these five clusters selected by g_cluster. These show the consistent presence of an α-helix at the N terminus, of ~ 40 residues, followed by a coiled region of ~ 20 residues and by another ~ 40-residue long α-helix in the C-terminal region, observed in two

of the five most populated clusters covering ~ 42% of the overall ensemble. A parallel analysis performed with FLEXIBLE-MECCANO without the use of SSP scores yielded a structural ensemble characterized by the absence of conserved extended secondary structure elements. The consistency of the calculated structural ensemble, obtained using FLEXIBLE-MECCANO and SSP scores, with experimental data obtained using NMR-based distance constraints was tested by determining the structure of Jaburetox in solution.

Solution structure of Jaburetox by NMR

The 3D structure elucidation of folded proteins in solution relies on the availability of long-range distance information obtained from the nuclear Overhauser enhancement (NOE). Regions of the protein distant in the primary sequence but close in space in the folded structure give rise to NOEs that are utilized to determine the global fold. As expected, in the case of Jaburetox, no long-range interactions indicative of the presence of stable tertiary structure were observed. However, a few medium-range NOE constraints indicative of helical or turn-like structures were observed, corresponding to the regions V4–E20, R48–G56 and I63–I74. The solution structure of Jaburetox was calculated using CYANA based on geometrical constraints derived from these NOEs and dihedral angle constraints obtained from TALOS+ (Table 1). In total, 844 NOE-based upper distance limits and 12 φ and ψ torsion angles were used to derive the Jaburetox structure. The geometrical constraints and coordinate files of the Jaburetox structural ensemble were deposited in the Protein Data Bank under the accession code 2MM8. The NMR-derived solution structural ensemble of Jaburetox, featuring large values of rmsd, confirms its disordered fold, as predicted by earlier [23] and the present bioinformatics studies (Fig. 3). However, some elements of secondary structure are found in three different parts of this protein consistently for all structure conformers of the selected ensemble (Fig. 6, Table 1): a small α-helical motif at the N terminus (A12–V16), and two turn-like structures located in the middle of the protein (R48–G56) and at its C terminus (I63–E74). These regions with transient secondary structure coincide with the potential disorder-based binding sites identified by the bioinformatics analysis described above (Fig. 3C). The presence of these regions with more structured fold is consistent with the presence of a peak in the thermal shift assays that implies an unfolding process, highlighting the power of this methodology to predict the folding state of proteins. Figure 6 illustrates the Jaburetox structural ensemble with the lowest target function superimposed using the three different fragments with residual secondary structure. To allow a more detailed investigation of the structural organization of these regions, the structure of each fragment was calculated separately from the rest of the protein and further refined following the same protocols as for the full protein (Fig. 7, Table 1). Although bioinformatics analysis predicted a slightly longer N-terminal α-helix composed of 13 amino acids (V4–E20), in fact only five of them (A12–V16) were experimentally confirmed to be involved in the α-helix formation as indicated by the presence of the characteristic NOE distance constraints. The rest of the residues in this region (V4–A11) exhibited some α-helical propensity which, together with the backbone relaxation data, may suggest that the formation of a more extended α-helix in principle could take place in slightly different sample conditions.

Overall, the NMR-based structural ensemble of Jaburetox shows some features that are similar to the ensemble determined by FLEXIBLE-MECCANO using only sequence and secondary chemical shift information: the helical fragment found by NMR close to the N terminus is composed within the much longer helix predicted to exist using the FLEXIBLE-MECCANO/SSP approach but shows a reduced extension; concomitantly, the helical region suggested to appear in the C-terminal portion of Jaburetox is in fact absent in the structural family determined by distance and dihedral constraints by NMR, and only two short sequences with some consistent prevalence of a turn motif are found in the NMR structure. Overall, these observations can be interpreted as indicating an overestimation of the helical propensity in Jaburetox as derived from the combination of intrinsic sequence properties and chemical shift index. We speculate, however, that helical regions could indeed be formed under solution conditions so far unattained.

In order to explore the protein folding under more physiological conditions, the disordered nature of Jaburetox was investigated by in-cell NMR spectroscopy, a technique that allows the acquisition of structural data on biomolecules in the cytoplasm [59–62]. ^{1}H-^{15}N HSQC spectra were recorded on *E. coli* cells overexpressing Jaburetox upon induction with IPTG and growth in ^{15}N-labeled media. A typical spectrum, shown in Fig. 8, demonstrates that, although some modifications of the backbone are evident by chemical shift perturbations compared to the spectrum in solution (possibly derived from differences in the physical parameters of the milieu), Jaburetox disorder is preserved within the cell, and it is not an *in vitro* artifact

Table 1. Structural statistics and geometrical constraints derived from NMR for Jaburetox.

Restraints used in structure calculation	
NOE constraints for the full protein	844
NOE constraints for the V4–E20 fragment	190
NOE constraints for the R48–G56 fragment	63
NOE constraints for the I63–I74 fragment	168
Torsion angle constraints for the full protein	12
Structure statistics	
CYANA target function value for the full protein (Å^2)	281.52 ± 0.73
CYANA target function value for the V4–E20 fragment	44.7 ± 0.09
CYANA target function value for the R48–G56 fragment	11.8 ± 0.05
CYANA target function value for the I63–I74 fragment	65.8 ± 0.04
Mean global backbone rmsd for the full protein (Å)	9.36 ± 2.45
Mean global backbone rmsd for the V4–E20 fragment (Å)	0.31 ± 0.18
Mean global backbone rmsd for the R48–G56 fragment (Å)	1.07 ± 0.86
Mean global backbone rmsd for the I63–I74 fragment (Å)	0.70 ± 0.41
Mean global heavy atom rmsd for the full protein (Å)	10.43 ± 2.55
Mean global heavy atom rmsd for the V4–E20 fragment (Å)	1.11 ± 0.25
Mean global heavy atom rmsd for the R48–G56 fragment (Å)	2.41 ± 1.16
Mean global heavy atom rmsd for the I63–I74 fragment (Å)	1.35 ± 0.58
Amber energies (kcal·mol^{-1})	
Amber energy for the full-length protein	−1.98E+05
Amber energy for the V4–E20 fragment	−2.91E+04
Amber energy for the R48–G56 fragment	−2.37E+05
Amber energy for the I63–I74 fragment	−2.14E+04
PROCHECK *NMR Ramachandran statistics*	
Residues in favorable regions for the full-length protein (%)	32.9
Residues in favorable regions for the V4–E20 fragment (%)	22.9
Residues in favorable regions for the R48–G56 fragment (%)	66.7
Residues in favorable regions for the I63–E74 fragment (%)	12.5
Residues in allowed regions for the full-length protein (%)	55.3
Residues in allowed regions for the V4–E20 fragment (%)	43.6
Residues in allowed regions for the R48–G56 fragment (%)	16.7
Residues in allowed regions for the I63–E74 fragment (%)	31.2
Residues in generously allowed regions for the full-length protein (%)	9.4
Residues in generously allowed regions for the V4–E20 fragment (%)	19.3
Residues in generously allowed regions for the R48–G56 fragment (%)	0
Residues in generously allowed regions for the I63–E74 fragment (%)	42.5
Residues in disallowed regions for the full-length protein (%)	2.4
Residues in disallowed regions for the V4–E20 fragment (%)	14.3
Residues in disallowed regions for the R48–G56 fragment (%)	16.7
Residues in disallowed regions for the I63–E74 fragment (%)	13.8

caused by the purification process. Similarly, in-cell NMR experiments have been used to demonstrate that disorder is maintained in the case of α-synuclein over-expressed in *E. coli* cells [63] or for the tau-protein microinjected into *Xenopus* oocytes [64].

NMR studies of Jaburetox dynamics

The results of the computational and structural analyses of chemical shifts described above prompted us to investigate more directly the protein dynamics of Jaburetox using ^{15}N relaxation measurements. NMR relaxation parameters provide valuable insights into the internal molecular motions of unfolded or partially folded proteins. The ^{15}N relaxation rates R_1 and R_2 and the ^{1}H-^{15}N NOE values of all assigned backbone amide groups of Jaburetox were determined and are shown in Fig. 9A,B,C, respectively. The presence of local internal motions in the picosecond–nanosecond time scales contribute to the R_1, R_2 and NOE values, while conformational exchange processes occurring on the microsecond–millisecond time scale additionally contribute to increase the R_2 rates [65]. Therefore, the analysis of these parameters can provide information

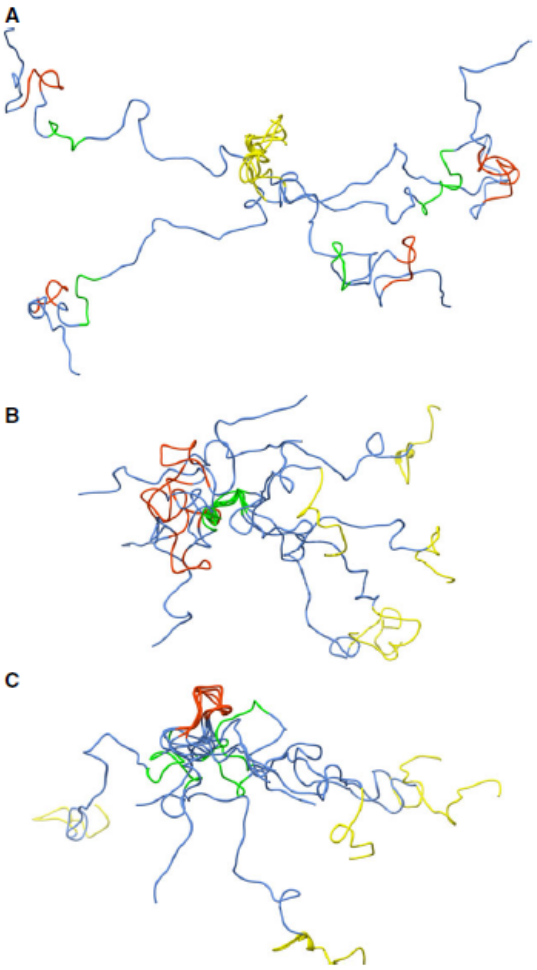

Fig. 6. Structure of Jaburetox by NMR. Ribbon scheme of the solution structure of Jaburetox calculated using CYANA, represented by the ensemble of five conformers with the lowest target function superimposed using three different and self-consistent protein fragments: (A) V4–E20, yellow; (B) R48–G56, green; (C) I63–I74, red. Figure made using CHIMERA [103].

on local backbone mobility of Jaburetox at different time scales. NOEs in particular are more sensitive to fast internal dynamics than R_1 and R_2 [66].

A qualitative analysis of the relaxation data for Jaburetox indicates that small NOE values are generally observed, indicative of a protein characterized by fast motion and high flexibility throughout the protein chain, consistently with the disordered nature of the protein revealed by the small chemical shift range of amide protons. The C-terminal region features larger NOE values compared to the N terminus, indicative of a relatively reduced mobility, in agreement with what is suggested by disorder predictions (see Fig. 3B). This difference somehow parallels the distinct biological activity of the two portions of Jaburetox, with the N terminus being involved in the toxicity of the protein against insects while the C terminus is not or less active [23]. Small or negative NOE values are found in the initial portion of the N terminus (4–10) and in the 30–40 region, indicating larger mobility in the nanosecond–picosecond time range. In the C-terminal region, several residues exhibit large values of R_2, which can be due either to a more structured conformation or to exchange processes occurring in the millisecond–microsecond time scale, or to both effects simultaneously.

A preliminary estimate of the rotational correlation time $\tau_m = 4.13 \pm 0.50$ ns was obtained according to $\tau_m = (1/2\omega_N)(6R_2/R_1 - 7)^{1/2}$ [67] using 14 experimental R_1 and R_2 relaxation rates selected by excluding residues characterized by significant internal mobility as shown by their small R_2 ($R_2 < (\bar{R}_2 - \sigma)$ and $(\bar{R}_2 - R_2)/R_2 > (\bar{R}_1 - R_1)/R_1$) and small NOE (NOE < 0.35). This value of τ_m was used to obtain a more accurate value by fitting the same 14 R_2/R_1 ratios to the general equation that correlates this ratio with the spectral densities assuming isotropic tumbling [66], an approach that yielded $\tau_m = 4.17 \pm 0.50$ ns. This value corresponds to a molecular mass of 7.0 ± 1.0 kDa estimated using the empirical relationship τ_m (ns) ~ 0.6 kDa determined for folded proteins [68]. This value supports the presence of the Jaburetox monomer in solution under the experimental conditions used, in agreement with the light scattering data reported above. The value estimated by NMR is slightly lower than expected, a difference possibly due to the large mobility of the protein that somehow simulates a smaller molecular mass.

Relaxation data were analyzed using the reduced spectral density mapping approach [69–72]. This represents a more suitable method than the model-free approach [73–76] because it does not make assumptions about the nature of the correlation function that describes the overall rotational diffusion, nor about the value of ^{15}N chemical shift anisotropy. In addition, it does not require knowledge of the protein structure, making it a more reliable approach in the case of IDPs. The spectral density function $J(\omega)$ describes the relative populations of HN bond vector fluctuations at different frequencies, namely at the frequency corresponding to the overall protein tumbling, as well as at ω_N and $0.87\omega_H$. $J(0)$ is influenced by low-frequency motions (nanoseconds) along with some fluctuations occurring on the millisecond to microsecond time scale arising from chemical exchange, $J(0.87\omega_H)$ is influ-

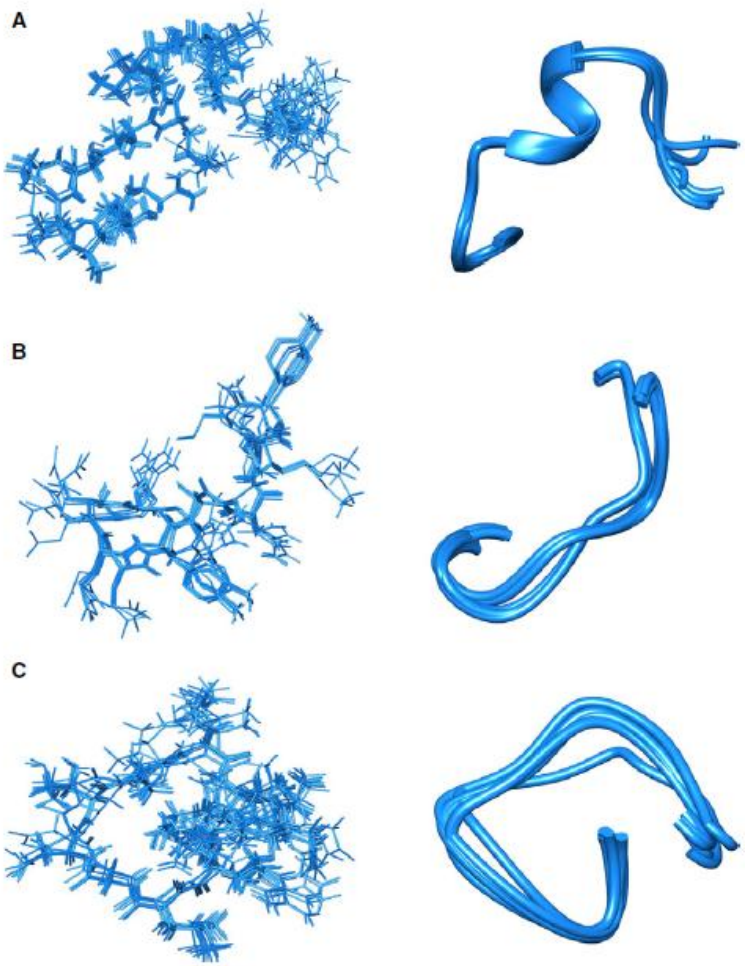

Fig. 7. Structure of Jaburetox ordered portions by NMR. Superimposition of the 10 conformers with the lowest target function represented as sticks (left panel) and ribbon (right panel) for the Jaburetox fragments V4–E20 (A), R48–G56 (B), I63–I74 (C). Figure made using CHIMERA [103].

enced by high-frequency motions (picoseconds) and $J(\omega_N)$ is the most sensitive to motions in the intermediate time scale. The results of this analysis are shown in Fig. 9D,E,F. Smaller than average values of $J(0)$ are observed in the N-terminal region of Jaburetox compared to the C-terminal region, indicating faster motions. $J(\omega_N)$ is particularly small at the beginning of the protein sequence, highlighting even faster dynamics. In the C-terminal region, a few residues display much higher values of $J(0)$, suggesting a contribution from conformational exchange phenomena. Consistently, $J(0.87\omega_H)$ decreases progressively from the N to the C terminus, paralleling a decrease of internal mobility. The possibility exists that exchange with the solvent, in addition to conformational processes, could influence the accurate determination of the relaxation times. Therefore, this treatment only provides a qualitative picture of the protein dynamics of Jaburetox and a comparative view of mobility along the protein sequence.

Discussion

The determination of the solution structure of plant proteins and peptides with insecticidal and/or antifungal activities is poorly explored in the literature. Some examples of antifungal polypeptides studied by NMR are Psd1, a 46-residue recombinant defensin from *Pisum sativum* [77,78], Rs-AFP1, a 51-residue defensin isolated from seeds of *Raphanus sativus* L. [79], Ib-AMP1, a 20-residue peptide derived from seeds of *Impatiens balsamina* [80], and EAFP2, a 41-residue polypeptide from *Eucommia ulmoides* [81]. Other plant-derived insecticides structurally characterized by

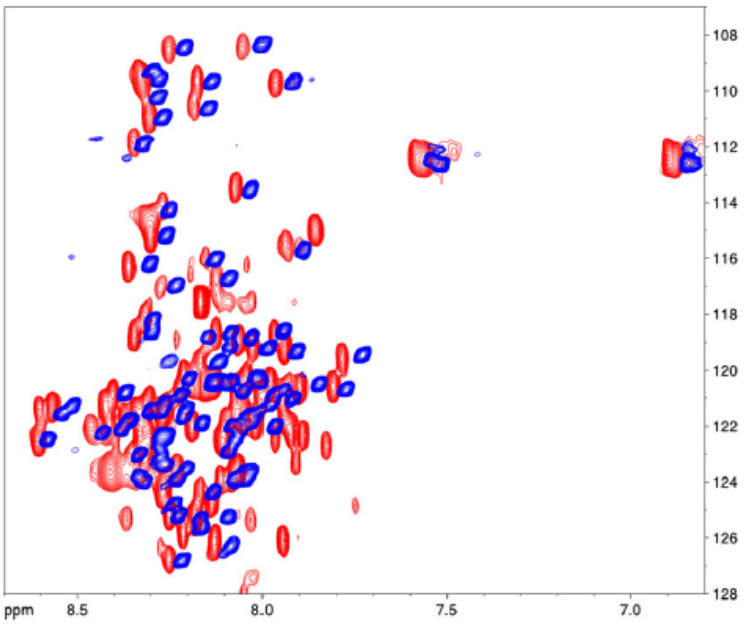

Fig. 8. In-cell NMR spectrum of Jaburetox. 950 MHz ^{1}H-^{15}N HSQC spectrum of Jaburetox-expressing *E. coli* cells induced with IPTG (shown in red) overlapped with the spectrum of isolated Jaburetox in solution (in blue). The experimental conditions are described in the text.

NMR are *Vigna radiata* VrD1, a plant defensin [82], Kalata B2, a cyclic peptide extracted from *Oldenlandia affinis* [83], PA1b, a 37-residue cysteine-rich plant defense peptide isolated from *P. sativum*, and NaD1, a 47-residue polypeptide isolated from flowers of *Nicotiana alata* [84]. In all these cases, a stable secondary and tertiary structure was determined.

In this work, we determined the solution properties of Jaburetox, characterizing this polypeptide as an IDP. We further used solution NMR spectroscopy, a powerful tool for studying IDPs [85–88], to establish the properties of the structural ensemble of Jaburetox conformations.

Considering the membrane-disturbing properties of Jaburetox [19,23,24], we would expect that the polypeptide would change its conformation to a folded state when in contact with membranes. The full assignment of Jaburetox reported here will allow us to perform NMR studies of this toxic polypeptide in contact with lipid micelles mimicking insect and fungus membranes [78], determining changes in its conformation properties based on modifications of the ^{1}H-^{15}N HSQC spectrum. Many IDPs are known to bind efficiently to artificial and natural membranes and this interaction is accompanied by a dramatic increase in their α-helical content [89]. It may be also that these conformational changes will not happen, since there are some IDPs that do not require protein folding to be active. Indeed, function can arise from any of these conformations and transitions between them [33,90]. With the currently established NMR assignment of Jaburetox, the study of its interaction with different targets is now possible, aiming to find a receptor to Jaburetox in insects and fungi.

Current efforts in our laboratories are aimed at further exploring the folding state of Jaburetox in *E. coli* cells, as well as *in vitro* in the presence of different crowding agents, membranes and non-interacting proteins, in order to understand whether some part of the protein undergoes significant conformational change in the cellular environment. In addition, we are setting up a method to determine the protein structure in cells of transgenic soybean plants that express the peptide using NMR spectroscopy.

The structural characterization of Jaburetox as an IDP is an important step towards understanding its toxic properties. Besides the structural peculiarities, the use of NMR, a powerful tool, could help us go further to unravel the pathways involved in the toxicity of Jaburetox, paving the way to exploring the potential applications for this naturally occurring polypeptide.

Materials and methods

Jaburetox production and purification

E. coli BL21(DE3) (Novagen, Madison, WI, USA) cells were transformed by heat shock with the construct pET23a-*Jaburetox* that expressed a protein containing a six-histidine tag at the C terminus [20]. Jaburetox analyzed

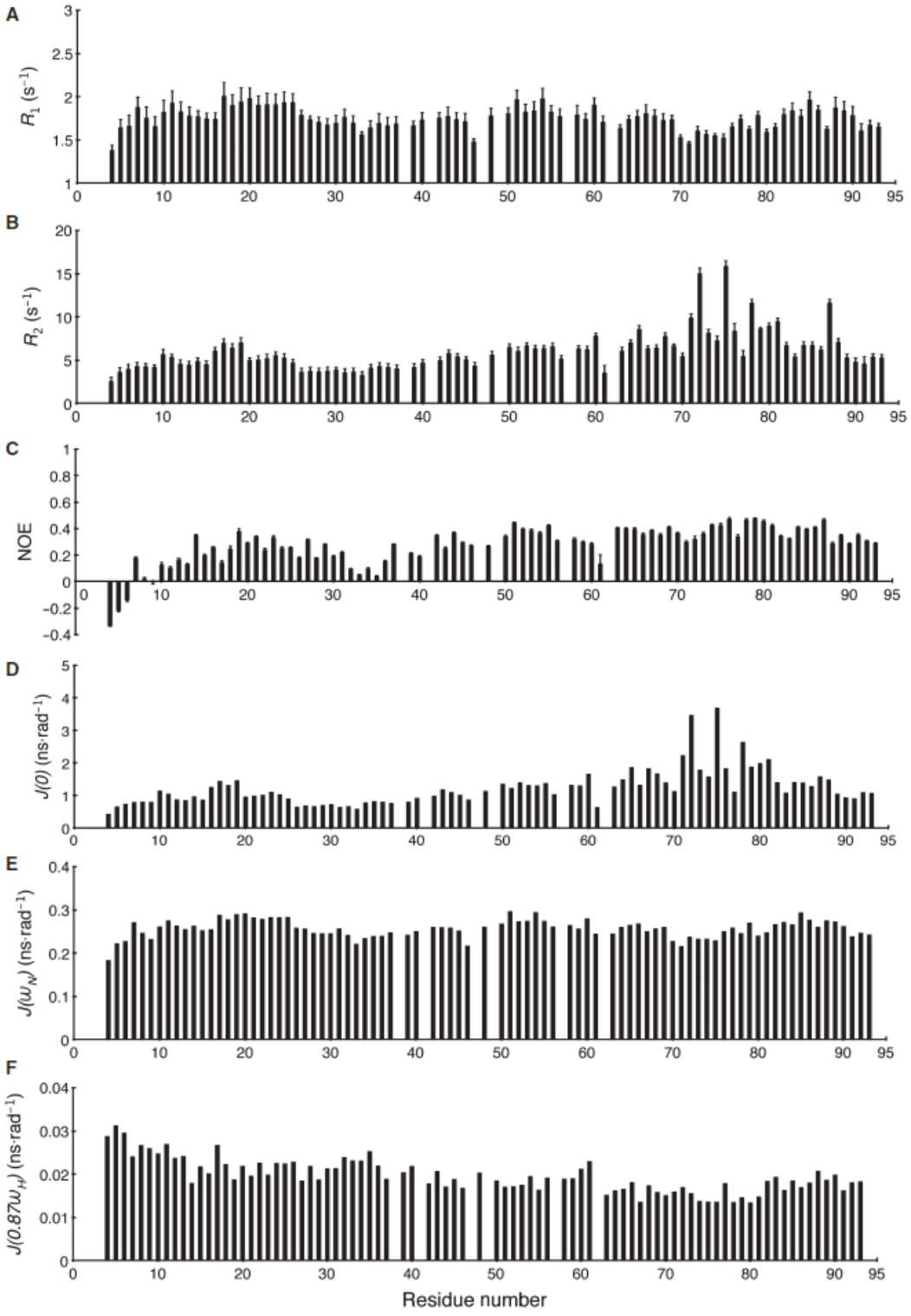
A
R_1 (s^{-1})
B
R_2 (s^{-1})
C
NOE
D
$J(0)$ (ns·rad^{-1})
E
$J(\omega_N)$ (ns·rad^{-1})
F
$J(0.87\omega_H)$ (ns·rad^{-1})
Residue number

in this study is the polypeptide corresponding to the residues 169–260 of the urease JBURE-II from *C. ensiformis* (UniProt ID Q8H6V8) containing the additional N-terminal methionine residue and the E195D substitution. Jaburetox expression was optimized in 25 mL cultures grown for 16 h, testing different values of temperature (16, 19, 26, 33 and 37 °C) and IPTG concentration (0.1, 0.23, 0.55, 0.87 and 1.0 mM) using a methodology that involved a total of 12 experiments to map a calculated response surface [91]. In all cases, the cells obtained after centrifugation (4500 ***g***) were incubated for 30 min at room temperature in 300 μL of 50 mM Tris/HCl buffer at pH 7.8, containing 60 μg of lysozyme, 6 μg of DNase and 0.3 mM $MgCl_2$. The resulting suspension of cell lysate and membranes was centrifuged to remove cell debris, and the supernatant was added to 50 μL of a slurry of Ni^{2+}-loaded Sepharose FF (GE Healthcare) resin. The yield of soluble Jaburetox produced under the different growth conditions was then quantified by evaluating the amount of protein bound to the resin using SDS/PAGE in 12% polyacrylamide gels and the software IMAGEJ 1.47 (National Institutes of Health, Bethesda, USA). The regression and graphical analysis of the data were performed using the STATISTICA 6.0 software (Statsoft, USA). After the best conditions for protein expression were selected, a recombinant cell pre-inoculum of 50 mL was cultured overnight, at 37 °C and 150 r.p.m., in 20 mL LB broth, supplemented with 1% glucose and 50 $\mu g \cdot mL^{-1}$ of carbenicillin. Subsequently, cells were inoculated in 1 L of LB broth containing 50 $\mu g \cdot mL^{-1}$ of carbenicillin and grown at 37 °C, 150 r.p.m., until D_{600} was 0.6–0.7. Cells were collected by centrifuging the culture at 4500 ***g*** for 30 min, and then the cells were resuspended in 250 mL of an M9 salt solution (6 $g \cdot L^{-1}$ Na_2HPO_4, 3 $g \cdot L^{-1}$ KH_2PO_4, 0.5 $g \cdot L^{-1}$ NaCl, 0.246 $g \cdot L^{-1}$ $MgSO_4$) and centrifuged again. The cell pellet was finally resuspended in 250 mL of M9 medium supplemented with 1.25 $g \cdot L^{-1}$ of $(NH_4)_2SO_4$ and 4 $g \cdot L^{-1}$ of glucose. Protein expression was induced after 1 h by addition of IPTG to a final concentration of 0.87 mM in the presence of 50 $\mu g \cdot mL^{-1}$ carbenicillin [25]. Cells expressing the protein were cultured for an additional 16 h at 20 °C. For isotope-labeled samples used in NMR experiments, 99% ^{13}C-labeled glucose and 98% ^{15}N-labeled ammonium sulfate (Sigma Aldrich) were used.

Cells were harvested by centrifugation at 11 300 ***g*** for 10 min at 4 °C and resuspended in 30 mL of buffer A (50 mM Tris/HCl buffer, pH 7.5, 500 mM NaCl) containing 5 mM imidazole and 200 $\mu g \cdot mL^{-1}$ lysozyme. The cell suspension was incubated at room temperature for 20 min, and then DNase I (20 $\mu g \cdot mL^{-1}$) was added followed by an additional incubation at 37 °C for 20 min. Subsequently, the cells were passed three times through a French pressure cell (SLM, Aminco) at 20 000 $lb \cdot in^{-2}$. The supernatant was separated by centrifugation at 27 200 ***g*** for 40 min at 4 °C and loaded onto a Ni^{2+}-loaded 5 mL His-Trap HP column (GE Healthcare), previously equilibrated with buffer A. Unbound proteins were washed from the column using 10 volumes of buffer A at a flow rate of 1 $mL \cdot min^{-1}$. Elution of Jaburetox was performed using 100 mL of a gradient of buffer A containing 5–500 mM imidazole. The fractions containing Jaburetox were collected, concentrated and loaded onto a Superdex 75 16/60 column (GE Healthcare) pre-equilibrated with buffer B (50 mM phosphate pH 7.5, 1 mM EDTA and 1 mM TCEP) and eluted at a flow rate of 1 $mL \cdot min^{-1}$. Sample purity was assessed by SDS/PAGE using NuPAGE Novex 12% Bis-Tris gels (Life Technologies) stained with ProBlue Safe Stain (Giotto Biotech). Fractions containing the protein were pooled and protein concentration was measured by Bradford assay [92].

Computational analysis of the intrinsic disorder propensity of Jaburetox

To better understand and visualize the relationships between sequence peculiarities and propensity for intrinsic disorder, the amino acid composition of the Jaburetox was analyzed using a tool developed for visualizing amino acid composition biases in proteins [39]. To this end, the fractional difference in amino acid compositions between Jaburetox and a set of representative ordered proteins with low mutual sequence identity [93] selected from the PDB [94], as well as the fractional difference in amino acid compositions between the latter group and a set of typical experimentally validated IDPs from the DisProt database [95], were calculated for each amino acid residue. The fractional difference is calculated as $(C_X - C_{order})/C_{order}$ values, where C_X is the content of a given residue in a protein/protein set of interest (Jaburetox or typical disordered proteins) and C_{order} is the corresponding value for the sample set of ordered proteins from the PDB [39]. Positive and negative values indicate residues in a given set that have more and less order, respectively. Confidence intervals were estimated using per-protein bootstrapping with 10 000 iterations.

Four different disorder predictors of the PONDR family evaluated the intrinsic disorder propensity of Jaburetox: (a) PONDR VL-XT [41], which applies various compositional probabilities and hydrophobic measures of amino acid as the input features of artificial neural networks for the prediction; although it is no longer the most accurate predictor, it is very sensitive to the local compositional biases and is thus capable of identifying potential molecular interaction motifs; (b) PONDR VSL2B [96], which is suitable for accurate evaluation of short and long disordered regions;

Fig. 9. Dynamics of Jaburetox by NMR. Backbone amide ^{15}N relaxation properties recorded at 298 K and 18.8 T on ^{15}N-labeled Jaburetox. (A) Longitudinal R_1 relaxation rate; (B) transverse R_2 relaxation rates; (C) steady-state heteronuclear ^1H-^{15}N NOE; values of $J(0)$ (D), $J(\omega_N)$ (E) and $J(0.87\omega_{H})$ (F) resulting from a reduced spectral density analysis of the relaxation data for Jaburetox.

(c) PONDR VL3 [97], which is suitable for finding long disordered regions; (d) PONDR-FIT [98], a meta-predictor that combines the six individual PONDR predictors VL-XT, VSL2, VL3, FoldIndex, IUPred and TopIDP; PONDR-FIT is moderately more accurate than each of the component predictors. Access to these predictors is provided by the DisProt database (http://www.disprot.org/metapredictor.php).

Molecular recognition features (MoRFs), defined as short order-prone motifs within a long disordered region and able to undergo disorder to order transitions during the binding to a specific partner, usually have much higher content of aliphatic and aromatic amino acids than disordered regions in general. Due to these peculiarities, MoRF regions are frequently observed as sharp dips in the corresponding plots representing per-residue distribution of PONDR VL-XT disorder scores. Hence, based on the PONDR VL-XT prediction and a number of other attributes (such as helical propensity), the α-MoRF regions in Jaburetox could be identified [42,43]. Intrinsically disordered regions can fold, upon interaction with specific binding partners, not only to α-helical but also to β-strand, irregular or complex structures; therefore another computational tool, MORFPRED, was used to find all MoRF types in Jaburetox (α, β, coil and complex) [44]. The MFSPSSMPRED tool was additionally used, which is a masked, filtered and smoothed position-specific scoring matrix-based predictor for finding potential MoRF regions in disordered proteins based on contextual local evolutionary conservation [45]. Finally, additional potential binding sites in Jaburetox were identified by the ANCHOR algorithm [46]. This approach relies on the pairwise energy estimation approach developed for the general disorder prediction method IUPRED, being based on the hypothesis that long regions of disorder contain localized potential binding sites that cannot form enough favorable intra-chain interactions to fold on their own, but are likely to gain stabilizing energy by interacting with a globular protein partner. Here we are using the term ANCHOR-indicated binding site (AIBS) to identify a region of a protein suggested by the ANCHOR algorithm to have significant potential to be a binding site for an appropriate but typically unidentified partner protein.

Hydrodynamic properties of Jaburetox

The molecular mass and hydrodynamic radius of Jaburetox in solution were determined using a combination of SEC, MALS and QELS. Jaburetox (140 μM, 400 μL) in buffer B was loaded onto a Superdex 75 10/300 GL column (GE Healthcare), pre-equilibrated with the same buffer, and eluted at room temperature at a flow rate of 0.6 mL·min^{-1}. The column was connected downstream to a multi-angle laser light (690.0 nm) scattering (MALS) DAWN EOS photometer and to a 90° angle quasi-elastic (dynamic) light scattering (QELS) device (Wyatt Technology). The concentration of the eluted protein was determined using a refractive index detector (Optilab DSP, Wyatt). Values of 0.185 mL·g^{-1} for the refractive index increment (dn/dc) and of 1.330 for the solvent refractive index were used. Molecular masses were determined from a Zimm plot, using the Zimm equation [99] with a fitting degree of 1. Data were analyzed using the ASTRA 4.90.07 software (Wyatt Technology), following the manufacturer's indications.

Circular dichroism spectroscopy

The CD spectra of Jaburetox (24 μM in 50 mM phosphate, pH 7.5) were measured using a Jasco 810 spectropolarimeter flushed with N_2 and a cuvette with 0.1 cm path length. The spectra were registered from 190 to 240 nm with 0.2 nm intervals, at 25 °C and 90 °C. Ten spectra for each condition were accumulated and averaged to achieve an appropriate signal-to-noise ratio. The spectrum of the buffer was subtracted. The web server CAPITO (CD Analysis and Plotting Tool, http://capito.nmr.fli-leibniz.de/index.php) [32] was used to evaluate the fold state (unfolded, pre-molten globule, molten globule and globular) of Jaburetox according to its CD spectrum.

Differential scanning fluorimetry

Differential scanning fluorimetry experiments were performed using the Slice pH (HR2-070) kit from Hampton Research (USA). The experiments were conducted in an Mx3000P qPCR system (Agilent). Fluorescent signals were acquired with excitation and emission wavelengths of 495 and 520 nm, respectively. Temperature scans were performed from 25 °C to 90 °C in 1 °C·min^{-1} increments. A solution of 500 × SYPRO Orange (Life Technologies) in 100% DMSO was prepared from the 5000 × stock solution and diluted 100-fold in MilliQ water to prepare the working solution (5×). Experiments were performed in a 96-well plate, each well containing 20 μL of final solution. The solutions were prepared with 2 μL kit buffer (final concentration 100 mM), 2 μL Jaburetox (final concentration 6.4 μM) and 4 μL SYPRO Orange 5 × working solution [100]. The fluorescence data were acquired and the curves were analyzed using the ORIGIN PRO8 software (1991–2007 Origin Lab Corporation). The melting temperatures (T_m) for every condition were calculated from the first derivative of the melting peak.

NMR spectroscopy data collection and analysis for backbone assignment

NMR spectra were acquired at 298 K on a Bruker Avance 800 spectrometer, operating at the proton nominal frequency of 800.13 MHz (18.8 T) on NMR samples containing 1 mM of ^{15}N and ^{13}C uniformly labeled Jaburetox in 50 mM phosphate buffer, pH 6.5, 1 mM EDTA, 1 mM

TCEP, in 90% H_2O/10% D_2O. The spectrometer was equipped with a TXI 5-mm triple resonance cryo-probe with pulsed field gradients along the *z*-axis, using the acquisition parameters provided in Table 2. 2D ^{15}N-^{1}H HSQC, 2D ^{1}H-^{13}C HSQC, 3D HNCA, HNcoCA, HNCACB, HNcoCACB, HNCO, HNcaCO, HCCH-TOCSY and ^{15}N-^{1}H/^{13}C-^{1}H NOESY experiments were used to obtain the sequential backbone and side chain resonance assignment. In these pulse schemes, water suppression is achieved using selective pulse and transverse signal cancellation with pulsed field gradients associated with a flip-back pulse. The NMR data were processed using TOPSPIN 3.2 (Bruker BioSpin). Spectral analysis for resonance assignment was performed using CARA 1.8.4.2 [47].

NMR spectroscopy data collection and analysis for backbone mobility

The experiments for the determination of ^{15}N longitudinal ($R_1 = 1/T_1$) and transverse ($R_2 = 1/T_2$) relaxation rates, and of the ^{1}H-^{15}N cross-relaxation rate measured via steady-state heteronuclear ^{1}H-^{15}N NOE, were acquired on a Bruker Avance 800 spectrometer, operating at the proton nominal frequency of 800.13 MHz (18.8 T) using NMR samples containing 1 mM of ^{15}N-labeled Jaburetox in 50 mM phosphate buffer, pH 6.5, 1 mM EDTA, 1 mM TCEP, in 90% H_2O/10% D_2O at 298 K, using phase-sensitive gradient-enhanced sequences (Table 2) [66,70]. In these pulse schemes, water suppression is achieved using selective pulse and transverse signal cancellation with pulsed field gradients with a flip-back pulse in order to avoid saturation of water magnetization that could affect the NOE values of solvent-exposed backbone amide protons. The NMR experiments used to measure relaxation rates consist of a series of ^{1}H-^{15}N HSQC experiments in which spectra are acquired at different time intervals after the radiofrequency pulse. T_1 measurements were based on inversion-recovery type experiments recorded using 10 different delays: 10, 150, 300, 450, 600, 750, 900, 1150, 1300 and 1500 ms. T_2 measurements were carried out using Carr–Purcell–Meiboom–Gill (CPMG) spin-echo pulse sequences recorded with 10 different delays prior to the 180° refocusing pulse: 16, 50, 100, 130, 160, 200, 250, 300, 350 and 400 ms. Recycle delays of 4 s were used in both experiments. ^{1}H-^{15}N NOE values were obtained recording two sets of spectra in the presence and absence of a 6 s proton saturation period. The two spectra were recorded in an interleaved manner to ensure identical conditions in the two experiments. Spectra were processed using TOPSPIN 3.2 (Bruker BioSpin) and peak intensities were analyzed using DYNAMICS CENTER 2.1.5 (Bruker BioSpin). The values of R_1 and R_2 were calculated by fitting the peak intensities in ^{1}H-^{15}N HSQC spectra acquired at different relaxation delays to a two-parameter exponential decay function, using a nonlinear Marquard algorithm. The errors on the parameters derived from the fit were estimated from the inverse of the weighted curvature matrix, using a confidence level of 95%. The heteronuclear NOE values were estimated as the ratio of the intensities in the saturated versus non-saturated spectra. In all cases, the uncertainty on the intensities was derived from the standard deviation of the noise in each spectrum. The DYNAMICS CENTER 2.1.5 (Bruker BioSpin) software was used to carry out the quantitative analysis of the relaxation data.

Calculation of the structure of Jaburetox using NMR spectroscopy

NOE cross-peaks were identified, assigned and integrated in ^{15}N-edited and ^{13}C-edited 3D NOESY-HSQC spectra

Table 2. NMR acquisition parameters of Jaburetox.

Experiment	Label	Sequence	TD	SI	SW (ppm)
^{1}H-^{15}N HSQC	^{15}N	hsqcfpf3gpphwg	1024 × 256	1024 × 1024	11.2 × 40
^{1}H-^{13}C HSQC	^{13}C	hsqcctetgpsisp	1536 × 256	1024 × 512	11.2 × 76
HNCA	^{15}N/^{13}C	hncagp3d	1024 × 64 × 110	512 × 64 × 128	11.2 × 22 × 44
HNCO	^{15}N/^{13}C	hncogp3d	1024 × 32 × 96	1024 × 32 × 128	11.2 × 36 × 9.2
CBCAcoNH	^{15}N/^{13}C	cbcaconhgp3d	1024 × 64 × 128	512 × 64 × 128	11.2 × 22 × 62
HNCACB	^{15}N/^{13}C	hncacbgp3d	1024 × 64 × 128	512 × 64 × 128	11.2 × 22 × 62
HNcoCA	^{15}N/^{13}C	hncocagp3d	1024 × 64 × 110	512 × 64 × 128	11.2 × 22 × 44
HNCACO	^{15}N/^{13}C	hncacogp3d	1024 × 32 × 96	512 × 32 × 64	11.2 × 36 × 9.2
HCCH-TOCSY	^{15}N/^{13}C	hcchdigp3d2	1536 × 64 × 128	1024 × 64 × 128	11.2 × 76 × 76
^{13}C-NOESY	^{15}N/^{13}C	noesyhsqcetgp3d	1536 × 56 × 164	1024 × 64 × 128	11.2 × 76 × 11.2
^{15}N-NOESY	^{15}N/^{13}C	noesyhsqcf3gp193d	1536 × 48 × 236	512 × 64 × 256	11.2 × 22 × 11.2
^{1}H-^{15}N HSQC (for R_1)	^{15}N	hsqct1etf3gpsi	1536 × 256	2048 × 1024	11.2 × 22
^{1}H-^{15}N HSQC (for R_2)	^{15}N	hsqct2etf3gpsi	1536 × 256	1024 × 1024	11.2 × 22
^{1}H-^{15}N HSQC (for NOEs)	^{15}N	hsqcnoef3gpsi	1536 × 512	2048 × 1024	11.2 × 22
^{1}H-^{15}N HSQC (for in-cell NMR)	^{15}N	sfhmqcf3gpph	1024 × 128	2048 × 128	16 × 50

TD is the total number of real+imaginary points collected. SI is the total number of real+imaginary points before the Fourier transform. SW is the spectral width.

using CARA 1.8.4.2 [47]. The CALIBA subroutine in CYANA 2.1 (www.cyana.org) was used to convert cross-peak intensities to distance constraints. Dihedral angle constraints were derived using TALOS+ [50]. The structure was calculated using the torsion angle dynamics program CYANA 2.1. A total of 100 random conformers were annealed in 8000 steps using NOE and dihedral angle constraints. Five conformers were selected on the basis of their lowest and consistent target function values. Their structures were placed in truncated octahedral water boxes using a 10-Å thick buffer zone of solvent around the protein. The Amber ff99SB force field [101] for the protein and the TIP3P water model [102] were used. Ions were added to reproduce the experimental ion concentration used for NMR structures. Each system was geometry optimized using GROMACS 4.6 [54–57]. The quality of the obtained structures was analyzed using the PROCHECK PDB validation server (http://deposit.pdb.org/validate/).

NMR spectroscopy data collection in cell

BL21(DE3) *E. coli* cells expressing Jaburetox were grown in 70 mL of LB medium containing 100 $\mu g \cdot mL^{-1}$ ampicillin, at 28 °C for 16 h. Subsequently, cells were centrifuged at 2000 ***g*** for 15 min at 25 °C, and gently resuspended into 50 mL of M9 medium containing $(^{15}NH_4)_2SO_4$. After 15 min, protein overexpression was induced with 0.8 mM IPTG and continued for 4 h. Then, 25 mL of the cellular culture was centrifuged at 2000 ***g*** for 15 min and gently resuspended with 300 µL of M9 medium containing 10% v/v D_2O. The obtained NMR sample reached a final volume of 600 µL and contained a 50% v/v cellular suspension. NMR spectra were acquired at 310 K on a Bruker Avance 950 spectrometer operating at the proton nominal frequency of 950.20 MHz (22.3 T). The spectrometer was equipped with a TCI 5-mm cryo-probe with pulsed field gradients along the *z*-axis, using a SOFAST-HMQC pulse sequence and the acquisition parameters provided in Table 2.

Acknowledgements

Massimo Lucci and Enrico Luchinat are thanked for acquiring respectively *in vitro* and in-cell NMR spectra at the Center for Magnetic Resonance (Sesto Fiorentino, Italy). Dr Cristian Follmer is acknowledged for critically reading the first version of the manuscript.

Funding

This project was financed by the Brazilian agency Conselho de Aperfeiçoamento de Pessoal de Nível Superior (CAPES), Projeto Pesquisador Visitante PVE 054/2012, Ciências sem Fronteiras (Science without Borders). F.C.L received from CAPES a split PhD fellowship at the University of Bologna for this project. O.D. was supported by a fellowship financed by Specialty Fertilizer Products (Leawood, KS, USA). The research is partially funded by CIRMMP (Consorzio Interuniversitario di Risonanze Magnetiche di Metallo-Proteine) [104]. The WeNMR project (European FP7 e-Infrastructure grant, contract no. 261572, www.wenmr.eu) supported by the European Grid Initiative (http://www.egi.eu/) through the national GRID Initiatives of Belgium, France, Italy, Germany, the Netherlands, Poland, Portugal, Spain, UK, South Africa, Malaysia, Taiwan, the Latin America GRID infrastructure via the Gisela project (http://www.gisela-grid.eu/), the International Desktop Grid Federation (http://desktopgridfederation.org/) with its volunteers and the US Open Science Grid (http://www.opensciencegrid.org/) are acknowledged for the use of web portals, computing and storage facilities.

Author contributions

FCL produced and purified Jaburetox, and carried out differential scanning fluorimetry experiments; OD analyzed the NMR data, performed the assignment, and calculated the structural and dynamic properties of Jaburetox; RRG produced labeled Jaburetox for initial NMR studies; VB complemented experiments on differential scanning fluorimetry; VNU carried out the bioinformatics analysis; BZ carried out light scattering and CD experiments, and in-cell NMR; FM carried out computational analysis of the experimental and theoretical structures; SC processed and analyzed the NMR data; CRC and SC designed the research; all authors contributed to data analysis and wrote the paper.

References

1 Maroney MJ & Ciurli S (2013) Nonredox nickel enzymes. *Chem Rev* **114**, 4206–4228.
2 Mobley HLT & Hausinger RP (1989) Microbial urease: significance, regulation and molecular characterization. *Microbiol Rev* **53**, 85–108.
3 Karplus PA, Pearson MA & Hausinger RP (1997) 70 years of crystalline urease: what have we learned? *Acc Chem Res* **30**, 330–337.
4 Krajewska B (2009) Ureases I. Functional, catalytic and kinetic properties: a review. *J Mol Cat B: Enzymatic* **59**, 9–21.
5 Zambelli B, Musiani F, Benini S & Ciurli S (2011) Chemistry of Ni^{2+} in urease: sensing, trafficking, and catalysis. *Acc Chem Res* **44**, 520–530.

6 Sumner JB (1926) The isolation and crystallization of the enzyme urease. *J Biol Chem* **69**, 435–441.
7 Dixon NE, Gazzola TC, Blakeley RL & Zermer B (1975) Jack bean urease (EC 3.5.1.5). A metalloenzyme. A simple biological role for nickel? *J Am Chem Soc* **97**, 4131–4133.
8 Pires-Alves M, Grossi-de-Sá MF, Barcellos GB, Carlini CR & Moraes MG (2003) Characterization and expression of a novel member (JBURE-II) of the urease gene family from jackbean [*Canavalia ensiformis* (L.) DC]. *Plant Cell Physiol* **44**, 139–145.
9 Mulinari F, Becker-Ritt AB, Demartini DR, Ligabue-Braun R, Stanisçuaski F, Verli H, Fragoso RR, Schroeder EK, Carlini CR & Grossi-de-Sá MF (2011) Characterization of JBURE-IIb isoform of *Canavalia ensiformis* (L.) DC urease. *BBA-Proteins Proteom* **1814**, 1758–1768.
10 Follmer C, Barcellos GB, Zingali RB, Machado OL, Alves EW, Barja-Fidalgo C, Guimarães JA & Carlini CR (2001) Canatoxin, a toxic protein from jack beans (*Canavalia ensiformis*), is a variant form of urease (EC 3.5.1.5): biological effects of urease independent of its ureolytic activity. *Biochem J* **360**, 217–224.
11 Carlini CR & Guimarães JA (1981) Isolation and characterization of a toxic protein from *Canavalia ensiformis* (jack bean) seeds, distinct from concanavalin A. *Toxicon* **19**, 667–675.
12 Carlini CR, Oliveira AE, Azambuja P, Xavier-Filho J & Wells MA (1997) Biological effects of canatoxin in different insect models: evidence for a proteolytic activation of the toxin by insect cathepsin-like enzymes. *J Econ Entomol* **90**, 340–348.
13 Ferreira Da Silva CT, Gombarovits MEC, Masuda H, Oliveira CM & Carlini CR (2000) Proteolytic activation of canatoxin, a plant toxic protein, by insect cathepsin-like enzymes. *Arch Insect Biochem* **44**, 162–171.
14 Carlini CR & Grossi-de-Sá MF (2002) Plant toxic proteins with insecticidal properties. A review on their potentialities as bioinsecticides. *Toxicon* **40**, 1515–1539.
15 Staniscuaski F, Ferreira-DaSilva C, Mulinari F, Pires-Alves M & Carlini C (2005) Insecticidal effects of canatoxin on the cotton stainer bug *Dysdercus peruvianus* (Hemiptera: Pyrrhocoridae). *Toxicon* **45**, 753–760.
16 Defferrari MS, Demartini DR, Marcelino TB, Pinto PM & Carlini CR (2011) Insecticidal effect of *Canavalia ensiformis* major urease on nymphs of the milkweed bug *Oncopeltus fasciatus* and characterization of digestive peptidases. *Insect Biochem Molec* **41**, 388–399.
17 Mulinari F, Staniscuaski F, Bertholdo-Vargas L, Postal M, Oliveira-Neto O, Rigden D, Grossi-de-Sa M & Carlini C (2007) Jaburetox-2Ec: an insecticidal peptide derived from an isoform of urease from the plant *Canavalia ensiformis*. *Peptides* **28**, 2042–2050.
18 Stanisçuaski F, Te Brugge V, Carlini CR & Orchard I (2009) *In vitro* effect of *Canavalia ensiformis* urease and the derived peptide Jaburetox-2Ec on *Rhodnius prolixus* Malpighian tubules. *J Insect Physiol* **55**, 255–263.
19 Barros PR, Stassen H, Freitas MS, Carlini CR, Nascimento MA & Follmer C (2009) Membrane-disruptive properties of the bioinsecticide Jaburetox-2Ec: implications to the mechanism of the action of insecticidal peptides derived from ureases. *Biochim Biophys Acta* **1794**, 1848–1854.
20 Postal M, Martinelli AH, Becker-Ritt AB, Ligabue-Braun R, Demartini DR, Ribeiro SF, Pasquali G, Gomes VM & Carlini CR (2012) Antifungal properties of *Canavalia ensiformis* urease and derived peptides. *Peptides* **38**, 22–32.
21 Balasubramanian A & Ponnuraj K (2010) Crystal structure of the first plant urease from jack bean: 83 years of journey from its first crystal to molecular structure. *J Mol Biol* **400**, 274–283.
22 Balasubramanian A, Balaji N, Gautham N & Ponnuraj K (2013) Molecular dynamics simulation and molecular modelling studies on the insecticidal domain from jack bean urease. *Mol Simulat* **39**, 357–366.
23 Martinelli AH, Kappaun K, Ligabue-Braun R, Defferrari MS, Piovesan AR, Stanisçuaski F, Demartini DR, Dal Belo CA, Almeida CG, Follmer C *et al.* (2014) Structure-function studies on jaburetox, a recombinant insecticidal peptide derived from jack bean (*Canavalia ensiformis*) urease. *Biochim Biophys Acta* **1840**, 935–944.
24 Piovesan AR, Martinelli AH, Ligabue-Braun R, Schwartz J-L & Carlini CR (2014) *Canavalia ensiformis* urease, Jaburetox and derived peptides form ion channels in planar lipid bilayers. *Arch Biochem Biophys* **547**, 6–17.
25 Marley J, Lu M & Bracken C (2001) A method for efficient isotopic labeling of recombinant proteins. *J Biomol NMR* **20**, 71–75.
26 Iakoucheva LM, Kimzey AL, Masselon CD, Smith RD, Dunker AK & Ackerman EJ (2001) Aberrant mobility phenomena of the DNA repair protein XPA. *Protein Sci: Pub Protein Soc* **10**, 1353–1362.
27 Receveur-Brechot V, Bourhis JM, Uversky VN, Canard B & Longhi S (2006) Assessing protein disorder and induced folding. *Proteins* **62**, 24–45.
28 Kozlowska M, Tarczewska A, Jakob M, Szpotkowski K, Wojtas M, Rymarczyk G & Ozyhar A (2014) Calponin-like chd64 is partly disordered. *PLoS One* **9**, e96809.
29 Follmer C, Pereira FV, Da Silveira NP & Carlini CR (2004) Jack bean urease (EC 3.5.1.5) aggregation

monitored by dynamic and static light scattering. *Biophys Chem* **111**, 79–87.
30 Boivin S, Kozak S & Meijers R (2013) Optimization of protein purification and characterization using Thermofluor screens. *Protein Expr Purif* **91**, 192–206.
31 Uversky VN (2002) What does it mean to be natively unfolded? *Eur J Biochem* **269**, 2–12.
32 Wiedemann C, Bellstedt P & Görlach M (2013) CAPITO–a web server-based analysis and plotting tool for circular dichroism data. *Bioinformatics* **29**, 1750–1757.
33 Uversky VN (2009) Intrinsically disordered proteins and their environment: effects of strong denaturants, temperature, pH, counter ions, membranes, binding partners, osmolytes, and macromolecular crowding. *Protein J* **28**, 305–325.
34 Zambelli B, Cremades N, Neyroz P, Turano P, Uversky VN & Ciurli S (2012) Insights in the (un) structural organization of *Bacillus pasteurii* UreG, an intrinsically disordered GTPase enzyme. *Mol BioSyst* **8**, 220–228.
35 Corrêa DHA & Ramos CHI (2009) The use of circular dichroism spectroscopy to study protein folding, form and function. *African J Biochem Res* **3**, 164–173.
36 Anderson VL, Ramlall TF, Rospigliosi CC, Webb WW & Eliezer D (2010) Identification of a helical intermediate in trifluoroethanol-induced alpha-synuclein aggregation. *Proc Natl Acad Sci USA* **107**, 18850–18855.
37 Park SHS, Shalongo WW & Stellwagen EE (1997) The role of PII conformations in the calculation of peptide fractional helix content. *Protein Sci* **6**, 1694–1700.
38 Radivojac P, Iakoucheva LM, Oldfield CJ, Obradovic Z, Uversky VN & Dunker AK (2007) Intrinsic disorder and functional proteomics. *Biophys J* **92**, 1439–1456.
39 Vacic V, Uversky VN, Dunker AK & Lonardi S (2007) Composition Profiler: a tool for discovery and visualization of amino acid composition differences. *BMC Bioinformatics* **8**, 211–217.
40 Uversky VN, Gillespie JR & Fink AL (2000) Why are "natively unfolded" proteins unstructured under physiologic conditions? *Proteins* **41**, 415–427.
41 Romero P, Obradovic Z, Li X, Garner EC, Brown CJ & Dunker AK (2001) Sequence complexity of disordered protein. *Proteins* **42**, 38–48.
42 Oldfield CJ, Cheng Y, Cortese MS, Romero P, Uversky VN & Dunker AK (2005) Coupled folding and binding with alpha-helix-forming molecular recognition elements. *Biochemistry* **44**, 12454–12470.
43 Cheng Y, Oldfield CJ, Meng J, Romero P, Uversky VN & Dunker AK (2007) Mining alpha-helix-forming molecular recognition features with cross species sequence alignments. *Biochemistry* **46**, 13468–13477.
44 Disfani FM, Hsu WL, Mizianty MJ, Oldfield CJ, Xue B, Dunker AK, Uversky VN & Kurgan L (2012) MoRFpred, a computational tool for sequence-based prediction and characterization of short disorder-to-order transitioning binding regions in proteins. *Bioinformatics* **28**, i75–i83.
45 Fang C, Noguchi T, Tominaga D & Yamana H (2013) MFSPSSMpred: identifying short disorder-to-order binding regions in disordered proteins based on contextual local evolutionary conservation. *BMC Bioinformatics* **14**, 300.
46 Dosztanyi Z, Meszaros B & Simon I (2009) ANCHOR: web server for predicting protein binding regions in disordered proteins. *Bioinformatics* **25**, 2745–2746.
47 Keller R & Wuthrich K (2004) Computer-Aided Resonance Assignment (CARA). Verlag Goldau, Cantina, Switzerland.
48 Jensen MR, Salmon L, Nodet G & Blackledge M (2010) Defining conformational ensembles of intrinsically disordered and partially folded proteins directly from chemical shifts. *J Am Chem Soc* **132**, 1270–1272.
49 Marsh JA, Singh VK, Jia Z & Forman-Kay JD (2006) Sensitivity of secondary structure propensities to sequence differences between α-and γ-synuclein: implications for fibrillation. *Protein Sci: Pub Protein Soc* **15**, 2795–2804.
50 Shen Y, Delaglio F, Cornilescu G & Bax A (2009) TALOS+: a hybrid method for predicting protein backbone torsion angles from NMR chemical shifts. *J Biomol NMR* **44**, 213–223.
51 Ozenne V, Bauer F, Salmon L, Huang JR, Jensen MR, Segard S, Bernado P, Charavay C & Blackledge M (2012) Flexible-meccano: a tool for the generation of explicit ensemble descriptions of intrinsically disordered proteins and their associated experimental observables. *Bioinformatics* **28**, 1463–1470.
52 Gast K, Damaschun H, Misselwitz R, Muller-Frohne M, Zirwer D & Damaschun G (1994) Compactness of protein molten globules: temperature-induced structural changes of the apomyoglobin folding intermediate. *EBJ* **23**, 297–305.
53 Wilkins DK, Grimshaw SB, Receveur V, Dobson CM, Jones JA & Smith LJ (1999) Hydrodynamic radii of native and denatured proteins measured by pulse field gradient NMR techniques. *Biochemistry* **38**, 16424–16431.
54 Berendsen HJC, Vanderspoel D & Vandrunen R (1995) Gromacs – a Message-Passing Parallel Molecular-Dynamics Implementation. *Comput Phys Commun* **91**, 43–56.
55 Lindahl E, Hess B & Van Der Spoel D (2001) GROMACS 3.0: a package for molecular simulation and trajectory analysis. *J Mol Model* **7**, 306–317.

56 Van der Spoel D, Lindahl E, Hess B, Groenhof G, Mark AE & Berendsen HJC (2005) Gromacs: Fast, flexible, and free. *J Comput Chem* **26**, 1701–1718.
57 Hess B, Kutzner C, van der Spoel D & Lindahl E (2008) GROMACS 4: Algorithms for highly efficient, load-balanced, and scalable molecular simulation. *J Chem Theory Comput* **4**, 435–447.
58 Daura X, Gademann K, Jaun B, Seebach D, van Gunsteren WF & Mark AE (1999) Peptide folding: when simulation meets experiment. *Angew Chem Int Ed* **38**, 236–240.
59 Reckel S, Hänsel R, Löhr F & Dötsch V (2007) In-cell NMR spectroscopy. *Prog Nucl Mag Res Sp* **51**, 91–101.
60 Selenko P & Wagner G (2007) Looking into live cells with in-cell NMR spectroscopy. *J Struct Biol* **158**, 244–253.
61 Pielak GJ, Li C, Miklos AC, Schlesinger AP, Slade KM, Wang G-F & Zigoneanu IG (2009) Protein nuclear magnetic resonance under physiological conditions. *Biochemistry* **48**, 226–234.
62 Sakakibara D, Sasaki A, Ikeya T, Hamatsu J, Hanashima T, Mishima M, Yoshimasu M, Hayashi N, Mikawa T & Wälchli M (2009) Protein structure determination in living cells by in-cell NMR spectroscopy. *Nature* **458**, 102–105.
63 McNulty BC, Young GB & Pielak GJ (2006) Macromolecular crowding in the *Escherichia coli* periplasm maintains α-synuclein disorder. *J Mol Biol* **355**, 893–897.
64 Bodart J-F, Wieruszeski J-M, Amniai L, Leroy A, Landrieu I, Rousseau-Lescuyer A, Vilain J-P & Lippens G (2008) NMR observation of Tau in *Xenopus* oocytes. *J Magn Reson* **192**, 252–257.
65 Palmer AG III (1993) Dynamic properties of proteins from NMR spectroscopy. *Curr Opin Biotechnol* **4**, 385–391.
66 Kay LE, Torchia DA & Bax A (1989) Backbone dynamics of proteins as studied by nitrogen-15 inverse detected heteronuclear NMR spectroscopy: application to staphylococcal nuclease. *Biochemistry* **28**, 8972–8979.
67 Fushman D, Weisemann R, Thüring H & Rüterjans H (1994) Backbone dynamics of ribonuclease T_1 and its complex with 2′ GMP studied by two-dimensional heteronuclear NMR spectroscopy. *J Biomol NMR* **4**, 61–78.
68 Rossi P, Swapna G, Huang YJ, Aramini JM, Anklin C, Conover K, Hamilton K, Xiao R, Acton TB & Ertekin A (2010) A microscale protein NMR sample screening pipeline. *J Biomol NMR* **46**, 11–22.
69 Peng JW & Wagner G (1992) Mapping of spectral density functions using heteronuclear NMR relaxation measurements. *J Magn Reson* **98**, 308–332.
70 Farrow NA, Muhandiram R, Singer AU, Pascal SM, Kay CM, Gish G, Shoelson SE, Pawson T, Forman-Kay JD & Kay LE (1994) Backbone dynamics of a free and a phosphopeptide-complexed Src homology 2 domain studied by ^{15}N NMR relaxation. *Biochemistry* **33**, 5984–6003.
71 Ishima R & Nagayama K (1995) Protein backbone dynamics revealed by quasi spectral density function analysis of amide N-15 nuclei. *Biochemistry* **34**, 3162–3171.
72 Farrow NA, Zhang O, Szabo A, Torchia DA & Kay LE (1995) Spectral density function mapping using ^{15}N relaxation data exclusively. *J Biomol NMR* **6**, 153–162.
73 Lipari G & Szabo A (1982) Model-free approach to the interpretation of nuclear magnetic resonance relaxation in macromolecules. 1. Theory and range of validity. *J Am Chem Soc* **104**, 4546–4559.
74 Lipari G & Szabo A (1982) Model-free approach to the interpretation of nuclear magnetic resonance relaxation in macromolecules. 2. Analysis of experimental results. *J Am Chem Soc* **104**, 4559–4570.
75 Clore GM, Szabo A, Bax A, Kay LE, Driscoll PC & Gronenborn AM (1990) Deviations from the simple two-parameter model-free approach to the interpretation of ^{15}N nuclear magnetic relaxation of proteins. *J Am Chem Soc* **112**, 4989–4991.
76 D'Auvergne EJ & Gooley PR (2008) Optimisation of NMR dynamic models II. A new methodology for the dual optimisation of the model-free parameters and the Brownian rotational diffusion tensor. *J Biomol NMR* **40**, 121–133.
77 Almeida MS, Cabral K, Kurtenbach E, Almeida FC & Valente AP (2002) Solution structure of *Pisum sativum* defensin 1 by high resolution NMR: plant defensins, identical backbone with different mechanisms of action. *J Mol Biol* **315**, 749–757.
78 de Medeiros LN, Angeli R, Sarzedas CG, Barreto-Bergter E, Valente AP, Kurtenbach E & Almeida FCL (2010) Backbone dynamics of the antifungal Psd1 pea defensin and its correlation with membrane interaction by NMR spectroscopy. *Biochim Biophys Acta* **1798**, 105–113.
79 Fant F, Vranken W, Broekaert W & Borremans F (1998) Determination of the three-dimensional solution structure of *Raphanus sativus* antifungal protein 1 by ^{1}H NMR. *J Mol Biol* **279**, 257–270.
80 Patel SU, Osborn R, Rees S & Thornton JM (1998) Structural studies of Impatiens balsamina antimicrobial protein (Ib-AMP1). *Biochemistry* **37**, 983–990.
81 Huang R-H, Xiang Y, Tu G-Z, Zhang Y & Wang D-C (2004) Solution structure of *Eucommia* antifungal peptide: a novel structural model distinct with a five-disulfide motif. *Biochemistry* **43**, 6005–6012.

82 Liu YJ, Cheng CS, Lai SM, Hsu MP, Chen CS & Lyu PC (2006) Solution structure of the plant defensin VrD1 from mung bean and its possible role in insecticidal activity against bruchids. *Proteins* **63**, 777–786.

83 Jennings CV, Rosengren KJ, Daly NL, Plan M, Stevens J, Scanlon MJ, Waine C, Norman DG, Anderson MA & Craik DJ (2005) Isolation, solution structure, and insecticidal activity of kalata B2, a circular protein with a twist: do Möbius strips exist in nature? *Biochemistry* **44**, 851–860.

84 Lay FT, Schirra HJ, Scanlon MJ, Anderson MA & Craik DJ (2003) The three-dimensional solution structure of NaD1, a new floral defensin from *Nicotiana alata* and its application to a homology model of the crop defense protein alfAFP. *J Mol Biol* **325**, 175–188.

85 Mittag T & Forman-Kay JD (2007) Atomic-level characterization of disordered protein ensembles. *Curr Opin Struct Biol* **17**, 3–14.

86 Jensen MR, Ruigrok RW & Blackledge M (2013) Describing intrinsically disordered proteins at atomic resolution by NMR. *Curr Opin Struct Biol* **23**, 426–435.

87 Wells M, Tidow H, Rutherford TJ, Markwick P, Jensen MR, Mylonas E, Svergun DI, Blackledge M & Fersht AR (2008) Structure of tumor suppressor p53 and its intrinsically disordered N-terminal transactivation domain. *Proc Natl Acad Sci USA* **105**, 5762–5767.

88 Mittag T, Marsh J, Grishaev A, Orlicky S, Lin H, Sicheri F, Tyers M & Forman-Kay JD (2010) Structure/function implications in a dynamic complex of the intrinsically disordered Sic1 with the Cdc4 subunit of an SCF ubiquitin ligase. *Structure* **18**, 494–506.

89 Tompa P (2012) Intrinsically disordered proteins: a 10-year recap. *Trends Biochem Sci* **37**, 509–516.

90 Uversky VN (2013) Unusual biophysics of intrinsically disordered proteins. *BBA-Proteins Proteom* **1834**, 932–951.

91 Haaland PD (1989) Experimental Design in Biotechnology. CRC press, New York, NY.

92 Bradford MM (1976) A rapid and sensitive method for the quantitation of microgram quantities of protein utilizing the principle of protein-dye binding. *Anal Biochem* **72**, 248–254.

93 Griep S & Hobohm U (2009) PDBselect 1992-2009 and PDBfilter-select. *Nucleic Acids Res* **38**, D318–D319.

94 Rose PW, Beran B, Bi C, Bluhm WF, Dimitropoulos D, Goodsell DS, Prlic A, Quesada M, Quinn GB, Westbrook JD *et al.* (2011) The RCSB Protein Data Bank: redesigned web site and web services. *Nucleic Acids Res* **39**, D392–D401.

95 Sickmeier M, Hamilton JA, LeGall T, Vacic V, Cortese MS, Tantos A, Szabo B, Tompa P, Chen J, Uversky VN *et al.* (2007) DisProt: the database of disordered proteins. *Nucleic Acids Res* **35**, D786–D793.

96 Peng K, Radivojac P, Vucetic S, Dunker AK & Obradovic Z (2006) Length-dependent prediction of protein intrinsic disorder. *BMC Bioinformatics* **7**, 208.

97 Peng K, Vucetic S, Radivojac P, Brown CJ, Dunker AK & Obradovic Z (2005) Optimizing long intrinsic disorder predictors with protein evolutionary information. *J Bioinformat Computat Biol* **3**, 35–60.

98 Xue B, Dunbrack RL, Williams RW, Dunker AK & Uversky VN (2010) PONDR-FIT: a meta-predictor of intrinsically disordered amino acids. *Biochim Biophys Acta* **1804**, 996–1010.

99 Zimm BH (1948) The dependence of the scattering of light on angle and concentration in linear polymer solutions. *J Phys Colloid Chem* **52**, 260–267.

100 Sheth PR, Ramanathan L, Ranchod A, Basso AD, Barrett D, Zhao J, Gray K, Liu YH, Zhang R & Le HV (2010) Expression, purification, stability optimization and characterization of human Aurora B kinase domain from *E. coli*. *Arch Biochem Biophys* **503**, 191–201.

101 Hornak V, Abel R, Okur A, Strockbine B, Roitberg A & Simmerling C (2006) Comparison of multiple Amber force fields and development of improved protein backbone parameters. *Proteins: Struct Funct Bioinform* **65**, 712–725.

102 Jorgensen WL, Chandrasekhar J, Madura JD, Impey RW & Klein ML (1983) Comparison of simple potential functions for simulating liquid water. *J Chem Phys* **79**, 926–935.

103 Pettersen EF, Goddard TD, Huang CC, Couch GS, Greenblatt DM, Meng EC & Ferrin TE (2004) UCSF Chimera—a visualization system for exploratory research and analysis. *J Comput Chem* **25**, 1605–1612.

104 Wassenaar TA, van Dijk M, Loureiro-Ferreira N, van der Schot G, de Vries SJ, Schmitz C, van der Zwan J, Boelens R, Giachetti A, Ferella L, *et al.* (2012) WeNMR: Structural Biology on the Grid. *J Grid Comp* **10**, 743–767.

5. DISCUSSÃO GERAL

A otimização da produção de proteínas recombinantes é necessária para estudos de caracterização biológica e estrutural, uma vez que são requeridas elevadas quantidades de proteínas para estes estudos. Uma das estratégias empregadas para otimizar condições de cultivo é a utilização de métodos estatísticos, que geralmente produzem resultados vantajosos comparados aos métodos clássicos, que modificam um fator por vez. As técnicas estatísticas nos permitem analisar múltiplas variáveis por experimento, reduzindo o número de experimentos e mostrando os efeitos das interações entre os parâmetros (DAROIT, CORRÊA & BRANDELLI, 2011). Na presente tese, o uso do Planejamento Fatorial, associado a Metodologia de Superfície de Resposta foi vantajoso no aumento da expressão da proteína de fusão GST-uSBU, aumentando sua produção de 2 mg para 5 mg por litro de cultivo, auxiliando, assim na caracterização biológica desta proteína. Na otimização da produção do Jaburetox também utilizamos um planejamento fatorial para determinar qual concentração de IPTG e qual temperatura eram mais adequadas para uma maior expressão do peptídeo (dados não mostrados). De acordo com MALUF et al., 2014, a temperatura e a concentração do agente indutor estão entre os parâmetros de maior impacto sobre a expressão e, portanto devem ser cuidadosamente avaliados. Neste caso, apesar de não ter sido possível gerar uma superfície de resposta por problemas estatísticos, os resultados preliminares nos auxiliaram no delineamento das condições ideias para produzir o peptídeo, principalmente para a realização da técnica de RMN, que demanda grandes quantidades da proteína a ser estudada, bem como a utilização de um meio pobre em nutrientes, como o meio mínimo M9, que pode ser um fator limitante para a produção da proteína.

Para aumentar a produção do Jaburetox, utilizamos a técnica estabelecida por Marley e colaboradores (MARLEY et al., 2001). Esta técnica utiliza duas etapas de inóculo, sendo a primeira para a multiplicação das células em meio rico (LB, por exemplo) e a segunda para a indução em meio pobre (M9) e em menor volume. Os autores demonstraram que a dimuinuição do volume em quatros vezes do primeiro para o segundo inóculo, aumenta a produção de proteínas. Esta técnica oferece vantagens no preparo de amostras para RMN, uma vez que há economia no uso de isótopos marcados. Contudo, ela também é vantajosa nos cultivos utilizando meios ricos, aumentando o rendimento da

proteína. Provavelmente, inoculando as células em um meio novo, essa técnica auxilia na remoção de subprodutos inibitórios do crescimento e da expressão, além de promover a indução com uma densidade elevada de células (MARLEY et al., 2001).

O meio M9 é requerido para a produção de Jaburetox marcado para as análises de RMN. Para outros fins, estamos utilizado o meio de auto-indução para a produção de Jaburetox. Este meio é considerado rico, por conter triptona, extrato de levedura, glicerol, $(NH_4)_2SO_4$, KH_2PO_4, Na_2HPO_4, glicose e micronutrientes (TICHOTA, 2014). A lactose é utilizada como indutor, ao invés do IPTG, trazendo como vantagem um menor custo. Além disso, altas concentrações de IPTG podem ser tóxicas para as células de *E. coli* (KILIKIAN et al. 2000). Como observamos no planejamento fatorial para GST-uSBU, altas concentrações de IPTG não resultaram necessariamente em altas concentrações de proteína, podendo ser esta toxicidade uma das causas do baixo rendimento. TOMAZETTO e colaboradores, reportaram que IPTG pode também apresentar toxicidade para humanos, podendo ser considerado não apropriado para a produção de proteínas para usos terapêuticos, bem como pode ser um gargalo na produção de proteínas recombinantes em larga escala, devido a seu alto custo (TOMAZETTO et al., 2007).

A estabilidade e a solubilidade de proteínas recombinantes são fatores críticos tanto na produção, quanto nos estágios pós-produção. Tanto uSBU, quanto Jaburetox são fusionados à uma cauda, GST e polihistidina, respectivamente. O principal objetivo das caudas, primeiramente, é facilitar a purificação, pois a utilização da cromatografia de afinidade facilita muito este processo, sendo muitas vezes o único passo necessário. Outro fator importante é o aumento de solubilidade, o que foi observado no caso da GST-uSBU. Quando foi efetuada a clivagem da cauda GST, a proteína clivada precipitou (MARTINELLI, 2007), dessa forma, a cauda atuou positivamente na solubilidade de uSBU. Quanto ao Jaburetox, não temos informações a respeito do peptídeo sem a cauda de histidina, mas observamos que esta cauda não afetou a atividade biológica de Jaburetox 2Ec e nem de Jaburetox (POSTAL et al., 2012), e por isso mantivemos a cauda de histidina para as caracterizações biológicas dos peptídeos e também na caracterização estrutural de Jaburetox.

Na literatura são relatados trabalhos nos quais proteínas fusionadas à GST, mantiveram suas atividades biológicas. SPIEZIA et al. (2012) expressaram conotoxina V2 de *Conus ventricosus* fusionada à GST. A proteína fusionada apresentou elevada atividade

inseticida em uma dose de 100 pM por grama de peso das larvas de *Galleria mellonella*. Os autores relataram que devido à elevada hidrofobicidade da conotoxina, não foi possível clivar a cauda de GST, por isso, utilizaram a proteína fusionada no ensaio biológico e como controle GST, estratégia utilizada também em nosso trabalho. GST não apresentou toxicidade à *G. mellonella*. Outro grupo relatou a produção heteróloga em *E. coli* da proteína de fusão heparinase I de *Bacteroides thetaiotaomicron*, fusionada à GST. A proteína fusionada facilitou a purificação, permitindo a realização de apenas um passo cromatográfico, bem como a heparinase I-GST exibiu parâmetros cinéticos similares comparados à heparinase I após a remoção da GST. Além disso, a presença da cauda de GST facilitou a imobilização de heparinase I em fase sólida (LUO et al., 2007). DELLA-CASA et al. (2010) reportaram o isolamento de uma desintegrina, a partir de veneno de *Bothrops insularis*, denominada Insularina. Neste trabalho também foi realizada a expressão de Insularina recombinante fusionada à GST. A proteína nativa e a recombinante inibiram a agregação de plaquetas induzidas por ADP e também atuaram na inibição da adesão de células endoteliais. Igualmente ao que observamos em nosso trabalho, a remoção da cauda de GST foi seguida da precipitação de Insularina, sendo que o grupo optou por trabalhar com a proteína fusionada, utilizando, da mesma forma, GST como controle.

Evitar a agregação durante a produção é um grande desafio, porém mesmo quando as proteínas são obtidas na forma solúvel, podem apresentar tendência a agregação, especialmente se são estocadas e manipuladas em altas concentrações (VAZQUEZ, CORCHERO, & VILLAVERDE, 2011). No caso da análise de RMN do Jaburetox, obter a estabilidade do peptídeo era um fator crucial e limitante. Esta técnica requer que a proteína esteja estável por pelo menos 7 dias, exposta a temperatura de 25 °C (para simular uma condição mais próxima da condição fisiológica) e em alta concentração (1 mM). Para estabilizar o Jaburetox, foi necessário alterar a formulação do tampão de estocagem, uma vez que, em vários trabalhos do grupo havíamos observado a tendência à agregação do Jaburetox, principalmente em pHs mais ácidos. Em trabalhos anteriores, tanto Jaburetox-2Ec, quanto Jaburetox haviam sido utilizados Ditiotreitol (DTT) (BARROS et al., 2009) ou β-mercaptoetanol. Dessa forma, substituimos o agente redutor utilizado na formulação por TCEP. O TCEP atua em uma ampla faixa de pH, entre 1,5 a 8,5, apresentando maior estabilidade e poder redutor que o DTT. Além disso, a fosfina da estrutura do TCEP é comparativamente mais estável do que o grupamento tiol do DTT em contato com o ar.

Outra vantagem é poder utilizar o TCEP em presença de Ni^{2+}, pois este metal não afeta o TCEP, ao contrário do DTT que é prontamente oxidado (HAN & HAN, 1994; GETZ et al., 1999; CLINE et al., 2004). Não encontramos estudos comparativos entre TCEP e β-mercaptoetanol na literatura, porém verificamos na rotina de laboratório e em algumas análises de SLS, que o Jaburetox apresenta tendência a agregar quando estocado em tampões contendo β-mercaptoetanol. Apesar do Jaburetox não formar pontes dissulfeto na sua forma monomérica, a importância de se utilizar um agente redutor, bem como um quelante de metais, como o EDTA, na formulação do tampão de estocagem, são importantes para prolongar o tempo de vida da proteína (BOIVIN et al., 2013).

Visando aplicação biotecnológica do Jaburetox, estamos trabalhando com o encapsulamento deste peptídeo em nanopartículas lipídicas, a fim de preparar uma formulação para uso agronômico e farmacêutico. Foram realizados testes de pré-formulação, pois o preparo de nanopartículas envolve aquecimento, para a fusão dos lipídios. Nestes testes o peptídeo foi mantido por 30 minutos a temperaturas que variaram entre 40 a 100 °C. Observamos que a incubação não trouxe prejuízo para sua atividade antifúngica contra *Pichia membranifasciens*, sendo que em algumas temperaturas houve um aumento da atividade antifúngica do peptídeo (TICHOTA, 2014). Esta termoestabilidade está de acordo com o fato do Jaburetox pertencer a classe das proteínas intrinsicamente desordenadas. Esta termoestabilidade faz o peptídeo ter grande interesse biotecnológico nas mais diversas áreas. Podemos explorar, de forma mais detalhada, possíveis aplicações do Jaburetox em outras áreas, como por exemplo, no uso deste peptídeo como conservante para a Indústria Alimentícia, principalmente devido à sua atividade antifúngica. Vale destacar que a atividade antifúngica do Jaburetox é de 2 a 3 ordens de grandeza mais potente do que a de outras proteínas e peptídeos antifúngicos obtidos de plantas já conhecidos (POSTAL et al., 2012), e o peptídeo parece ser inócuo para mamíferos, seja injetado ou por via oral (MULINARI et al., 2007). Estudos para verificar se o Jaburetox é ativo contra bactérias estão sendo conduzidos pelo nosso grupo e poderão ampliar ainda mais as futuras aplicações deste peptídeo, mediante prévios estudos de toxicidade.

6. ANEXO

TÉCNICAS PARA ESTUDOS ESTRUTURAIS E DE ENOVELAMENTO DE PROTEÍNAS E PEPTÍDEOS

6.1. RESSONÂNCIA MAGNÉTICA NUCLEAR

Os concomitantes avanços em biologia molecular e em espectroscopia por Ressonância Magnética Nuclear (RMN) multidimensional tiveram como reflexo um aumento surpreendente na utilização do RMN, a fim de obter informações estruturais e dinâmicas de macromoléculas biológicas, incluindo ácidos nucleicos, carboidratos e proteínas. Essa combinação única de determinação de estrutura e de dinâmica, é que torna a técnica de RMN importante, em particular nos sistemas que já são inerentemente dinâmicos, como as IDPs. A estrutura tridimensional de uma proteína, determinada a partir de dados de RMN, consiste em um conjunto de diferentes confôrmeros que igualmente satisfazem as restrições experimentais (FERELLA, ROSATO, & TURANO, 2012; ALMEIDA, 2014). A possibilidade de medir movimentos na escala de tempo de ns a ms tem revelado a complexidade de conjuntos de confôrmeros de proteínas em solução. A dinâmica do *backbone* de uma proteína pode ser monitorada por medidas de relaxação, tipicamente relaxação longitudinal ^{15}N (T1), relaxação tranversal ^{15}N (T2) e Efeito Nuclear Overhauser ^{15}N-^{1}H NOE (Nuclear Overhauser Effect) heteronuclear (NEVES et al., 2010).

O espectro bidimensional de ^{1}H-^{15}N HSQC (heteronuclear single-quantum coherence), onde cada pico corresponde ao nitrogênio amídico de um aminoácido do *backbone* da proteína, é uma importante técnica de *screening* para determinar o grau de enovelamento de uma proteína, bem como a qualidade da amostra. Quando o espectro de ^{1}H-^{15}N HSQC é de uma proteína totalmente enovelada, todos os picos são intensos e distribuídos em um ampla faixa de deslocamento químico e o número de ressonâncias atribuídas às amidas do *backbone* conferem com o número de resíduos da proteína (com exceção das prolinas). Em proteínas parcialmente desenoveladas, os picos são menos dispersos na dimensão do ^{1}H, os picos mais intensos são largos e colapsados em uma região estreita ao redor de 8,5 ppm, típico de estruturas *random coil*. Picos fora desta faixa

são fracos. Por fim, proteínas completamente desenoveladas apresentam espectro com picos colapsados, localizados próximos a 8,3 ppm na dimensão de deslocamento químico do ^{1}H. A resolução também diminui com o aumento do grau de desenovelamento (FERELLA, ROSATO & TURANO., 2012; ALMEIDA, 2014).

Para o estudo de proteínas por RMN, cada sinal de ressonância deve ser associado a um núcleo específico. Este processo é denominado de atribuição de ressonâncias. A atribuição das ressonâncias de uma proteína é obtida através da análise em conjunto dos espectros de NOESY (Nuclear Overhauser Effect), TOCSY (Total Correlated Spectroscopy), espectros bidimensionais, heteronucleares e de tripla ressonância, onde o intuito é correlacionar cada um dos sinais de ressonância encontrados nestes espectros, com os prótons, carbonos e nitrogênios de cada um dos aminoácidos da proteína, sendo assim, necessário o conhecimento prévio da sequência de aminoácidos da proteína em estudo (ALMEIDA, 2014).

Atualmente, o número de estruturas resolvidas por cristalografia, depositadas no *Protein Data Bank*, supera em aproximadamente cinco vezes às resolvidas por RMN (ALMEIDA, 2014; CAPRILES et al., 2014). Uma das vantagens da técnica de RMN em relação à técnica de Cristalografia de Raios X, é que não é necessária a cristalização prévia da amostra, um fator limitante para a cristalografia. A análise por RMN é realizada em solução, condição que é mais próxima da fisiológica. Contudo, a técnica de RMN necessita que a proteína esteja solúvel e em altas concentrações, no mínimo 1 mM. Normalmente há a necessidade de marcação desta proteína com isótopos ^{13}C e ^{15}N, o que aumenta os custos da análise. Uma outra limitação inerente desta técnica, é que a mesma está limitada a proteínas de tamanhos pequenos a médios (de até 30 a 40 kDa), o que não ocorre com a técnica de cristalografia.

6.2. CRISTALOGRAFIA POR DIFRAÇÃO DE RAIOS X

A Cristalografia de raios-X moderna apresenta aplicações amplas nas ciências dos materiais, química, mineralogia, física e biologia. Sua aplicação para determinação da estrutura tridimensional de biomoléculas, com destaque para as proteínas, deu origem à

cristalografia de proteínas, caracterizada como um processo complexo que engloba uma variedade de estratégias e métodos tradicionais e modernos, integrando especilialidades como a física, matemática, química, biologia, bioquímica e bioinformática. A técnica de Cristalografia de raios X é a melhor opção para caracterizar estruturalmente proteínas grandes, ou complexos macromoleculares, a uma resolução atômica. Sistemas que são ainda maiores (ou não podem ser cristalizados) podem ser investigados pela Criomicroscopia Eletrônica (FERELLA, ROSATO & TURANO, 2012; MALUF et al., 2014). A Criomicroscopia Eletrônica apresenta como vantagens em relação às técnicas de RMN e de Cristalografia de raios X: requerer pequenas quantidades de proteína (0,1 mg pode ser suficiente), possuir poucas restrições quanto à pureza da amostra e não requerer a cristalização da proteína. Porém, no que se refere à resolução, as técnicas de RMN e Cristalografia, superam a técnica de Criomicroscopia Eletrônica (BAI, MCMULLAN, & SCHERES, 2014).

A grande heterogeneidade, insolubilidade e grande polidispersidade de JBU em solução podem ter sido os motivos pelos quais sua estrutura cristalográfica tenha sido resolvida apenas 83 anos após a cristalização por Sumner em 1926. Além disso, o fato de JBU não ser a única isoforma de urease em *C. ensiformis*, aumenta a heterogeneidade da amostra, impactando significativamente na obtenção da proteína com elevado teor de pureza e, consequentemente na qualidade e formação dos cristais (FOLLMER, 2008, MALUF et al., 2014).

O processo para obtenção da estrutura tridimensional de uma proteína por Cristalografia de raios X compreende etapas de produção e purificação da proteína alvo, cristalização, coleta e processamento dos dados, resolução da estrutura (empregando informações da sequência de aminoácidos e diferentes programas) e, por fim refinamento da estrutura (CAPRILES et al, 2014).

6.3. DICROÍSMO CIRCULAR

O Dicroísmo Circular (CD, do inglês Circular Dichroism) é uma técnica espectroscópica utilizada para estudar uma grande variedade de moléculas quirais, tais

como fármacos, polímeros e biopolímeros, em solução. Para sistemas enovelados e estruturados tridimensionalmente, como proteínas globulares, o CD é uma técnica de baixa resolução quando comparado à RMN e Cristalografia de Raios-X. Isto ocorre porque o CD, ao contrário destes métodos, não possui resolução atomística, ou seja, não é capaz de identificar átomos específicos das moléculas em estudo. No entanto, o CD é capaz de lidar com suas estruturas desordenadas (LIMA et al., 2014).

O CD é uma técnica bem estabelecida e um dos métodos espectroscópicos mais utilizados em química de proteínas. Esta técnica apresenta numerosas vantagens: não sendo necessária a marcação da proteína para a análise, requerendo pequenas quantidades do material e curto tempo de análise (WHITMORE et al., 2010). De maneira geral, os espectros de CD podem ser utilizados para diversos tipos de estudos, incluindo-se: 1) enovelamento e estrutura secundária de proteínas, 2) estruturas de proteínas de membranas inseridas em bicamadas lipídicas; 3) interação entre moléculas; 4) interações entre macromoléculas (destacadamente, proteínas, ácidos nucleicos e carboidratos); 5) monitoramento da integridade estrutural de moléculas sob aquecimento e mudanças de pH; 6) quantificação de alterações conformacionais; 7) caracterização de domínios de proteínas, a qual pode ser empregada em comparações com modelos gerados computacionalmente; 8) análise de carboidratos; 9) cinética rápida de enovelamento de proteínas e montagem de complexos macromoleculares, dentre outros (WOODY, 2015; LIMA et al., 2014). Além disso, estudos de CD podem ser realizados em solução, em condições bem próximas das fisiológicas, fazendo deste método uma ferramenta ideal para investigar as interações entre moléculas envolvidas nos mais diversos processos biológicos (LIMA et al., 2014).

O CD é uma técnica de grande valor para o estudo de proteínas em solução, pois muitos motivos conformacionais incluindo α-hélices, folhas β, bem como proteínas desenoveladas, apresentam características bem definidas no espectro de CD no Ultravioleta (UV) distante (178-250 nm). Hélices α apresentam grandes bandas de CD com elipiticidade negativa em 222 e 208 nm, e uma forte banda positiva em torno de 193 nm. O CD de folhas β exibe uma grande banda negativa de máxima absorção em 218 nm e uma grande banda positiva próximo da região entre 195-200 nm, enquanto proteínas desordenadas possuem uma banda larga e fraca próximo a 217 nm e forte banda negativa

próximo a 200 nm. O espectro de CD de uma proteína é basicamente a soma dos espectros de seus elementos conformacionais (GREENFIELD, 1999; LIMA et al., 2014).

6.4. ESPALHAMENTO DE LUZ ESTÁTICO E DINÂMICO

O espalhamento de luz é uma das técnicas de maior importância para caracterizar macromoléculas e colóides. Estas técnicas são muito convenientes e efetivas na investigação do formato, massa, agregação e interações de moléculas biológicas, em condições próximas de seu estado natural. Utilizando moderna instrumentação, é possível obter informação sobre a massa molecular, o raio de giro e raio hidrodinâmico da proteína em estudo (BANACHOWICZ, 2006; BLOOMFIELD, 2000).

O Espalhamento de luz dinâmico (DLS, do inglês Dynamic Light Scattering) determina os parâmetros hidrodinâmicos das macromoléculas em solução, como o Raio Hidrodinâmico. Uma vantagem da técnica de DLS comparada a outras técnicas hidrodinâmicas é que a DLS é rápida, não invasiva e os estudos podem ser realizados em uma grande variedade de condições. Já o espalhamento de luz estático (SLS, do inglês Static Light Scattering) permite a determinação da massa molecular de partículas, que é um complemento das medidas das dimensões hidrodinâmicas (GAUST & MODLER, 2012).

A determinação da massa molecular de proteínas, muitas vezes, é realizada por Cromatografia de Exclusão por Tamanho (SEC, em inglês Size Exclusion Chromatography) que é um método simples e rápido para estimar a massa molecular de uma proteína em seu estado nativo, baseando-se no seu volume de eluição. Contudo, um problema relacionado a esta técnica é que o volume de eluição depende não apenas da massa molecular da proteína, mas também de seu formato. Outros problemas são: o volume de eluição irá mudar, caso ocorra interação com a matriz da coluna ou com a fase móvel e para proteínas ou complexos protéicos contendo carboidratos, estes carboidratos podem causar uma distorção no volume de eluição. Portanto, a grande vantagem de usar não somente a SEC, mas usar a SEC acoplada ao SLS para a determinação da massa molecular de proteínas, é que a determinação da massa molecular é independente do volume de eluição (referida como massa molecular absoluta). Uma vez que o detector foi

calibrado, os únicos parâmetros necessários para o *software* realizar o cálculo da massa molecular é o índice refractivo diferencial (dn/dc) e a concentração da proteína. Além disso, a SEC pode realizar a prévia separação de diferentes estados oligoméricos de uma proteína, antes da análise de SLS, podendo assim, determinar a massa moleceular de cada oligômero em separado (OLIVA & FARIN, 2001; YE, 2006).

6.5. FLUORIMETRIA DIFERENCIAL DE VARREDURA

Técnicas baseadas em desnaturação térmica tem sido cada vez mais utilizadas para caracterizar a estabilidade de proteínas e de interações. Estas técnicas tem sido escolhidas para a realização de *screening* de proteínas contra bibliotecas de compostos e de condições ótimas de tampão, que podem estabilizar as proteínas em estudo, reduzindo agregação e precipitação das mesmas (SENISTERRA, CHAU & VEDADI, 2012).

Uma das técnicas empregadas, é a técnica de Fluorimetria Diferencial de Varredura, na qual a proteína é exposta a temperaturas crescentes a uma taxa controlada, geralmente 1 °C por minuto, variando de 25 °C a 95 °C, na presença de fluoróforos. O sinal de fluorescência pode ser monitorado utilizando uma variedade de leitores de placa, incluindo equipamentos de PCR em tempo real, utilizando placas de 96 poços ou até mesmo de 384 poços. A metodologia é baseada no fato de determinados corantes fluorescentes se ligarem inespecificamente a proteínas. Estes corantes emitem fluorescência quando há aumento da hidrofobicidade. Para muitas proteínas, o aumento gradual de temperatura tem pouco efeito sobre seu enovelamento da proteína, até atingir determinada temperatura, na qual a proteína desenovela rapidamente. Neste ponto, a proteína desenovelada irá expor seu *core* hidrofóbico e o corante irá tornar-se fluorescente. A curva sigmoidal obtida permite o cálculo da temperatura de *melting* (T_m), que corresponde à temperatura na qual a proteína está 50% enovelada e 50 % desenovelada (BOIVIN, KOZAK, & MEIJERS, 2013; SENISTERRA et al., 2012).

Na otimização de um tampão para estabilizar uma proteína, desvios na T_m maiores que 2 ºC são considerados significativos. Um desvio positivo da T_m pode ser relacionado a um aumento de ordem estrutural e redução da flexibilidade conformacional, enquanto um

desvio negativo indica que determinado tampão induz mudanças estruturais na proteína para uma conformação mais desorganizada (BOIVIN, KOZAK & MEIJERS, 2013). As T_m obtidas pelo método de fluorimetria diferencial de varredura se correlacionam adequadamente com os valores de T_m determinados por outros métodos biofísicos, como dicroísmo circular, medidas de turbidimetria e calorimetria diferencial de varredura (ERICSSON et al., 2006).

7. CONCLUSÕES

Capítulo 1

- A proteína de fusão GST-uSBU teve sua expressão otimizada pela Metodologia de Superfície de Resposta, obtendo-se quantidade suficiente para o estudo de suas propriedas biológicas;
- GST-uSBU apresentou propriedades antifúngicas, inseticida e de agregação de plaquetas e de hemócitos;
- GST-uSBU não apresentou atividade antibacteriana contra bactérias de importância médica;
- GST-uSBU afeta o metabolismo secundário de fungos filamentosos, principalmente a produção de pigmentos, além de causar mudanças morfológicas (produção de pseudo-hifas) em leveduras como *C. albicans*, *C. tropicalis* e *P. membranifasciens*;
- A proteína de fusão GST-uSBU mostrou ser um modelo adequado para estudos das propriedades biológicas da urease ubíqua de soja.

Capítulo 2

- O peptídeo Jaburetox pertence à classe das proteínas intrinsicamente desordenadas, no estado "*pre molten globule*";
- O uso do agente redutor TCEP estabilizou o peptídeo na sua forma monomérica;
- A caracterização como proteína intrinsicamente desordenada foi confirmada pelo elevado Raio Hidrodinâmico determinado por DLS, pelos dados obtidos por CD, pelas análises de algoritmos de desordem (PONDR) e pela técnica de RMN;
- Segundo os dados de RMN, o espectro ^{1}H-^{15}N HSQC demonstrou picos sobrepostos e largos, característicos de IDPs, além disso, os deslocamentos químicos do *backbone* demonstraram a baixa propensão do Jaburetox a apresentar estrutura secundária;
- A estrutura tridimensional do Jaburetox em solução (pH 6,5) apresenta um motivo α-hélice na região N-terminal e duas estruturas do tipo volta, uma na região central do peptídeo e outra próxima da região C-terminal;
- Análise de Fluorimetria Diferencial de Varredura, demonstrou que o Jaburetox, apesar de ser uma IDP, apresenta um certo grau de enovelamento;

- O RMN-*in cell* comprovou a natureza desordenada do peptídeo dentro da célula de *Escherichia coli*;
- Com a utilização de técnicas de Bioinformática, foram preditas no Jaburetox regiões potenciais de ligações com outras proteínas, sendo que a maioria das regiões preditas estão localizadas na região N-terminal do peptídeo.

8. PERSPECTIVAS

Estudos Estruturais

- Estudos de oligomerização do peptídeo Jaburetox em diferentes tampões (condições de estocagem e dos ensaios biológicos) por espectrometria de massas MALDI-TOF;

Estudos do Mecanismo de Ação Antifúngico

- Realizar estudos de microscopia confocal e microscopia eletrônica de transmissão, além de citometria de fluxo, buscando evidências do mecanismo de ação fungitóxico de GST-uSBU, Jaburetox e Soyuretox;

- Estudos da ação de GST-uSBU, Jaburetox e Soyuretox contra biofilmes (evitando sua formação ou eliminando o biofilme), utilizando *C. albicans* e *C. tropicalis* como fungos modelo;

- Realizar ensaios de Fluorimetria Diferencial de Varredura com possíveis ligantes de fungos e insetos (ex. quitina) com GST-uSBU, Jaburetox e Soyuretox;

9. REFERÊNCIAS

ABU-ELTEEN, K.H. & HAMAD, M. Antifungal Agents for Use in Human Therapy Fungi Biology and Applications, John Willy & Sons (2005).

ALMEIDA, M. S. Ressonância Magnética Nuclear. In: Bioinformática: da Biologia à Flexibilidade Molecular (org. Hugo Verli), 282 p., 2014.

ALVES, E. W.; FERREIRA, A T.; FERREIRA, C. T. & CARLINI, C. R. Effects of canatoxin on the $Ca2^{+}$-ATPase of sarcoplasmic reticulum membranes. *Toxicon*, *30*:1411–1418, 1992.

BAI, X.; MCMULLAN, G.; & SCHERES, S. H. W. How cryo-EM is revolutionizing structural biology. *Trends in Biochemical Sciences*, *40*(1): 49–57, 2014.

BAKER, R. A. & TATUM, J.H. Novel anthraquinones from stationary cultures of Fusarium oxysporum. Journal of *Fermentation and Bioengineering* 85: 359–361, 1998.

BALASUBRAMANIAN, A.; DURAIRAJPANDIAN, V.; ELUMALAI, S.; MATHIVANAN, N.; MUNIRAJAN, A. K. & PONNURAJ, K. Structural and functional studies on urease from pigeon pea (*Cajanus cajan*). *International Journal of Biological Macromolecules*, *58*: 301–309, 2013.

BALASUBRAMANIAN, A. & PONNURAJ, K. Crystal Structure of the First Plant Urease from Jack Bean: 83 Years of Journey from Its First Crystal to Molecular Structure. *Journal of Molecular Biology*, *400*(3): 274–283, 2010.

BANACHOWICZ, E. Light scattering studies of proteins under compression, *Biochimica et Biophysica Acta*, *1764*: 405–413, 2006.

BARJA-FIDALGO, C.; GUIMARÃES, J. A. & CARLINI, C. R.. Lipoxygenase-mediated secretory effect of canatoxin the toxic protein from Canavalia ensiformis seeds. *Toxicon*, *29*: 453–459, 1991.

BARJA-FIDALGO, C.; GUIMARAES, J. A. & CARLINI, C. R. Canatoxin, a Plant Protein, Induces Insulin Release from Isolated Pancreatic Islets. *Endocrinology*, *128*(2): 675–679, 1991a.

BARROS, P. R.; STASSEN, H.; FREITAS, M. S.; CARLINI, C. R.; NASCIMENTO, M. A C. & FOLLMER, C. Membrane-disruptive properties of the bioinsecticide Jaburetox-2Ec: implications to the mechanism of the action of insecticidal peptides derived from ureases. *Biochimica et Biophysica Acta*, *1794*(12): 1848–54, 2009.

BECKER-RITT, A. B.; MARTINELLI, A. H. S.; MITIDIERI, S.; FEDER, V.; WASSERMANN, G. E.; SANTI, L. & CARLINI, C. R. Antifungal activity of plant and bacterial ureases. *Toxicon*, *50*: 971–983, 2007.

BENINI, S.; RYPNIEWSKI, W. R.; WILSON, K. S.; MILETTI, S.; CIURLI, S. & MANGANI, S. A new proposal for urease mechanism based on the crystal structures of the native and inhibited enzyme from *Bacillus pasteurii*: why urea hydrolysis costs two nickels. *Structure*, *7*(2): 205–216, 1999.

BENJAMIN, C. F.; CARLINI, C. R. & BARJA-FIDALGO, C. Pharmacological characterization of rat paw edema induced by canatoxin, the toxic protein from *Canavalia ensiformis* (jack bean) seeds. *Toxicon*, *30*: 879–885, 1992.

BLOOMFIELD, V. A. Static and dynamic light scattering from aggregating particles. *Biopolymers*, *54*(3): 168–172, 2000.

BOIVIN, S.; KOZAK, S. & MEIJERS, R. Optimization of protein purification and characterization using Thermofluor screens. *Protein Expression and Purification*, *91*(2): 192–206, 2013.

BRADFORD, M.M. A rapid and sensitive method for the quantitation of microgram quantities of protein utilizing the principle of protein-dye binding. *Analytical Biochemistry*. 72, 248–254, 1976.

CAPRILES, P. V. S. Z.; TREVIZANI, R.; ROCHA, G. K.; DARDENNE, L. E. & CUSTÓDIO, F.L. Modelos Tridimensionais. In: Bioinformática: da Biologia à Flexibilidade Molecular (org. Hugo Verli), 282 p., 2014.

CARLINI, C. R.; GOMES, C.; GUIMARÃES, J. A.; MARKUS, R. P. & SATO, H. TROLIN, G. Central Nervous Effects of the Convulsant Protein Canatoxin. *Acta Pharmacologica et Toxicologica*, *54*(3): 161–166, 1984.

CARLINI, C. R. & GROSSI-DE-SÁ, M. F. Plant toxic proteins with insecticidal properties. A review on their potentialities as bioinsecticides. *Toxicon*, *40*: 1515–1539, 2002.

CARLINI, C. R. & GUIMARÃES, J. A. Isolation and characterization of a toxic protein from *Canavalia ensiformis* (jack bean) seeds, distinct from concanavalin A. *Toxicon*, *19*(5): 667–675, 1981.

CARLINI, C. R.; GUIMARÃES, J. A. & RIBEIRO, J. M. Platelet release reaction and aggregation induced by canatoxin, a convulsant protein: evidence for the involvement of the platelet lipoxygenase pathway. *British Journal of Pharmacology*, *84*: 551–560, 1985.

CARLINI, C. R. & GUIMARÃES, J. A. Plant and microbial toxic proteins as hemilectins: emphasis on canatoxin. *Toxicon*, *29*(7): 791–806, 1991.

CARLINI, C. R.; OLIVEIRA, A. E. A.; AZAMBUJA, P.; XAVIER-FILHO, J. & WELLS, M. A. Biological effects of canatoxin in different insect models: evidence for a proteolytic activation of the toxin by insect cathepsinlike enzymes. *Journal of Economic Entomology*, *90*(2): 340–348, 1997.

CARLINI, C. R. & POLACCO, J. C. Toxic properties of urease. *Crop Science*, *48*: 1665–1672, 2008.

CARTER, E. L.; FLUGGA, N.; BOER, J. L.; MULROONEY, S. B. & HAUSINGER, R. P. Interplay of metal ions and urease. *Metallomics*, *1*(3): 207–221, 2009.

CARTER, E. L.; TRONRUD, D. E.; TABER, S. R.; KARPLUS, P. A. & HAUSINGER, R. P. Iron-containing urease in a pathogenic bacterium. *Proceedings of the National Academy of Sciences of the United States of America*, *108*(32): 13095–13099, 2011.

CHOUIKHA, I., & HINNEBUSCH, B. J. Silencing urease : A key evolutionary step that facilitated the adaptation of *Yersinia pestis* to the flea-borne transmission route, *111*(52): 18709–18714, 2014.

CLEMENS, D. L., LEE, B. Y. & HORWITZ, M. Purification, characterization, and genetic analysis of *Mycobacterium tuberculosis* urease, a potentially critical determinant of host- pathogen interaction. *Journal of Bacteriology*, *177*(19): 5644–5652, 1995.

CLINE, D. J., REDDING, S. E., BROHAWN, S. G., PSATHAS, J. N., SCHNEIDER, J. P. & THORPE, C. New water-soluble phosphines as reductants of peptide and protein disulfide bonds: Reactivity and membrane permeability. *Biochemistry*, *43:* 15195–15203, 2004.

CONRAD, J. P. The nature of the catalyst causing the hydrolysis of urea in soils. *Soil Science*, *50*(2): 119–134, 1940.

DAROIT, D. J.; CORRÊA, A. P. F. & BRANDELLI, A. Production of keratinolytic proteases through bioconversion of feather meal by the Amazonian bacterium *Bacillus* sp. P45. *International Biodeterioration and Biodegradation*, *65*:45–51, 2011.

DEFFERRARI, M. S., DEMARTINI, D. R., MARCELINO, T. B., PINTO, P. M., & CARLINI, C. R. Insecticidal effect of Canavalia ensiformis major urease on nymphs of the milkweed bug Oncopeltus fasciatus and characterization of digestive peptidases. *Insect Biochemistry and Molecular Biology*, *41*(6), 388–399, 2011.

DELLA-CASA, M.S.; JUNQUEIRA-DE-AZEVEDO, I.; BUTERA, D.; BIANCA, P.; LOPES, D.S.; SERRANO, S.M.T.; PIMENTA, D.C.; MAGALHÃES, G.S.; LEE, P. & MOURA-DA-SILVA, A.M., 2011. Insularin , a disintegrin from Bothrops insularis venom : Inhibition of platelet aggregation and endothelial cell adhesion by the native and recombinant GST-insularin proteins . Toxicon 57: 125–133, 2011.

DIXON, N. E.; GAZZOLA, C.; BLAKELEY, R. L. & ZERNER, B. Jack bean urease (EC 3.5.1.5). Metalloenzyme. Simple biological role for nickel. *Journal of the American Chemical Society*, *97*(14): 4131–4133, 1975.

DYSON, H. J. & WRIGHT, P. E. Intrinsically unstructured proteins and their functions. *Nature Reviews. Molecular Cell Biology*, *6:* 197–208. 2005

ELSEBAI, M.F., SALEEM, M., TEJESVI, M. V, KAJULA, M., MATTILA, S., MEHIRI, M., TURPEINEN, A. & PIRTTILÄ, A.M. Fungal phenalenones: chemistry, biology, biosynthesis and phylogeny. Natural Product Reports. 31, 628–45, 2014.

ERICSSON, U. B.; HALLBERG, B. M.; DETITTA, G. T.; DEKKER, N. & NORDLUND, P. Thermofluor-based high-throughput stability optimization of proteins for structural studies. *Analytical Biochemistry*, *357*: 289–298, 2006.

FEARON, W. R. Urease. Part I. The Chemical Changes Involved in the Zymolysis of Urea. *The Biochemical Journal*, *17*: 84–93, 1923.

FEDER, V.; KMETZSCH, L.; STAATS, C. C.; VIDAL-FIGUEIREDO, N.; LIGABUE-BRAUN, R.; CARLINI, C. R. & VAINSTEIN, M. H. *Cryptococcus gattii* urease as a virulence factor and relevance of enzymatic activity in cryptococcosis pathogenesis. *FEBS Journal*, 2005.

FERELLA, L.; ROSATO, A.; TURANO, P. & PLAVEC, J. What Can be Learned about the Structure and Dynamics of Biomolecules from NMR, in: NMR of Biomolecules: Towards Mechanistic Systems Biology (eds I. Bertini, K. S. McGreevy and G. Parigi), Wiley-VCH Verlag GmbH & Co. KGaA, Weinheim, Germany, 2012.

FERREIRA-DASILVA, C. T.; GOMBAROVITS, M. E.; MASUDA, H.; OLIVEIRA, C. M. & CARLINI, C. R. Proteolytic activation of canatoxin, a plant toxic protein, by insect cathepsin-like enzymes. *Archives of Insect Biochemistry and Physiology*, *44*: 162–171, 2000.

FOLLMER, C. Insights into the role and structure of plant ureases. *Phytochemistry*, *69*: 18–28, 2008.

FOLLMER, C.; BARCELLOS, G. B.; ZINGALI, R. B.; MACHADO, O. L.; ALVES, E. W.; BARJA-FIDALGO, C. & CARLINI, C. R. Canatoxin, a toxic protein from jack beans (*Canavalia ensiformis*), is a variant form of urease (EC 3.5.1.5): biological effects of urease independent of its ureolytic activity. *The Biochemical Journal*, *360*: 217–224, 2001.

FOLLMER, C.; CARLINI, C. R.; YONEAMA, M. L. & DIAS, J. F. PIXE analysis of urease isoenzymes isolated from *Canavalia ensiformis* (jack bean) seeds. *Nuclear Instruments and Methods in Physics Research, Section B: Beam Interactions with Materials and Atoms*, *189*: 482–486, 2002.

FOLLMER, C., PEREIRA, F. V., DA SILVEIRA, N.P. & CARLINI, C.R. Jack bean urease (EC 3.5.1.5) aggregation monitored by dynamic and static light scattering. Biophysical Chemistry 111: 79–87, 2004a.

FOLLMER, C.; REAL-GUERRA, R.; WASSERMANN, G. E.; OLIVERA-SEVERO, D. & CARLINI, C. R. Jackbean, soybean and *Bacillus pasteurii* ureases: Biological effects unrelated to ureolytic activity. *European Journal of Biochemistry*, *271*: 1357–1363, 2004.

GAST, K. & MODLER, A.J. Dynamic and Static Light Scattering of Proteins. In: Methods in Protein Structure and Stability Analysis--Conformational Stability, Size, Shape and Surface of Protein Molecules. V. N. Uversky (Ed.). Nova Publishers, 2007.

GATEHOUSE, J. A. Plant resistance towards insect herbivores: a dynamic interaction. *New Phytologist*, *156*(140): 145–169, 2002.

GEE, D.J.M.C.; MAY, C. A.; GARNER, R.M.; HIMPSL, J.M. & MOBLEY, H.L.T., ACTERIOL, J.B. Isolation of *Helicobacter pylori* genes that modulate urease activity. *Journal of Bacteriology*, 181: 2477–2484, 1999.

GETZ, E. B.; XIAO, M.; CHAKRABARTY, T.; COOKE, R. & SELVIN, P. R. A comparison between the sulfhydryl reductants tris(2-carboxyethyl)phosphine and dithiothreitol for use in protein biochemistry. *Analytical Biochemistry*, *273*, 73–80, 1999.

GHAZALEH, F. A.; FRANCISCHETTI, I. M.; GOMBAROVITS, M. E. & CARLINI, C. R. Stimulation of calcium influx and platelet activation by canatoxin: methoxyverapamil inhibition and downregulation by cGMP. *Archives of Biochemistry and Biophysics*, *339* (2): 362–367, 1997.

GOLDRAIJ, A.; BEAMER, L. J. & POLACCO, J. C. Interallelic Complementation at the Ubiquitous Urease Coding Locus of Soybean 1, 132*:* 1801–1810, 2003.

GRASSI-KASSISSE, D. M. & RIBEIRO-DASILVA, G. Canatoxin triggers histamine secretion from rat peritoneal mast cells. *Agents and Actions*, *37*(3-4): 204–209, 1992.

GREENFIELD, N. J. Applications of circular dichroism in protein and peptide analysis, *18*(4):236–244, 1999.

HA, N. C.; OH, S. T.; SUNG, J. Y.; CHA, K. A.; LEE, M. H. & OH, B.H. Supramolecular assembly and acid resistance of *Helicobacter pylori* urease. *Nature Structural & Molecular Biology*, *8*(6): 505–509, 2001.

HAALAND, P.D., 1989. Experimental design in biotechnology. CRC press.

HAN, J. C. & HAN, G. Y. A procedure for quantitative determination of tris(2-carboxyethyl)phosphine, an odorless reducing agent more stable and effective than dithiothreitol. *Analytical Biochemistry*, 220: 5-10, 1994.

HENDERSON, B.; LUND, P. A. & COATES, A. R. M. Multiple moonlighting functions of mycobacterial molecular chaperones. *Tuberculosis*, *90*(2): 119–124, 2010.

HILDER, V. A. & BOULTER, D. Genetic engineering of crop plants for insect resistance: a critical review. *Crop Protection*, *18*: 177-191, 1999.

HUBERTS, D. H. E. W. & VAN DER KLEI, I. J. Moonlighting proteins: An intriguing mode of multitasking. *Biochimica et Biophysica Acta - Molecular Cell Research*, *1803*(4): 520–525, 2010.

JABRI, E.; CARR, M. B.; HAUSINGER, R. P. & KARPLUS, P. A. The crystal structure of urease from *Klebsiella aerogenes*. *Science*, *268*(5213): 998–1004, 1995.

KAMOUN, S. Molecular Genetics of Pathogenic Molecular Genetics of Pathogenic Oomycetes. *Eukariotic Cell* 2: 191–199, 2003.

KAPPAUN, K. Clonagem e expressão da urease da bactéria diazotrófica *Azospirillum brasilense* FP2 e do peptídeo soyuretox, derivado da urease ubíqua de soja (*Glycine max*). Dissertation, Universidade Federal do Rio Grande do Sul, Porto Alegre, RS, Brazil, 2014.

KILIKIAN, B. V.; SUÁREZ, I. D.; LIRIA, C. W. & GOMBERT, A. K. Process strategies to improve heterologous protein production in *Escherichia coli* under lactose or IPTG induction. *Process Biochemistry*, *35*: 1019–1025, 2000.

KIM, J. K.; MULROONEY, S. B. & HAUSINGER, R. P. Biosynthesis of active *Bacillus subtilis* urease in the absence of known urease accessory proteins. *Journal of Bacteriology*, *187*(20): 7150–7154, 2005.

KRAJEWSKA, B. (2009). Ureases I. Functional, catalytic and kinetic properties: A review. *Journal of Molecular Catalysis B: Enzymatic*. *59*, 9–21, 2009.

KUMAR, S.; DWEVEDI, A. & KAYASTHA, A. M. Enzymatic Immobilization of soybean (*Glycine max*) urease on alginate and chitosan beads showing improved stability: Analytical applications. *Journal of Molecular Catalysis* B, *58*: 138–145, 2009.

LANE, N.J.; LESLIE, R. A. & SWALES, L.S.,. Insect peripheral nerves: accessibility of neurohaemal regions to lanthanum. *Journal of Cell Science*, 18, 179–197, 1975

LEE, H. S. Fungicidal property of active component derived from *Acorus gramineus* rhizome against phytopathogenic fungi. *Bioresource Technology*, *98*: 1324–1328, 2007.

LEITES, A.; PAULA, A.; ARGONDIZZO, C.; ESTEVES, S.; JESSOURON, E.; GALLER, R. & ALBERTO, M., 2011. Cloning and optimization of induction conditions for mature PsaA (pneumococcal surface adhesin A) expression in *Escherichia coli* and recombinant protein stability during long-term storage. *Protein Expression and Purification* 78: 38–47, 2011.

LIGABUE-BRAUN, R.; ANDREIS, F. C.; VERLI, H. & CARLINI, C. R. 3-to-1: unraveling structural transitions in ureases. *Naturwissenschaften*, *100*(5): 459–467, 2013.

LIMA, M.A.; YATES, E.A.; TERSARIOL, I. L. S. & NADER, H. B. Dicroísmo Circular. In: Bioinformática: da Biologia à Flexibilidade Molecular (org. Hugo Verli), 282 p., 2014.

LUO, Y.; HUANG, X. & MCKEEHAN, W.L.. High yield , purity and activity of soluble recombinant *Bacteroides thetaiotaomicron* GST-heparinase I from *Escherichia coli*. *Archives of Biochemistry and Biophysics*, 460: 17–24, 2007

MALUF, F. V.; MUNIZ, J. R.C.; OLIVA, G. & GUIDO, R. V. C. Cristalografia de Proteínas. In: Bioinformática: da Biologia à Flexibilidade Molecular (org. Hugo Verli), 282 p., 2014.

MARLEY, J.; LU, M. & BRACKEN, C. A method for efficient isotopic labeling of recombinant proteins. Journal of Biomolecular NMR, 71–75, 2001.

MARTINELLI, A. H. S. Expressão da urease ubíqua de soja em *Escherichia coli*. Dissertation, Universidade Federal do Rio Grande do Sul, Porto Alegre, RS, Brazil, 2007.

MARTINELLI, A. H. S. Toxicidade de urease de soja (Glycine max) a fitopatógenos. Trabalho de Conclusão, Universidade do Vale do Sinos, São Leopoldo, RS, Brazil, 2004.

MARTINELLI, A. H. S.; KAPPAUN, K.; LIGABUE-BRAUN, R.; DEFFERRARI, M. S.; PIOVESAN, A. R.; STANISÇUASKI, F.; DEMARTINI, D.R.; DAL BELO, C.A.;.ALMEIDA, C.G.M; FOLLMER, C.; VERLI, H.; CARLINI, C.R. & PASQUALI, G. Structure-function studies on jaburetox, a recombinant insecticidal peptide derived from jack bean (*Canavalia ensiformis*) urease. *Biochimica et Biophysica Acta - General Subjects*, *1840*(3): 935–944, 2014.

MEDEIROS-SILVA, M.; FRANCK, W. L.; BORBA, M. P.; PIZZATO, S. B.; STRODTMAN, K. N.; EMERICH, D. W. & CARLINI, C. R. Soybean ureases, but not that of *Bradyrhizobium japonicum*, are involved in the process of soybean root nodulation. *Journal of Agricultural and Food Chemistry*, *62*, 3517–3524, 2012.

MEDENTSEV, A. G. & AKIMENKO, V.K. Naphthoquinone metabolites of the fungi. *Phytochemistry* 47: 935–959, 1998.

MENEGASSI, A.; WASSERMANN, G. E.; OLIVERA-SEVERO, D.; BECKER-RITT, A. B.; MARTINELLI, A. H. S.; FEDER, V. & CARLINI, C. R. Urease from cotton (*Gossypium hirsutum*) seeds: Isolation, physicochemical characterization, and antifungal properties of the protein. *Journal of Agricultural and Food Chemistry*, *56*: 4399–4405, 2008.

MOBLEY, H. L. & HAUSINGER, R. P. Microbial ureases: significance, regulation, and molecular characterization. *Microbiological Reviews*, *53*(1): 85–108, 1989.

MOBLEY, H. L.; ISLAND, M. D. & HAUSINGER, R. P. Molecular biology of microbial ureases. *Microbiological Reviews*, *59*(3): 451–480, 1995.

MORA, D. & ARIOLI, S. (2014). Microbial Urease in Health and Disease, 10(12), 10–13, *Plos Pathogens*, 2014.

MULINARI, F.; BECKER-RITT, A. B.; DEMARTINI, D. R.; LIGABUE-BRAUN, R.; STANISÇUASKI, F.; VERLI, H.; FRAGOSO, R. R.; SCHROEDER, E. K.; CARLINI, C. R. & GROSSI-DE-SÁ, M. F. Characterization of JBURE-IIb isoform of *Canavalia ensiformis* (L.) DC urease. *Biochimica et Biophysica Acta - Proteins and Proteomics*, *1814*(12): 1758–1768, 2011.

MULINARI, F.; STANISÇUASKI, F.; BERTHOLDO-VARGAS, L. R.; POSTAL, M.; OLIVEIRA-NETO, O. B.; RIGDEN, D. J. & CARLINI, C. R. Jaburetox-2Ec: an insecticidal peptide derived from an isoform of urease from the plant *Canavalia ensiformis*. *Peptides*, *28*(10): 2042–50, 2007.

NEVES, L.; MEDEIROS, D.; ANGELI, R.; SARZEDAS, C. G.; BARRETO-BERGTER, E.; PAULA, A. & ALMEIDA, F. C. L. Backbone dynamics of the antifungal Psd1 pea defensin and its correlation with membrane interaction by NMR spectroscopy. Biochimica et Biophysica Acta *BBA – Biomembranes*. *1798*(2): 105–113, 2010.

OERKE, E. C. & DEHNE, H. W. Safeguarding production - Losses in major crops and the role of crop protection. *Crop Protection*, *23*, 275–285, 2004.

OERKE, E.C. Crop losses to pests. *The Journal of Agricultural Science*, *144*, 31, 2006.

OERKE, E.C. & DEHNE, H.W. Safeguarding production - Losses in major crops and the role of crop protection. *Crop Protection*. 23, 275–285, 2004.

OLIVA, A. & FARIN, B. Comparative study of protein molecular weights by size-exclusion chromatography and laser-light scattering, *25*, 833–841, 2001.

OLIVEIRA, A. E. A.; GOMES, V. M.; SALES, M. P.; FERNANDES, K. V. S.; CARLINI, C. R. & XAVIER-FILHO, J. The toxicity of jack bean [*Canavalia ensiformis* (L.) DC.] canatoxin to plant pathogenic fungi. *Revista Brasileira de Biologia*, *59*(1): 59–62, 1999.

OLIVERA-SEVERO, D.; WASSERMANN, G. E. & CARLINI, C. R. Ureases display biological effects independent of enzymatic activity. Is there a connection to diseases caused by urease-producing bacteria? *Brazilian Journal of Medical and Biological Research*, *39*, 851–861: 2006.

PAPANEOPHYTOU, C.P. & KONTOPIDIS, G. Statistical approaches to maximize recombinant protein expression in *Escherichia coli*: A general review. Protein Expression and Purification. 94, 22–32, 2014.

PETI, W. & PAGE, R. Strategies to maximize heterologous protein expression in *Escherichia coli* with minimal cost. *Protein Expression and Purification*, *51*, 1–10, 2007.

PIOVESAN, A. R.; MARTINELLI, A. H. S.; LIGABUE-BRAUN, R.; SCHWARTZ, J. & CARLINI, C. R. *Canavalia ensiformis* urease, Jaburetox and derived peptides form ion channels in planar lipid bilayers. *Archives of Biochemistry and Biophysics*, *547*, 6–17, 2014.

PIRES-ALVES, M.; GROSSI-DE-SÁ, M. F.; BARCELLOS, G. B. S.; CARLINI, C. R. & MORAES, M. G. Characterization and expression of a novel member (JBURE-II) of the urease gene family from jackbean [*Canavalia ensiformis* (L.) DC]. *Plant and Cell Physiology*, *44*(2): 139–145, 2003.

POLACCO, J. C. & HOLLAND, M. A. Roles of urease in plant cells. *International Review of Cytology*, *145*: 65–103, 1993.

POLACCO, J. C. & WINKLER, R. G. Soybean leaf urease: a seed enzyme? *Plant Physiology*, *74*: 800–803, 1984.

POLACCO, J. C. & HAVIR, E. A. Comparisons of soybean urease isolated from seed and tissue culture. The Journal of Biological Chemistry, 1707–1715, 1979.

POMPILIO, A.; SCOCCHI, M.; POMPONIO, S.; GUIDA, F.; DI PRIMIO, A.; FISCARELLI, E.; GENNARO, R. & DI BONAVENTURA, G. Antibacterial and anti-biofilm effects of cathelicidin peptides against pathogens isolated from cystic fibrosis patients. *Peptides* 32: 1807–1814, 2011..

POSTAL, M.; MARTINELLI, A. H. S.; BECKER-RITT, A. B.; LIGABUE-BRAUN, R.; DEMARTINI, D. R.; RIBEIRO, S. F. F. & CARLINI, C. R. Antifungal properties of *Canavalia ensiformis* urease and derived peptides. *Peptides*, *38*(1), 22–32, 2012.

RADFORD, D.R.; CHALLACOMBE, S.J. & WALTER, J.D. A scanning electronmicroscopy investigation of the structure of colonies of different morphologies produced by phenotypic switching of *Candida albicans*, Analytical Biochemistry 40: 416–423, 1994.

REAL-GUERRA, R., STANISÇUASKI, F. & CARLINI, C. R. Soybean Urease : Over a Hundred Years of Knowledge, Intech, 317-340, 2013.

RIBEIRO-DASILVA, G.; PIRES-BARBOSA, R. & CARLINI, C. R. Effect of canatoxin on the circulating levels of gonadotropins and prolactin in rats. *Brazilian Journal of Medical and Biological Research 22*(3): 387–395, 1988.

RIBEIRO-DASILVA, G. & PRADO, J. F. Increased insulin circulating levels induced by canatoxin in rats. *Toxicon*, *31*, 1131–1136, 1993.

RUTHERFORD, J. C. The Emerging Role of Urease as a General Microbial Virulence Factor. *PLoS Pathogens*, *10*(5): 1–3, 2014.

SALVADORI, J. D. M.; DEFFERRARI, M. S.; LIGABUE-BRAUN, R.; YAMAZAKI LAU, E.; SALVADORI, J. R. & CARLINI, C. R. Characterization of entomopathogenic nematodes and symbiotic bacteria active against *Spodoptera frugiperda* (Lepidoptera: Noctuidae) and contribution of bacterial urease to the insecticidal effect. *Biological Control*, *63*(3): 253–263, 2012.

SCHMUTZ, J.; CANNON, S. B.; SCHLUETER, J.; MA, J.; MITROS, T.; NELSON, W. & JACKSON, S. A. Genome sequence of the palaeopolyploid soybean. *Nature*, *463*(7278): 178–183, 2010.

SELITRENNIKOFF, C. P. Antifungal Proteins. *Applied and Environmental Microbiology*, *67*(7): 2883–2894, 2001.

SENISTERRA, G., CHAU, I. & VEDADI, M. Thermal Denaturation Assays in Chemical Biology. *Assay and Drug Developments Technologies*, 128–136, 2012.

SIRKO, A. & BRODZIK, R. Plant ureases: Roles and regulation. *Acta Biochimica Polonica*. *47*(4): 1189–1195, 2000.

SPIEZIA, M.; CHIARABELLI, C. & POLTICELLI, F. Recombinant expression and insecticidal properties of a Conus ventricosus conotoxin-GST fusion protein. Toxicon 60: 744–751, 2012.

SRIRAM, G.; MARTINEZ, J. A.; MCCABE, E. R. B.; LIAO, J. C. & DIPPLE, K. M. Single-gene disorders: what role could moonlighting enzymes play? *American Journal of Human Genetics*, *76*: 911–924, 2005.

STANISÇUASKI, F. & CARLINI, C. R. Plant ureases and related peptides: Understanding their entomotoxic properties. *Toxins*, *4*: 55–67, 2012.

STANISÇUASKI, F.; FERREIRA-DASILVA, C. T.; MULINARI, F.; PIRES-ALVES, M. & CARLINI, C. R. Insecticidal effects of canatoxin on the cotton stainer bug *Dysdercus peruvianus* (Hemiptera: Pyrrhocoridae). *Toxicon*, *45*: 753–760, 2005.

STANISÇUASKI, F.; TE BRUGGE, V.; CARLINI, C. R. & ORCHARD, I. Invitro effect of *Canavalia ensiformis* urease and the derived peptide Jaburetox-2Ec on *Rhodnius prolixus* Malpighian tubules. *Journal of Insect Physiology*, *55*(3): 255–63, 2009.

STANISÇUASKI, F.; TE BRUGGE, V.; CARLINI, C. R. & ORCHARD, I. Jack bean urease alters serotonin-induced effects on *Rhodnius prolixus* anterior midgut. *Journal of Insect Physiology*, *56*: 1078–1086, 2010.

SUMNER, J. B. The isolation and crystalization of the enzyme urease. *The Journal of Biological Chemistry*, 69: 435-441, 1926.

SMYTH, D.R.; MROZKIEWICZ, M.K.; MCGRATH, W.J.; LISTWAN, P. & KOBE, B., Crystal structures of fusion proteins with large-affinity tags, *Protein Science* 1313–1322, 2003.

TAN, V. P. Y. & WONG, B. C. Y. *Helicobacter pylori* and gastritis: Untangling a complex relationship 27 years on. *Journal of Gastroenterology and Hepatology*, *26 Suppl 1*, 42–45, 2011.

TATUM, H. J.; BAKER, A. R.& BERRY, E. R. Naphthofurans produced by *Fusarium oxysporum* isolated from citrus. *Phytochemistry* 26, 2499–2500, 1987.

TICHOTA, D. M. Encapsulação do peptídeo fungitóxico Jaburetox em nanopartículas lipídicas. Trabalho de Conclusão de Curso de Farmácia, Universidade Federal do Rio Grande do Sul, Porto Alegre, RS, 2014.

TOMAZETTO, G.; MULINARI, F.; STANISÇUASKI, F.; SETTEMBRINI, B.; CARLINI, C. R., & AYUB, M. A. Z. Expression kinetics and plasmid stability of recombinant *E. coli* encoding urease-derived peptide with bioinsecticide activity. *Enzyme and Microbial Technology*, *41*(6-7): 821–827, 2007.

TOMPA, P. Unstructural biology coming of age. *Current Opinion in Structural Biology*, *21*(3): 419–425, 2011.

TOMPA, P. Intrinsically disordered proteins : a 10-year recap, *Trends in Biochemical Sciences*, *37*(12): 509–516, 2012.

TOMPA, P. & FERSHT, A. Structure and function of intrinsically disordered proteins. *CRC Press*, 2009.

TORISKY, R. S., GRIFFIN, J. D., YENOFSKY, R. L. & POLACCO, J. C. A single gene (Eu4) encodes the tissue-ubiquitous urease of soybean. *Molecular & General Genetics : MGG*, *242*: 404–414, 1994.

TORISKY, R. S. & POLACCO, J. C. Soybean Roots Retain the Seed Urease Isozyme Synthesized during Embryo Development. *Plant Physiology*, *94*: 681–689, 1990.

TOWBIN, H.; STAEHELIN, T. & GORDON, J. Electrophoretic transfer of proteins from polyacrylamide gels to nitrocellulose sheets: procedure and some applications. *Proceeding of the National Academy of Sciences of U. S. A.* 76, 4350–4354, 1979.

UBERTI, A. F.; OLIVERA-SEVERO, D.; WASSERMANN, G. E.; SCOPEL-GUERRA, A.; MORAES, J. A.; BARCELLOS-DE-SOUZA, P. & CARLINI, C. R. Pro-inflammatory properties and neutrophil activation by *Helicobacter pylori* urease. *Toxicon*, *69*: 240–249, 2013.

UVERSKY, V. N. Natively unfolded proteins : A point where biology waits for physics. *Protein Science* (2002), 11:739–756, 2002.

UVERSKY, V. N., & DUNKER, A K. Understanding protein non-folding. *Biochimica et Biophysica Acta*, *1804*(6): 1231–64, 2010.

UVERSKY, V. N.; GILLESPIE, J. R. & FINK, A. L.. Why are "natively unfolded" proteins unstructured under physiologic conditions? *Proteins: Structure, Function, and Bioinformatics*, *41*(3): 415–427, 2000.

VANDENBORRE, G.; SMAGGHE, G. & DAMME, E. J. M. VAN. Phytochemistry Plant lectins as defense proteins against phytophagous insects. *Phytochemistry*, *72*(13): 1538–1550, 2011.

VAZQUEZ, E., CORCHERO, J. L. & VILLAVERDE, A. Post-production protein stability : trouble beyond the cell factory. *Microbial Cell Factories*, *10*(1): 60, 2011.

WALKER, T. S.; BAIS, H. P.; GROTEWOLD, E. & VIVANCO, J. M. Root exudation and rhizosphere biology. *Plant Physiology*, *132*(1): 44–51, 2003.

WASSERMANN, G. E.; OLIVERA-SEVERO, D.; UBERTI, A. F. & CARLINI, C. R. (2010). *Helicobacter pylori* urease activates blood platelets through a lipoxygenase-mediated pathway. *Journal of Cellular and Molecular Medicine*, *14*(7): 2025–2034, 2010.

WHITMORE, L.; WOOLLETT, B.; MILES, A. J.; JANES, R. W. & WALLACE, B. A. The Protein Circular Dichroism Data Bank, A Web-Based Site for Access to Circular Dichroism Spectroscopic Data. *Structure*, *18*(10): 1267–1269, 2010.

WIEBKE-STROHM, B.; PASQUALI, G.; MARGIS-PINHEIRO, M.; BENCKE, M.; BÜCKER-NETO, L.; BECKER-RITT, A. B. & BODANESE-ZANETTINI, M. H. Ubiquitous urease affects soybean susceptibility to fungi. *Plant Molecular Biology*, *79*: 75–87, 2012.

WIEDEMANN, C.; BELLSTEDT, P. & GO, M. Structural bioinformatics CAPITO — a web server-based analysis and plotting tool for circular dichroism data, *29*(14): 1750–1757, 2013.

WITTE, C. P. Urea metabolism in plants. *Plant Science*, *180*(3): 431–438, 2011.

WITTE, C. P.; ROSSO, M. G. & ROMEIS, T. Identification of three urease accessory proteins that are required for urease activation in *Arabidopsis*. *Plant Physiology*, *139*:1155–1162, 2005.

WOODY, R. W. (2015). The development and current state of protein circular dichroism. *Biomedical Spectroscopy and Imaging*, *4*: 5–34, 2015.

YE, H. Simultaneous determination of protein aggregation , degradation , and absolute molecular weight by size exclusion chromatography – multiangle laser light scattering, *Analytical Biochemistry*, *356*: 76–85, 2006.

ZAMBELLI, B.; MUSIANI, F.; BENINI, S. & CIURLI, S. Chemistry of Ni^{2+} in urease: sensing, trafficking, and catalysis. *Accounts of Chemical Research*, *44*(7): 520–530, 2011.

ZHAN, Y.; SONG, X. & ZHOU, G.W. Structural analysis of regulatory protein domains using GST-fusion proteins. *Gene* 281, 1–9, 2001

10. *CURRICULUM VITAE* RESUMIDO

LOPES, F.C.

I. DADOS PESSOAIS

Nome: Fernanda Cortez Lopes

Local e data de nascimento: Porto Alegre, Rio Grande do Sul, 03/08/1984

Endereço profissional: Avenida Bento Gonçalves, 9500 Prédio 43.431 Laboratório 114, Campus do Vale CEP: 91501-970

Telefone profissional: +55 51 3308-7600/ 3308-7606

E-mail: fernandalopes@cbiot.ufrgs.br

II. FORMAÇÃO ACADÊMICA

- **2011-em andamento**: Curso de Pós-Graduação *stricto senso* (doutorado) em Biologia Celular e Molecular (Universidade Federal do Rio Grande do Sul)
- **2009-2011:** Curso de Pós-Graduação *stricto senso* (mestrado) em Biologia Celular e Molecular (Universidade Federal do Rio Grande do Sul)
- **2008-2012**: Habilitação em Análises Clínicas (Universidade Federal do Rio Grande do Sul)
- **2004-2008**: Graduação em Farmácia (Universidade Federal do Rio Grande do Sul)

Formação Complementar (restrito ao período de desenvolvimento da tese)

- **Methods to Characterize Protein Folding and Chemistry** (Carga horária: 15h), Universidade Federal do Rio Grande do Sul, Drª Barbara Zambelli, 2014.
- **Advanced Topics in Insect Neurobiology** (Carga horária: 21h), Pontifícia Universidade Católica do Rio Grande do Sul, Dr. Ian Orchard e Drª Angela Lange, 2014.
- **Bioinorganic Chemistry** (Carga horária: 20h), Universidade Federal do Rio Grande do Sul, Dr. Stefano Ciurli, 2014.
- **Protein NMR** (Carga horária: 30h), Universidade Federal do Rio Grande do Sul, Dr. Stefano Ciurli, 2013.
- **Workshop em Microscopia Eletrônica** (Carga horária: 16h), Universidade Federal do Rio Grande do Sul, Dr. Roland Fleck e Dr. Daniel Lorscheitter Baptista, 2013.

III. ESTÁGIOS

- **Doutorado-Sanduíche:** Università di Bologna, Bologna, Itália (Estudos das Propriedades Estruturais do Jaburetox). Período: abril a outubro de 2013.
- **Missão de Curta Duração:** Instituto Max Planck de Química Ecológica, Jena, Alemanha (Estudos de herbivoria utilizando soja (*Glycine max*) como planta modelo, realizando um estudo comparativo com o equipamento MecWorm (mimetiza a mordida de lagarta) e a mordida da lagarta *Spodoptera littoralis*). Período: 02 a 12 de novembro de 2014.

IV. PRÊMIOS E DISTINÇÕES

- 2011: Menção honrosa ao trabalho "Propriedades antioxidantes de linhagens de *Lactobacillus*" (co-autoria), 26º Congresso Brasileiro de Microbiologia (Simpósio Internacional de Bactérias Láticas).
- 2006: Trabalho destaque na sessão de Microbiologia do Salão de Iniciação Científica UFRGS.

V. EDUCAÇÃO E POPULARIZAÇÃO DE CIÊNCIA E TECNOLOGIA

- 2014-atual: Professora Voluntária de Biologia na Organização Não-Governamental para o Ensino Popular (ONGEP)
- 2013: Monitoria Curso de Férias PPGBCM: Você conhece a célula?
- 2012: Monitoria Curso de Férias PPGBCM: Alimentos.
- 2011: Monitoria Curso de Férias PPGBCM: Plantas..para que mesmo?
- 2010: Monitoria Curso de Férias PPGBCM: Você conhece a célula?
- 2009: Monitoria Curso de Férias PPGBCM: Micro-organismos – mocinhos ou bandidos?

VI. PUBLICAÇÕES EM PERIÓDICOS ESPECIALIZADOS

- **LOPES, F. C.**, DOBROVOLSKA, O., REAL-GUERRA, R., BROLL, V., ZAMBELLI, B., MUSIANI, F., UVERSKY, V., CARLINI, C. R., CIURLI, S. Pliable natural biocide: Jaburetox is an intrinsically disordered insecticidal and fungicidal polypeptide derived from jack bean urease. *The FEBS Journal*, 2015.

- PEREIRA, J. Q., **LOPES, F. C.,** PETRY, M. V., MEDINA, L. F. C., BRANDELLI, A. Isolation of three novel Antarctic psychrotolerant feather-degrading bacteria and partial purification of keratinolytic enzyme from *Lysobacter* sp. A03. *International Biodeterioration & Biodegradation*, 88: 1 - 7, 2014.
- **LOPES, F. C.**, TICHOTA, D. M., SAUTER, I. P., MEIRA, S. M. M., SEGALIN, J., ROTT, M. B., RIOS, A. O., BRANDELLI, A. Active metabolites produced by *Penicillium chrysogenum* IFL1 growing on agro-industrial residues. *Annals of Microbiology*, 63: 771 - 778, 2013.
- **LOPES, F. C.**, TICHOTA, D. M., PEREIRA, J. Q., SEGALIN, J., RIOS, A. O., BRANDELLI, A. Pigment Production by Filamentous Fungi on Agro-Industrial Byproducts: an Eco-Friendly Alternative. *Applied Biochemistry and Biotechnology*, 171: 616 - 625, 2013.
- MEIRA, S. M. M., HELFER, V. E., VELHO, R. V., **LOPES, F. C.**, BRANDELLI, A. Probiotic potential of *Lactobacillus* spp. isolated from Brazilian regional ovine cheese. *Journal of Dairy Research* (Print), 79: 119 - 127, 2012.
- CORREA, A. P. F., DAROIT, D. J., COELHO, J., MEIRA, S. M. M., **LOPES, F.C.**, SEGALIN, J., RISSO, P., BRANDELLI, A. Antioxidant, antihypertensive and antimicrobial properties of ovine milk caseinate hydrolyzed with a microbial protease. *Journal of the Science of Food and Agriculture*, 91: 2247 - 2254, 2011.
- **LOPES, F. C**., SILVA, L. A. D. E., TICHOTA, D. M., DAROIT, D. J., VELHO, R. V., PEREIRA, J. Q., CORREA, A. P. F., BRANDELLI, A. Production of proteolytic enzymes by a keratin-degrading *Aspergillus niger*. *Enzyme Research* (Online), 1 – 9, 2011.
- DEDAVID E SILVA, L. A., **LOPES, F. C.**, SILVEIRA, S. T., BRANDELLI, A. Production of cellulolytic enzymes by *Aspergillus phoenicis* in grape waste using response surface methodology. *Applied Biochemistry and Biotechnology*, 152 (2): 295-305, 2008.

VII. TRABALHOS CIENTIFICOS APRESENTADOS EM CONGRESSOS

(restrito ao período de desenvolvimento da tese)

Eventos Internacionais

- DEFFERRARI, M. S., FRUTTERO, L. L., DEMARTINI, D. R., LIGABUE-BRAUN, R., **LOPES, F. C.**, KRUG, M. S., SETTEMBRINI, B. P., CARLINI, C. R. Jaburetox and UDP-N-Acetyl glucosamine pyrophosphorylase: an unexpected interaction opening doors to the understanding of the entomotoxic mechanism of action of urease-derived peptides, Insect Biotech Conference, Toronto, Canadá, 2014.
- **LOPES, F. C.**, ZAMBELLI, B., CIURLI, S., CARLINI, C. R. Solution studies on Jaburetox: an entomotoxic peptide derived from jack bean (*Canavalia ensiformis*) urease. Convegno Nazionale della Divisione di Chimica dei Sistemi Biologici, Bertinoro, Itália, 2013.
- BROLL, V., SULIS, D. B., **LOPES, F. C.**, LIGABUE-BRAUN, R., POSTAL, M., DEMARTINI, D. R., CARLINI, C. R. Purification and Characterization of recombinant urease from *Proteus mirabilis*. Convegno Nazionale della Divisione di Chimica dei Sistemi Biologici, Bertinoro, Itália, 2013.
- FUCK, W. F., **LOPES, F. C**., GRASSELLI, L. P., ODY, D., BRANDELLI, A., GUTTERRES, M. Development of Fungal Dyes and Application in Leather Dyeing. XXXII. Congress of the International Union of Leather Technologists and Chemist Societies (IULTCS), Istanbul, Turquia, 2013.
- **LOPES, F. C.**, MARTINELLI, A. H. S., KAPPAUN, K., TICHOTA, D. M., PASQUALI, G., CARLINI, C. R. Atividade fungitóxica de urease ubíqua de soja (*Glycine max*) recombinante. XXI Congresso Latinoamericano de Microbiologia (ALAM), Santos, 2012.
- **LOPES, F. C.,** PELEGRINI, A. L., BECKER-RITT, A. B., NÖR, C., VERLI, H., SACHETT, L. G., ALMEIDA, M., BARBIERI, N. L., PERINI, P., LIGABUE-BRAUN, R., CARLINI, C. R. Curso de Férias PPGBCM: Uma alternativa didática ou uma didática alternativa? XXI Congresso Latinoamericano de Microbiologia (ALAM), Santos, 2012.

Eventos Nacionais

- PEREZ, K. J., CRISPINI, S. M., **LOPES, F. C.,** VELHO, R. V., BRANDELLI, A., NARDI, R. M. D. Potencial antifúngico de *Bacillus* sp. P5 isolado de puba de mandioca. 4º Simpósio de Segurança Alimentar, 2012, Gramado, 2012.
- MEIRA, S. M. M., HELFER, V. E., VELHO R. V., **LOPES, F. C.**, BRANDELLI, A. Bactérias lácticas potencialmente probióticas isoladas de queijo de ovelha. 26º Congresso Brasileiro de Microbiologia, 2011, Foz do Iguaçu, 2011.
- MEIRA, S. M. M., HELFER, V. E., **LOPES, F. C.**, BRANDELLI, A. . Propriedades Antioxidantes de linhagens de *Lactobacillus.* 26º Congresso Brasileiro de Microbiologia, Foz do Iguaçu, 2011.
- PEREZ, K. J., CRISPINI, S. M., **LOPES, F. C.**; BRANDELLI, A., NARDI, R. M. D. Indução (Ativação/Estímulo) da produção de substâncias antimicrobianas de *Bacillus* sp P5 por meio de co-cultivo com bactérias e fungos filamentosos. 26º Congresso Brasileiro de Microbiologia, Foz do Iguaçu, 2011.
- PEREIRA, J. Q., UTPOTT, M., **LOPES, F. C.**, MEDINA, L. F. C., BRANDELLI, A. Identificação e Caracterização de uma protease queratinolítica produzida por uma bactéria isolada das Ilhas Shetland do Sul, Antártida. 26º Congresso Brasileiro de Microbiologia, Foz do Iguaçu, 2011.
- MÜLLER, D., POSTAL, M., **LOPES, F. C.**, CARLINI, C. R. Mecanismo de ação fungitóxica da urease de *Canavalia ensiformis* e identificação das regiões da proteína responsáveis por essa atividade. 26º Congresso Brasileiro de Microbiologia, Foz do Iguaçu, 2011.
- CORRÊA, A. P. F., DAROIT, D. J., COELHO, J., MEIRA, S. M. M., **LOPES, F. C.**, BRANDELLI, A. Atividade Antibacteriana e Antifúngica de hidrolisados de caseína ovina pela protease de *Bacillus* sp. P7. 26º Congresso Brasileiro de Microbiologia, Foz do Iguaçu, 2011.

VIII. PALESTRAS

- **Lopes, F.C.** Do DNA ao Consultório Odontológico: A Importância da Biologia Molecular para a Odontologia. 2014, Faculdade Especializada na Área de Saúde do Rio Grande do Sul (FASURGS), Passo Fundo, 2014.

- **Lopes, F.C.**, Teixeira, T., Maciel, M.J., Hickert, L.R. Pós-Graduação no ICTA, XII Semana Acadêmica da Engenharia de Alimentos, Universidade Federal do Rio Grande do Sul, Porto Alegre, 2010.